Advanced Reactor Technologies

Radial Deconsolidation Leach-Burn-Leach of Five AGR-3/4 TRISO Fuel Compacts after Post-Irradiation Heating Tests

M3TG-24IN04020318

SEPTEMBER 2024

John D. Stempien
Lu Cai

Idaho National Laboratory

Idaho National Laboratory

Radial Deconsolidation Leach-Burn-Leach of Five AGR-3/4 TRISO Fuel Compacts after Post-Irradiation Heating Tests

John D. Stempien
Lu Cai
Idaho National Laboratory

September 2024

Idaho National Laboratory
Advanced Reactor Technologies
Idaho Falls, Idaho 83415

http://www.ART.INL.gov

Page intentionally left blank
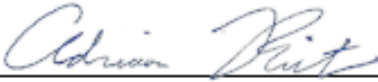
INL ART Program

Radial Deconsolidation Leach-Burn-Leach of Five AGR-3/4 TRISO Fuel Compacts after Post-Irradiation Heating Tests

INL/RPT-24-80406

September 2024

Technical Reviewer: (Confirmation of mathematical accuracy, and correctness of data and appropriateness of assumptions.)
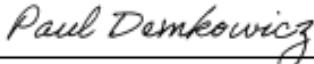
_____   9/5/2024
Adriaan A. Riet, PhD   Date
ART AGR Computational Scientist

Approved by:

_____   9/13/2024
Paul A. Demkowicz, PhD   Date
ART AGR Fuels Technical Director

_____   9/5/2024
Travis R. Mitchell   Date
ART AGR Program Manager

_____   9/13/2024
Michelle T. Sharp   Date
INL Quality Assurance

Page intentionally left blank

ABSTRACT

Five AGR-3/4 fuel compacts were previously heated in the Fuel Accident Condition Simulator (FACS) furnace. Three of these compacts were also reirradiated in the 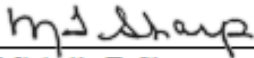Neutron Radiography (NRAD) reactor before the FACS tests. One of these was heated to 1200°C, two were heated to 1400°C, one was heated to 1600°C, and one was held for a period of time at 1600 and 1700°C. After these FACS tests, the compacts were subjected to destructive post-irradiation examination (PIE) via radial-deconsolidation-leach-burn-leach (RDLBL) at INL. The RDLBL process deconsolidated the compacts in multiple radial steps, followed by a final, single-step axial deconsolidation. The samples generated at each step were analyzed for isotopes of key fission products and actinides. After each deconsolidation step, the compact volume was assessed, and this was used to normalize the measured quantities of nuclides of interest to give volumetric concentrations as a function of radial position within the compact. The total inventories of measured fission products and actinides and the radial concentration profiles were compared with their sibling compacts within the same capsule (similar irradiation conditions) that went through RDLBL in the as-irradiated state. These data will be used to refine the fission product transport models.

Page intentionally left blank

ACKNOWLEDGEMENTS

Page intentionally left blank

CONTENTS

FIGURES

TABLES

Page intentionally left blank

ACRONYMS

AGR	Advanced Gas Reactor
AL	Analytical Laboratory
ART	Advanced Reactor Technologies
ATR	Advanced Test Reactor
DLBL	deconsolidation leach-burn-leach
DTF	Designed-to-fail
EOI	End of irradiation
FACS	Fuel Accident Condition Simulator
FGMS	Fission Gas Monitoring System
HTGR	High-temperature gas-cooled reactor
ICP-MS	inductively coupled plasma mass spectrometry
INL	Idaho National Laboratory
IPyC	inner pyrolytic carbon
M/C	measured-to-calculated ratio
MDA	Minimum detectable activity
NRAD	Neutron Radiography
OPyC	Outer pyrolytic carbon
ORNL	Oak Ridge National Laboratory
PGS	precision gamma scanner
PIE	Post-irradiation examination
PyC	pyrolytic carbon
RDLBL	Radial deconsolidation leach-burn-leach
TAVA	Time-average volume-average
TRISO	Tristructural isotropic

Page intentionally left blank

Radial Deconsolidation Leach-Burn-Leach of Five AGR-3/4 TRISO Fuel Compacts after Post-Irradiation Heating Tests

1.   INTRODUCTION

1.1. Overall Program Purpose

The Advanced Gas Reactor (AGR) Fuel Development and Qualification Program was established to perform research and development on tristructural isotropic (TRISO)-coated particle fuel to support deployment of a high-temperature gas-cooled reactor (HTGR). This work continues as part of the Advanced Reactor Technologies (ART) Program. The overarching goal of the ART AGR program is to provide a data set to support TRISO fuel qualification and the licensing and operation of HTGRs. This program includes the elements of fuel fabrication, irradiation, post-irradiation examination (PIE) and high-temperature tests, fuel performance modeling, and fission product transport (Idaho National Laboratory 2022). The fourth and final AGR TRISO fuel irradiation (designated AGR-5/6/7) was completed at the Advanced Test Reactor (ATR) at Idaho National Laboratory (INL) in July 2020.

1.2. Purpose of AGR-3/4 and Related Status

The AGR-1 and AGR-2 experiments focused on the performance of high-quality TRISO fuel, and PIE for those experiments focused on quantifying the very small rates of silicon carbide (SiC) and TRISO coating failures. In contrast, the AGR-3/4 experiment was primarily a fission-product transport experiment focused on observing the migration of fission products throughout fuel and nuclear-grade graphites. Following irradiation, measurements of the fission-product concentration profiles (both axially and radially) within AGR-3/4 samples (primarily the graphite rings and compacts) have constituted the bulk of PIE (Stempien et al. 2018b; Stempien 2021; Harp, Stempien, and Demkowicz 2021; Riet 2022). Most recently, a report on the measurements of fission product concentration profiles within as-irradiated AGR-3/4 compacts was completed at INL (Stempien and Cai 2024a) to accompany similar reporting completed by staff at Oak Ridge National Laboratory (ORNL) (Hunn et al. 2020, Helmreich et al. 2021, Helmreich et al. 2022). The subject of this report is the measurement of fission product concentration profiles at INL in AGR-3/4 fuel compacts after post-irradiation heating tests were conducted. These data are being used to support refinement of fission product transport models and HTGR source-term analyses (Riet and Stempien 2022; Riet 2023).

1.3. AGR-3/4 Fuel Description

The cylindrical AGR-3/4 fuel compacts contained TRISO-coated driver-fuel particles, similar to AGR-1 baseline fuel (Collin 2015a; Hunn and Lowden 2007; Hunn et al. 2014), and designed-to-fail (DTF) particles to intentionally release fission products during irradiation to migrate radially outward through the surrounding concentric rings of graphitic matrix and nuclear-grade graphite that made up the balance of the AGR-3/4 irradiation capsules. Each AGR-3/4 compact contained 20 DTF particles, in addition to the approximately 1,898 TRISO-coated "driver" fuel particles. DTF fuel kernels were coated only with a thin (20-μm-thick) pyrolytic carbon (PyC) layer. This PyC layer was intentionally fabricated with high anisotropy, such that it would be likely to fail during the irradiation (Collin 2015a; Hunn and Miller 2009; and Kercher et al. 2011), resulting in 20 exposed fuel kernels per compact. As shown at right in Figure 1, the DTF particles (highlighted in red) were aligned roughly along the compact radial centerline. DTF particles were intended to provide a known source of fission products to migrate radially outward in the irradiation capsules. However, PIE has also found evidence of axial fission product transport, which has complicated the analyses (Stempien 2021). It was expected that intact DTF particles would behave like TRISO particles with SiC layer failures (releasing substantial Cs, but retaining fission

gases), and failed DTF particles (DTF particles with breached pyrocarbon layers) would behave like TRISO particles with failed TRISO coatings (releasing both Cs and fission gases).

The white particles in the image on the right side of Figure 1 are the driver particles. AGR-3/4 driver-particle fuel kernels were fully TRISO-coated with buffer layer, inner pyrolytic carbon (IPyC) layer, SiC layer, and outer pyrolytic carbon (OPyC) layer characteristics similar to the Baseline fuel from the AGR-1 experiment (Collin 2015b; Hunn and Lowden 2007). Both the AGR-3/4 driver and DTF fuel particles contain uranium oxycarbide (a heterogeneous mixture of uranium carbide and uranium oxide) fuel kernels (approximately 350 μm in diameter) manufactured at BWXT. The U-235 enrichment was 19.7 wt%. The DTF pyrocarbon coating and the driver fuel TRISO coatings were applied to the kernels at ORNL. Driver particle and DTF particle properties were summarized by Collin (2015a). Complete kernel and particle characterization and fabrication data were compiled in several AGR program reports and publications (Kercher and Hunn 2006; Hunn and Lowden 2007; Hunn and Miller 2009; Kercher et al., 2011). The average dimensions of driver fuel particles and DTF particles are summarized in Table 1.

AGR-3/4 driver and DTF particles were over-coated with a precursor to graphitic matrix material and formed into cylindrical fuel compacts at ORNL. The compact graphitic matrix material is composed of multiple types of graphite and a carbonized phenolic resin. Compacts were nominally 12.3 mm in diameter and 12.5 mm long (in contrast to the AGR-1 and AGR-2 compacts, which were approximately 12.3 mm in diameter and 25 mm long). A summary of AGR-3/4 fuel compact properties is provided in the AGR-3/4 Final As-Run Report (Collin 2015a). Detailed characterization data of the as-fabricated compacts have been compiled in an AGR program report (Hunn, Trammel, and Montgomery 2011).

Each compact has a unique identifier denoting its position in the irradiation test train. In the X-Y compact naming convention, X denotes the capsule number, and Y denotes the level of the compact within the capsule (with level 1 at the bottom and level 4 at the top of the capsule). In AGR-3/4 there were four compacts per capsule. Thus, for example, Compact 3-3 is the third compact from the bottom of Capsule 3, and Compact 12-1 is the bottom compact from Capsule 12.
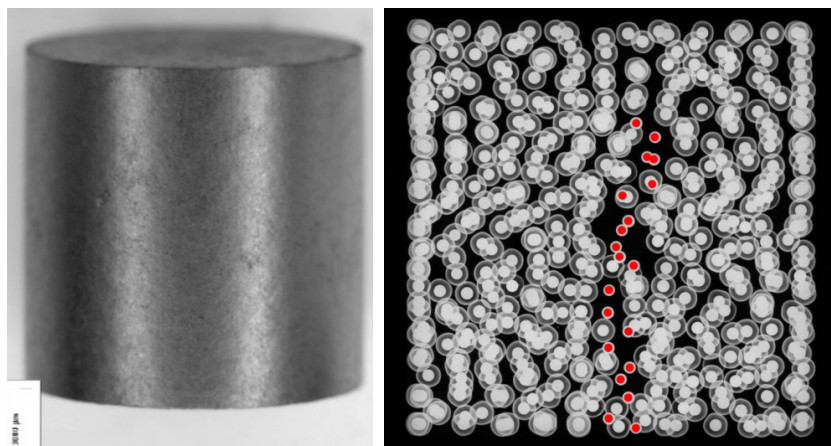
Figure 1. Image of an AGR-3/4 fuel compact (left) and x-radiograph of a 2.5-mm-thick section taken from the center of an AGR-3/4 compact (right) (Hunn, Trammell, and Montgomery 2011). DTF particles are highlighted with red dots in the x-ray image.

Table 1. As-fabricated particle dimensions and standard deviations from Table A-2 of the "AGR-3/4 Irradiation Test Final As-Run Report" (Collin 2015a).

DTF Particle Properties	
Kernel diameter (µm)	357.3 ± 10.5
DTF pyrocarbon thickness (µm)	20.0 ± 9
DTF particle overall diameter (µm)	400.0 ± 9.2
Driver Particle Properties	
Kernel diameter (µm)	357.3 ± 10.5
Buffer thickness (µm)	109.7 ± 7.7
IPyC thickness (µm)	40.4 ± 2.3
SiC thickness (µm)	33.5 ± 1.1
OPyC thickness (µm)	41.3 ± 2.1
Driver particle overall diameter (µm)	818.9 ± 14.2

2. SAMPLE SELECTION, EXPERIMENTAL PROCESSES, AND DATA PROCESSING

2.1. Past and Present RDLBL Samples

Table 2 lists the five compacts subjected to the radial deconsolidation leach-burn-leach (RDLBL) process at INL after heating in the Fuel Accident Condition Simulator (FACS) furnace. These compacts are the subject of this report. Some information on the ATR irradiation history of these compacts, the temperatures used during the FACS heating tests, and whether these compacts had been reirradiated in the Neutron Radiography (NRAD) reactor prior to FACS heating is also included. Table 3 summarizes the AGR-3/4 FACS-tested compacts that were sent to ORNL for RDLBL and reported previously. In addition to the FACS-tested compacts listed in Table 2 and Table 3, Table 4 lists the AGR-3/4 compacts that were analyzed via as-irradiated RDLBL: eight at INL and four at ORNL. As referenced in those tables, the results from these as-irradiated RDLBL exams (meaning compacts that were neither heated nor reirradiated) were reported previously. Preliminary results from only the as-irradiated FACS tests (meaning compacts tested in FACS without reirradiation) of Compacts 3-2, 10-2, and 10-4 were given previously by Stempien et al. (2018a), but the final results from the as-irradiated FACS tests of AGR-3/4 fuel compacts will be referenced in the discussions that follow (Stempien and Cai 2024b). Preliminary results from the reirradiation/FACS tests of Compacts 3-1, 8-1, and 10-1 were also given previously by Stempien et al. (2021b). A final report on the reirradiation/FACS tests will be prepared at a later date, which may require revisions to some of the results in this report.

Table 2. AGR-3/4 fuel compacts subjected to RDLBL at INL after heating in the FACS furnace. These are the subject of this report. The irradiation properties, FACS temperatures, and reirradiation statuses are also listed. The neutronic and thermal calculations were performed by Sterbentz (2015) and Hawkes (2016), respectively.

	Burnup (% FIMA[c])	Neutron Fluence (10^{25} n/m^2, E>0.18 MeV)	TAVA[d] Temp (°C)	TA[e] Min Temp (°C)	TA Peak Temp (°C)	FACS Temp (°C)	NRAD Reirradiation
1-2	5.91	1.66	941	910	971	1400	Yes
3-1	12.16	4.04	1138	1041	1214	1600	Yes
3-2	12.49	4.17	1196	1154	1240	1600 1700[a]	No
8-1	14.51	5.13	1165	1063	1242	1200[b]	Yes
8-2	14.58	5.11	1213	1171	1257	1400	No

a. After the initial isothermal hold at 1600°C for 300 h, the temperature was raised to 1700°C for 48 h.

b. Temperature held at 1200°C for about 300 h. Then three cycles between temperatures <200°C and 1200°C.

c. Fissions per initial metal atom.

d. Time-average volume-average.

e. Time-averaged.

Table 3. AGR-3/4 fuel compacts subjected to RDLBL at ORNL after heating in the FACS furnace. The irradiation properties, FACS temperatures, and reirradiation statuses are also listed. The results for Compacts 4-3, 10-1, and 10-2 were reported by Helmreich et al. (2022). The results for Compact 10-4 were reported by Hunn et al. (2020). The neutronic and thermal calculations were performed by Sterbentz (2015) and Hawkes (2016), respectively.

	Burnup (% FIMA)	Neutron Fluence (10^{25} n/m^2, E>0.18 MeV)	TAVA Temp (°C)	TA Min Temp (°C)	TA Peak Temp (°C)	FACS Temp (°C)	NRAD Reirradiation
4-3	14.29	4.89	1035	992	1084	1000	Yes
10-1	12.08	4.12	1172	1080	1238	1400	Yes
10-2	11.96	4.01	1213	1179	1249	1200	No
10-4	11.43	3.75	1168	1079	1231	1400	No

Table 4. AGR-3/4 fuel compacts subjected to as-irradiated RDLBL, their irradiation properties, and the reports discussing their results. The neutronic and thermal calculations were performed by Sterbentz (2015) and Hawkes (2016), respectively.

	Burnup (% FIMA)	Neutron Fluence (10^{25} n/m², E>0.18 MeV)	TAVA Temp (°C)	TA Min Temp (°C)	TA Peak Temp (°C)	RDLBL Lab	References
3-3	12.73	4.28	1205	1170	1242	INL	Stempien and Cai 2024a
5-3	14.92	5.22	1050	1001	1102		
5-4	14.98	5.23	989	858	1084		
7-3	15.00	5.27	1376	1335	1418		
8-3	14.54	5.07	1213	1171	1257		
10-3	11.75	3.89	1210	1174	1248		
12-1	5.87	1.8	849	802	883		
12-3	5.17	1.41	864	844	884		
1-4	6.85	2.10	929	866	972	ORNL	Hunn et al. 2020[a]
7-4	14.90	5.24	1319	1206	1397		Helmreich et al. 2021[a]
8-4	14.43	5.02	1169	1068	1242		
1-3	6.37	1.87	959	942	978		Helmreich et al. 2022[a]

a. Results from these studies were also discussed and compiled by Stempien and Cai (2024a).

2.2. FACS Testing and NRAD Reirradiations Before RDLBL

To enable assessments of short-lived fission product retention in the DTF particles, three of the five AGR-3/4 fuel compacts comprising this report (Compacts 1-2, 3-1, and 8-1) were reirradiated for 120 h in NRAD to generate short-lived isotopes such as I-131 ($t_{1/2}$ = 8.02 d) and Xe-133 ($t_{1/2}$ = 5.2 d) before FACS testing. Figure 2 shows a process diagram for these operations. Both FACS and NRAD are located at the Hot Fuels Examination Facility (HFEF), which enabled rapid transfer of the reirradiated fuel from NRAD to the precision gamma scanner (PGS) and FACS furnace. Compacts were reirradiated, one at a time, in aluminum holders in the C4SW position of the NRAD core. Table 5 summarizes the dates and times for NRAD start and stop and FACS start. NRAD was operated at full power (250 kW). Additional details on NRAD and the documentation specific to the compact reirradiations are available from Bess, Briggs, and Lell (2014) and Gleicher (2018), respectively. Gleicher also performed additional inventory calculations to account for the effects of reirradiation, which were most significant for nuclides with short half-lives. That work has not been reported as of yet. The reirradiated fuel compacts were retrieved from NRAD and gamma scanned via PGS before loading into the FACS furnace. Additionally, Compacts 1-2 and 8-1 were re-scanned on PGS after the FACS tests had finished. The FACS furnace's Fission Gas Monitoring System (FGMS) enabled measurement of the usual Kr-85 nuclide as well as the short-lived Xe-133 nuclide. The FACS furnace's condensation plates were used to quantify the I-131 released from the fuel. This required timely analysis of each condensation plate using the HFEF out-of-cell gamma system (HOGS). The other two compacts (Compacts 3-2 and 8-2) were tested in FACS without any NRAD exposure.
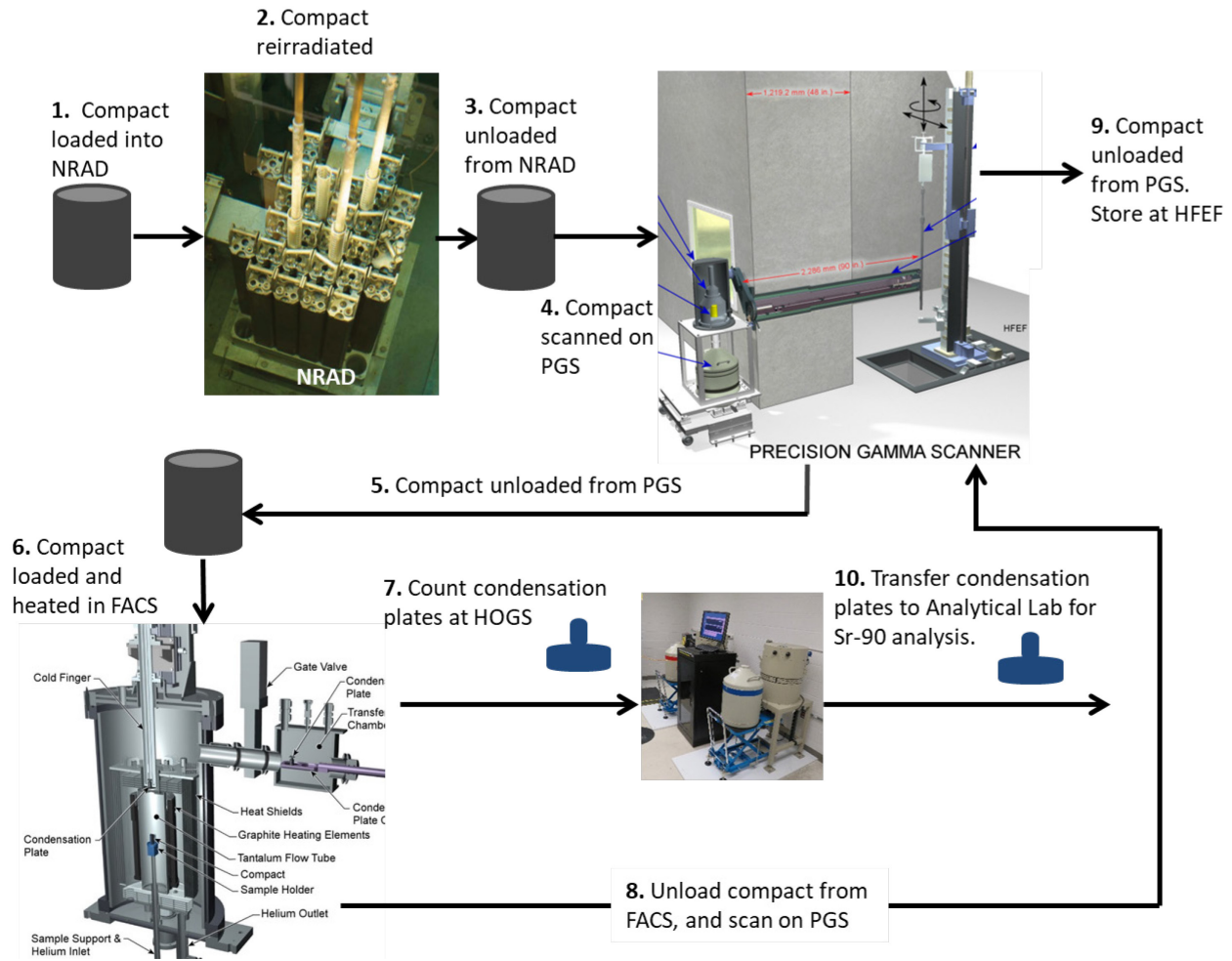
Figure 2. Flow chart of compact reirradiation in NRAD, gamma scanning via PGS, and heating in FACS.

Table 5. Summary of NRAD reirradiation dates and FACS start dates. Total reirradiation time is the time NRAD was at full power (250 kW). At the beginning, from initial reactor startup (at about 70 milliwatts of power) to full power was about 15-30 minutes.

Compact	FACS Test Temperature (°C)	Total Reirradiation Time (hrs)	NRAD Reirradiation Start Date	NRAD Reirradiation End Date	FACS Start Date	Additional Notes
3-1	1600	113.8	7/12/2019 8:38	7/17/2019 2:25	7/25/2019 8:00	
8-1	1200	120.0	9/4/2019 9:10	9/09/2019 9:05	9/17/2019 8:00	
10-1 [a]	1400	119.7	8/6/2019 8:00 [b]	8/11/2019 9:20	8/16/2019 8:00	
4-3 [a]	1000	120.0	7/12/2021 8:58	7/17/2021 8:58	7/23/2021 8:00	
1-2	1400	120.0	8/2/2021 18:31	8/7/2021 18:31	8/12/2021 8:00	Placed in storage rack Position K during Compact 4-3 reirradiation

a. RDLBL results reported in Helmreich et al. (2022).
b. Reirradiation was interrupted. First period ran from 8/6/2019 8:01 to 8/8/2019 7:45. Second period ran from 8/8/2019 9:20 to 8/11/2019 9:20.

Demkowicz et al. (2012) previously described the FACS furnace and its associated systems. In these tests, FACS was operated using the same processes described previously (Demkowicz et al. 2015a). A schematic of the furnace was shown in the bottom left of Figure 2. Figure 3 displays the furnace temperature profiles for all the AGR-3/4 FACS tests. The compacts that this report focuses on are plotted with dashed lines in Figure 3. Compared to AGR-1 FACS tests, the AGR-3/4 tests used an initial hold at 300°C (instead of 400°C) for two hours to drive off adsorbed moisture. Then, the AGR-3/4 FACS temperature program ramped from 300°C directly to the isothermal hold (1000, 1200, 1400, or 1600°C) over the course of 1.5 to 2 h depending on the specific isothermal hold temperature. In contrast, the AGR-1 and AGR-2 tests ramped from 400 to 1250°C over the course of 12 h, and this temperature was maintained for 12 h to allow the fuel to equilibrate at a typical irradiation temperature. Following that 12-h hold, the AGR-1 FACS tests ramped to 1600 or 1800°C at a rate of 50°C/h. The lower hold at 300°C, the elimination of the intermediate hold at 1250°C, and the use of faster ramps to the isothermal holds were chosen for these AGR-3/4 tests to minimize the time spent at temperatures other than the isothermal hold temperature. Given each compact started the test with the 20 DTF particles, the motivation was also to ensure that release of fission products retained in those kernels would still be observable at the hold temperature, as opposed to having been released during a gradual ramp or intermediate temperature hold.

The aforementioned condensation plates in the FACS furnace were suspended on a water-cooled cold finger to act as a comparatively cool surface for condensable fission products to deposit on. These plates were periodically exchanged throughout each test so they could be analyzed for gamma-emitting fission products (e.g., Cs-134, Cs-137, Eu-154, and I-131) and beta-emitting Sr-90. All FACS tests utilized a total flow of 1 L/min helium. This sweep gas carried any evolved fission gases from the fuel to the FGMS for collection and gamma counting. Preliminary results from the as-irradiated FACS tests of Compacts 3-2, 10-2, and 10-4 were presented by Stempien et al. (2018a), and a report including the results from those three compacts plus results from Compact 8-2 was recently completed by Stempien and Cai (2024b). Preliminary results from the NRAD/FACS tests of Compacts 3-1, 8-1, and 10-1 were presented by Stempien et al. (2021b). Those FACS and NRAD/FACS test results will be finalized and integrated with the RDLBL results in future reports.

As Figure 3 shows, some tests (Compact 1-2 and 8-1) were interrupted to repair parts of the FACS/FGMS systems, one test (Compact 3-2) had both 1600 and 1700°C holds, and one test (Compact 8-1) had several temperature cycles applied.

With relatively small amounts of fission products released from Compact 3-2 during the 1600°C hold, a decision was made to increase the temperature to 1700°C after 300 h at 1600°C had been acrued to see how much additional fission product release could be induced (Stempien and Cai 2024b). For Compact 8-1, 1200°C was maintained for 90 hours before a problem with the condensation plate exchanges forced an uncontrolled cooldown back to ambient temperature. The cold finger was repaired, and 1200°C was regained at a total elapsed time of 123 h. The test was terminated after a total of 305 h (including the downtime for repairs), and a total time of 272 h was spent at 1200°C. After allowing the system to cool to ambient temperature, three ramps from near ambient temperature up to 1200°C were performed to see if temperature cycling noticeably affected fission product release. Each ramp consisted of heating to 1200°C in 2 h, holding 1200°C for 24 h, cooling for 3 h, and then ramping back to 1200°C. As Figure 3 shows, the 1400°C test of AGR-3/4 Compact 1-2 was interrupted so the FGMS traps could be baked out. Because of this interruption, only about 250 h were spent at 1400°C.
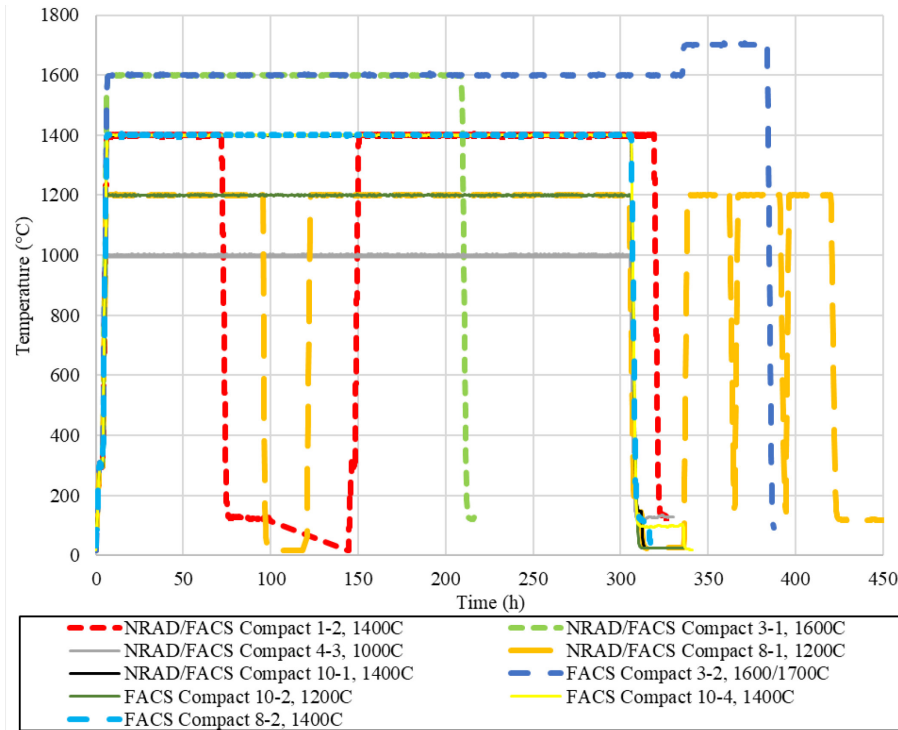
Figure 3. FACS test temperature histories for all AGR-3/4 compacts. The compacts that are the subject of this report are plotted with dashed lines. All others were reported previously.

2.3. Radial Deconsolidation-Leach-Burn-Leach

The traditional, single-step axial deconsolidation leach-burn-leach (DLBL) method has been detailed in various PIE reports (e.g., Hunn et al. 2013; Stempien 2020). The INL RDLBL process has been discussed by Stempien (2017) and Stempien and Cai (2024a). An abbreviated description will be given here.

The RDLBL process is a stepwise DLBL that uses multiple (typically three) radial deconsolidation steps and a final axial deconsolidation step (like the traditional DLBL process). In either process, the deconsolidation step electrolytically oxidizes and breaks down the compact graphitic matrix to liberate TRISO particles and matrix debris into the deconsolidation acid.

Figure 4 shows the first iteration of the radial-deconsolidation apparatus developed at INL that was installed in Cell 5 at the Analytical Laboratory (AL). One end of the compact was epoxied to one end of a 6-mm diameter, hollow stainless-steel shaft (referred to here as a "rod"). At the other end of the rod was a gear driven at 10 revolutions per minute by a direct current electric gearmotor. Nitric acid (concentration: 8M) was added to the beaker, which also filled the thimble through the porous frit in the bottom of the thimble and the holes toward the top. With a complete electrical circuit between the anode, cathode, compact, and nitric acid, contact between the compact and the anode screen helped remove deconsolidated matrix material, which together with TRISO particles fell to the bottom of the thimble. Material was removed in this fashion in three discrete steps. Each step of the electrolytic radial deconsolidation proceeded for a period of time (typically 15 to 20 minutes to remove approximately 0.5–1 mm of the compact diameter). Then, the deconsolidation solution was changed, and a new thimble was put in place. From each radial deconsolidation step, the solids were separated from the deconsolidation solutions, and each solution was analyzed for nuclides of interest using gamma-spectrometry, inductively coupled-plasma mass spectrometry (ICP-MS), and gas proportional counting.

8

The solids collected from each radial deconsolidation step were then leached twice in near-boiling nitric acid via a Soxhlet extractor, and those leachates were subjected to the same panel of radiochemical analyses. Following those two pre-burn leaches, the particles and matrix debris were oxidized ("burned") in air at 750°C. After the burn, the burn-back particles (particles with their OPyC layers removed) and any other remaining solids were leached twice in boiling nitric acid, and those leachates were analyzed.

When the epoxy holding the compact to the rod (and/or the deconsolidation rod itself) began to contact the anode screen, the compact itself was no longer in uniform contact with the anode screen, and the radial deconsolidation was halted. At this point, the core of the compact remained (Figure 5). This core was deconsolidated in a single axial step, and the remaining leach-burn-leach steps were followed as usual. Thirty TRISO particles from each of the three radial segments and the core were loaded into individual vials for gamma counting.

Whether the DLBL or RDLBL approach is used, actinides and fission products not contained within the boundary of normally retentive SiC layers are subject to dissolution in the DLBL leachates (contingent upon the individual fission-product solubilities and the ability of the acid to access their location). The dissolved actinides and fission products may include those that (a) had migrated through intact SiC coatings of the TRISO-coated driver particles, but were still retained within the compact, (b) were related to uranium contamination present in the compact matrix and/or OPyC at the time the compact was fabricated, (c) were externally introduced by contamination from sources present in the hot cell, (d) were from particles with compromised SiC (with or without the presences of concurrent compromised PyC coatings), (e) were retained in the DTF particles specific to AGR-3/4, and (f) migrated out of the DTF kernels and into the surrounding compact matrix. Combinations of two or more of these sources are common.

RDLBL has three benefits over a one-step axial deconsolidation. First, RDLBL enables measurements of the radial fission-product-concentration profile within a compact outside of the TRISO SiC layer. Second, RDLBL allows collection and analysis of particles from specific radial regions of a compact. Temperature gradients in compacts during irradiation may result in differences in fission-product retention between particles from different radial zones. It might be possible to observe such differences by separately analyzing the particles recovered from the different radial zones. Third, RDLBL allows radial segments of the compact to be removed without disturbing the DTF particles located approximately in the center of the compact. If failed DTF particles were deconsolidated along with other portions of the compact, the fission-product inventory of the OPyC and compact matrix would be difficult or impossible to distinguish from that still retained in the DTF fuel kernels.
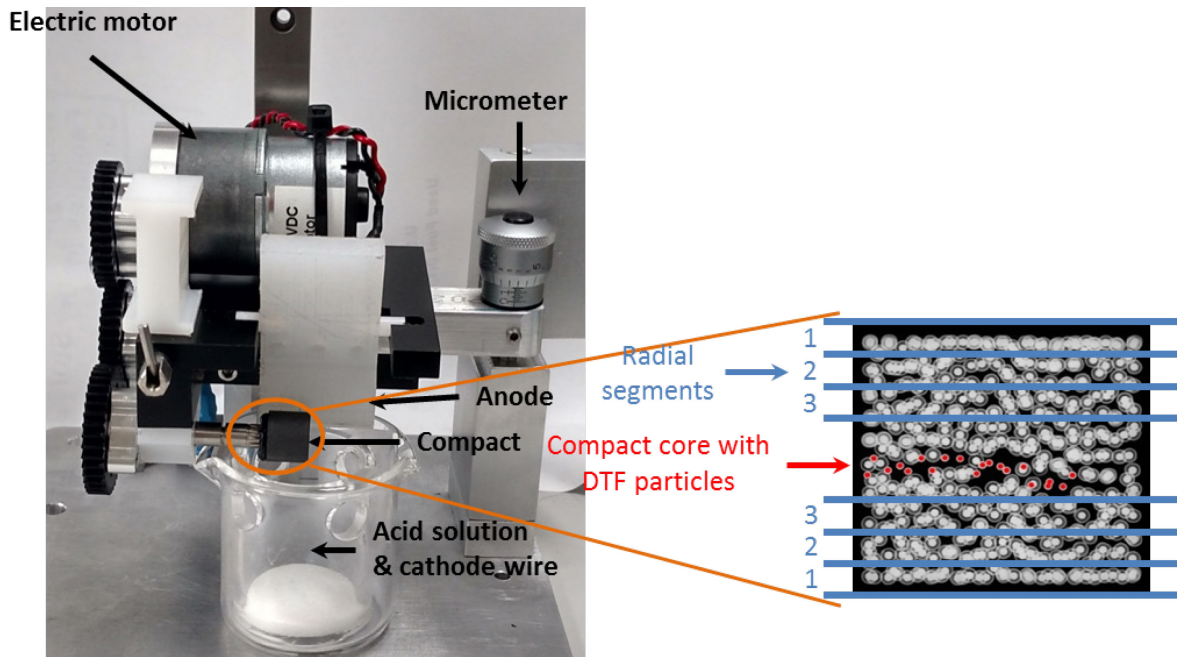
Figure 4. Radial deconsolidation apparatus and depiction of compact (x-ray image) indicating three radial segments and a central core with the DTF particles.
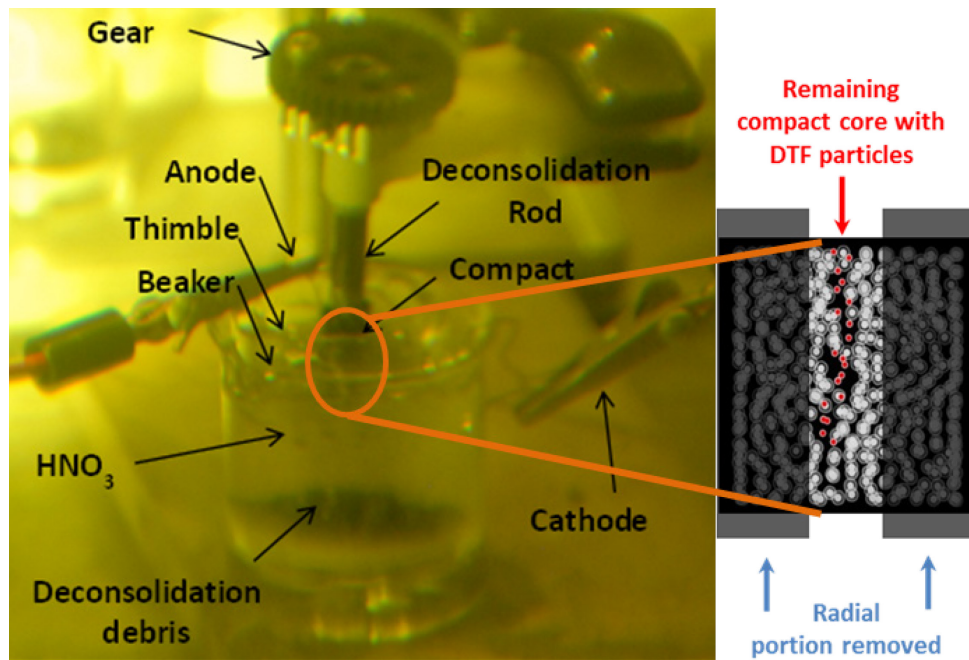
Figure 5. Axial deconsolidation (at left) of compact core remaining after radial deconsolidation. At right, x-ray of AGR-3/4 compact with depiction of core remaining after radial deconsolidation.

2.4. Compact Dimensional Measurements by Image Analysis

The main goals of the AGR-3/4 experiment were to study fission product transport in TRISO fuels and related materials, via the measurement of spatial variations in fission-product concentrations in compacts and graphite, and the derivation of new transport parameters for use in predictive models. To get concentration profiles in the fuel compacts, the fission-product content in multiple radial segments in the compacts was measured (using the processes described in Section 2.3), and the diameter of the compact must be known at the beginning of radial deconsolidation and at the end of each segment of radial deconsolidation (using the process briefly described in this section). The development work performed at ORNL produced a program called FrameGrabber (written in MATLAB) for measuring the diameter of a compact by analyzing video captured while the compact rotated (Helmreich et al. 2015). FrameGrabber was used during benchtop development work at INL; however, the program proved difficult to use with video captured through the hot-cell window at AL. FrameGrabber was rewritten by Helmreich, and the version dubbed FrameGrabber v11 has proven to be easier to use for analysis of video captured in the hot-cell environment.

To aid video collection, a circular polarizer was used in some instances to reduce reflections caused by the hot-cell windows or from liquid remaining on the compact after a deconsolidation step. Detailed instructions for setting up the deconsolidation apparatus, lighting, and digital camera to effectively capture videos of the rotating compact through the hot cell window were discussed previously (Stempien 2017). The use of FrameGrabber v11 to process the videos and measure the diameter of the compact at each step of the radial deconsolidation was discussed by Stempien (2017) and Stempien and Cai (2024a).

For each frame analyzed, FrameGrabber generates an image of that frame with overlays of the boundaries of the compact that it has determined and linear projections of the upper and lower edges and center of the deconsolidation rod. An example of a frame with the overlay and projections generated by FrameGrabber is given in Figure 6 for frame 31 of video file name "DSC_138" from Compact 3-1. The known diameter of the rod (6 mm) is used as a standard to determine the diameter of the compact. For a given frame, the outputted diameter is the average diameter along the length of the compact. FrameGrabber repeats this process for each specified frame of the video. Videos were typically 30 seconds long, meaning that five full rotations of the compact were captured. Ten frames per rotation (for a total of 50 frames) were then analyzed in FrameGrabber. Because the user-defined region around the rod and compact can vary slightly in size from one analysis to the next, the 50 frames were analyzed three different times. The diameters determined from the three different analyses of each of the 50 analyzed frames were averaged, and a standard deviation was determined from that population. Knowing the length of the compact from metrology (Stempien et al. 2016) and the compact diameter determined from this image analysis, the volume of the radial deconsolidation segment was calculated. This process was performed for videos taken prior to the start of radial deconsolidation and for videos taken at the end of each approximately 15 to 20-minute segment of radial deconsolidation.
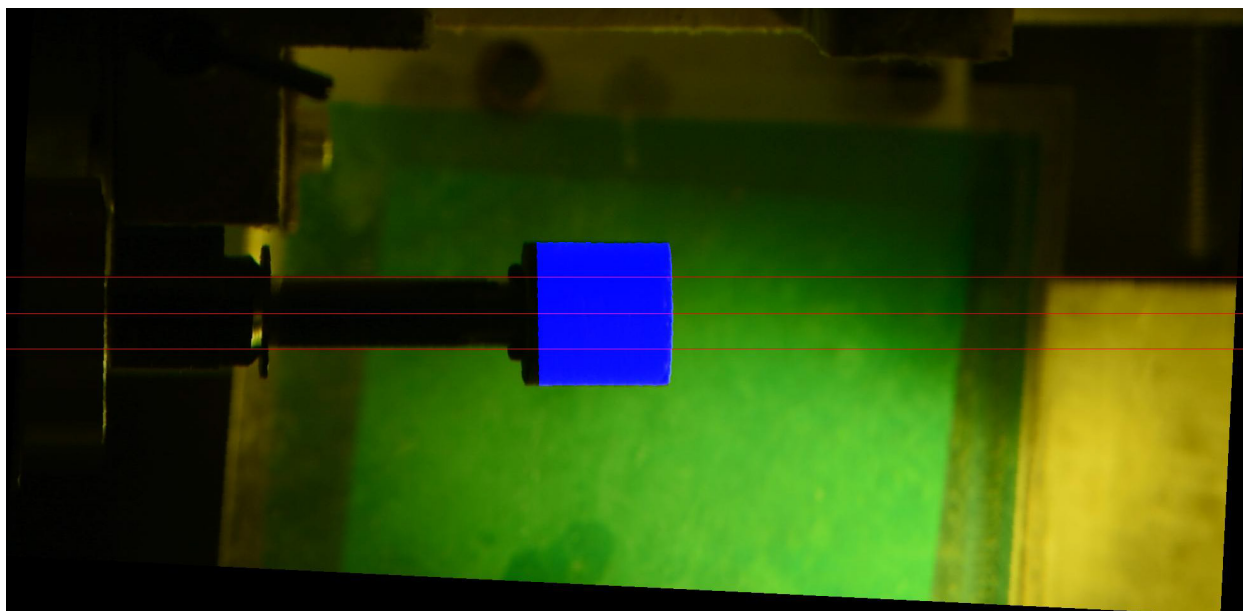
Figure 6. Blue shading shows the compact region determined by FrameGrabber for AGR-3/4 Compact 3-1. (Frame 31 from DSC_0138). Red lines denote deconsolidation rod center and upper and lower edges.

FrameGrabber has adjustments that can be made to tune the program for different lighting conditions. These adjustments are made using four variables called: "num_rod_thresh", "num_com_thresh", "keep_rod_thresh", and "keep_com_thresh". The variables num_rod_thresh and num_com_thresh set the number of segmentation thresholds (up to 20) that the user-defined boxed regions will be divided into based on the brightness of the green channel minus the red channel and the blue channel (Helmreich 2017). The second set of variables (keep_rod_thresh and keep_com_thresh) sets the number of the calculated thresholds (set by the first set of variables) that will be retained and used in the measurement. The second set of variables must be less than or equal to the values in the first set. In Table 6, the default values for these variables are summarized, along with other combinations of these variables that have produced reasonable results for videos taken through the hot cell window.

Table 6. Combinations of threshold variables used for analyses in FrameGrabber.

	v11 Default	v11e	v11h	v11j	v11k	v11t	v11w	v11x	v11y
num_rod_thresh	2	3	3	3	3	11	10	9	5
num_com_thresh	2	4	7	9	9	3	9	9	9
keep_rod_thresh	1	2	2	2	2	4	4	4	1
keep_com_thresh	1	2	3	3	4	2	3	3	3

2.5. Processing Radiochemical Results

RDLBL is used to measure gamma-emitting fission products, beta-emitting Sr-90, and actinides outside of the TRISO SiC layers. These measured quantities can then be compared to inventories determined via physics calculations to have been produced in the compacts during irradiation and reirradiation (if applicable).

For compacts not subjected to reirradiation in NRAD, all fission product activities measured in the RDLBL solutions (and in individual deconsolidated particles) were decay-corrected back to the end of the AGR-3/4 irradiation in ATR (end of irradiation [EOI], April 12, 2014 5:00 AM MST) plus one day (April 13, 2014 5:00 AM MST) using Equation (1).

$$A = A_o e^{-\lambda t} \tag{1}$$

where

A =   activity at time t

A_o =   activity at $t = 0$

λ =   decay constant ($\lambda = ln(2)/t_{1/2}$, and $t_{1/2}$ is the half-life).

Isotope half-lives were taken from the ENDF/B-VII.1 library. The uranium and plutonium nuclides measured via mass spectrometry were not decay-corrected, and their measured quantities were compared to the calculated inventories at EOI + 1 year. The reference time of EOI plus one year was selected to account for the appreciable production of some stable actinides of interest during the first year after the irradiation. After the first year, inventory changes in these nuclides were deemed insignificant (Hunn et al. 2013, Table 1). To compute the fraction of the compact inventory measured in the solutions (sometimes referred to as the measured-to-calculated ratio [M/C]), the measured fission product and uranium/plutonium values were divided by the inventories predicted by physics calculations to exist in the compacts at the reference times. ECAR-2753 (Sterbentz 2015) provided the calculated inventories of fission products and actinides for all AGR-3/4 compacts after the ATR irradiation. Values for selected isotopes are listed in Table 7 and Table 8 for Compacts 3-2 and 8-2.

Measured-to-calculated ratios were also computed for results from compacts that were reirradiated in NRAD prior to FACS testing and RDLBL. Short-lived fission product inventories were also calculated, but these could not be analyzed via RDLBL because they decayed away quickly. Therefore, the calculated values for those nuclides were not included here. Because Compacts 1-2, 3-1, and 8-1 were reirradiated in NRAD for 5 consecutive days, the fission product inventories were recalculated from ECAR-2753 (Sterbentz 2015) by Dr. Frederick Gleicher to account for additional fission in NRAD. The updated fission product inventories for reirradiated compacts were not formally documented at the time of this writing, but they are listed in Table 9 through Table 11, together with the actinide predictions from ECAR-2753 (Sterbentz 2015). Changes in the inventories of the actinide were evaluated, but the long half-life of these nuclides and the short reirradiation in NRAD with a low neutron fluence relative to the length of the ATR irradiation meant these changes were negligible. For example, the total (non-energy-resolved) neutron fluence for a 120-h reirradiation in the C4SW position in NRAD is 3.7E20 n/m^2. The AGR-3/4 compact with the lowest total fast-fluence (E>0.18 MeV) was Compact 1-2, at 1.7E25 n/m^2. Its total neutron fluence in ATR would be even higher.

For gamma-emitting nuclides, a minimum 3% two-sigma error was applied for all measurements; however, the reported error could be higher based on gamma-ray counting statistics. For beta-emitting Sr-90, a minimum of 2% error at two-sigma was applied; however, the reported error could have been higher due to counting statistics. Where multiple measurements were added together (for example, to sum the total Cs-134 measured from all the different RDLBL steps), the errors from the individual measurements were combined by adding them in quadrature. In instances where no activity was detected for a given nuclide, minimum detectable activities (MDAs) were reported. Like the measured activities, these MDAs were also decay-corrected and were denoted by "<". These MDAs were considered an upper bound on the activity of a given nuclide, but they were treated as zero (MDA = 0) any time activities were summed.

For the measurements made via ICP-MS, the uncertainty was estimated at AL using the GUM Workbench Pro Version 2.4.1.406 computer program. In samples where the uncertainty in the signal intensity was small, the uncertainties from the instrument calibration, sample weights, and dilutions dominated, and the estimated total uncertainty was reported as 5% at two-sigma. This value (5%) was the lowest reported uncertainty in any of the ICP-MS results from AL. For measurements where uncertainty in the signal intensity was greater than 5%, which occurred when the analyte concentration was low (closer to the instrument's detection limits), the uncertainty was rounded up to the nearest 10%. Where multiple measurements were added together (for example, to sum the total U-238 measured from all the different RDLBL steps), the errors from the individual measurements were combined by adding them in quadrature. In instances where a given analyte was not detected, a minimum detectable mass was reported. These were denoted by "<". These less-than values were considered an upper bound on the quantity of a given nuclide, but they were treated as zero anytime values from multiple RDLBL steps were summed.

Table 7. Inventories of fission products and actinides calculated to have been produced in Compact 3-2.

Isotope	Inventory (Bq) at AGR-3/4 EOI + 1 Day
Ag-110m	6.68E+07
Ce-144	9.54E+10
Cs-134	6.75E+09
Cs-137	6.27E+09
Eu-154	2.19E+08
Eu-155	1.48E+08
Ru-106	1.96E+10
Sb-125	4.83E+08
Sr-90	5.48E+09
Isotope	Inventory (g) at AGR-3/4 EOI + 1 Year
U-234	4.55E-04
U-235	3.19E-02
U-236	9.81E-03
U-238	3.43E-01
Pu-239	5.04E-03
Pu-240	1.75E-03

Table 8. Inventories of fission products and actinides calculated to have been produced in Compact 8-2.

Isotope	Inventory (Bq) at AGR-3/4 EOI + 1 Day
Ag-110m	1.08E+08
Ce-144	1.09E+11
Cs-134	9.46E+09
Cs-137	7.33E+09
Eu-154	2.95E+08
Eu-155	1.94E+08
Ru-106	2.54E+10
Sb-125	5.80E+08
Sr-90	6.29E+09
Isotope	Inventory (g) at AGR-3/4 EOI + 1 Year
U-234	4.22E-04
U-235	2.44E-02
U-236	1.08E-02
U-238	3.39E-01
Pu-239	5.01E-03
Pu-240	1.96E-03

Table 9. Inventories of fission products and actinides calculated to have been produced in reirradiated Compact 1-2.

Isotope	Inventory (Bq) at AGR-3/4 EOI + 1 Day*
Ag-110m	1.98E+04
Ce-144	3.34E+08
Cs-134	1.11E+08
Cs-137	2.50E+09
Eu-154	2.39E+07
Eu-155	1.77E+07
Ru-106	6.96E+07
Sb-125	2.01E+08
Sr-90	2.31E+09
Isotope	Inventory (g) at AGR-3/4 EOI + 1 Year**
U-234	5.55E-04
U-235	5.93E-02
U-236	5.58E-03
U-238	3.53E-01
Pu-239	3.68E-03
Pu-240	6.69E-04

∗ Fission products from calculation by Gleicher in August 2024 to account for production of these isotopes from reirradiation in NRAD. These are the inventories at the end of the NRAD reirradiation after decay-correcting them to the end of the ATR irradiation plus 1 day.

∗∗ All actinides were from ECAR-2753, which accounts only for the initial irradiation in ATR.

Table 10. Inventories of fission products and actinides calculated to have been produced in reirradiated Compact 3-1.

Isotope	Inventory (Bq) at AGR-3/4 EOI + 1 Day*
Ag-110m	7.30E+07
Ce-144	1.09E+11
Cs-134	6.32E+09
Cs-137	6.11E+09
Eu-154	2.09E+08
Eu-155	1.48E+08
Ru-106	1.95E+10
Sb-125	4.81E+08
Sr-90	5.36E+09
Isotope	Inventory (g) at AGR-3/4 EOI + 1 Year**
U-234	4.60E-04
U-235	3.33E-02
U-236	9.62E-03
U-238	3.43E-01
Pu-239	5.27E-03
Pu-240	1.75E-03

* Fission product inventories from calculation by Gleicher to account for reirradiation in NRAD. These are the calculated inventories at the end of the NRAD reirradiation after decay-correcting them to the end of the ATR irradiation plus 1 day.

** All actinides were from ECAR-2753 which accounts only for the initial irradiation in ATR.

Table 11. Inventories of fission products and actinides calculated to have been produced in reirradiated Compact 8-1.

Isotope	Inventory (Bq) at AGR-3/4 EOI + 1 Day*
Ag-110m	1.26E+08
Ce-144	1.24E+11
Cs-134	9.21E+09
Cs-137	7.29E+09
Eu-154	2.91E+08
Eu-155	2.00E+08
Ru-106	2.59E+10
Sb-125	5.93E+08
Sr-90	6.26E+09
Isotope	Inventory (g) at AGR-3/4 EOI + 1 Year**
U-234	4.60E-04
U-235	3.33E-02
U-236	9.62E-03
U-238	3.43E-01
Pu-239	5.27E-03
Pu-240	1.75E-03

* Fission product inventories from calculation by Gleicher to account for reirradiation in NRAD. These are the calculated inventories at the end of the NRAD reirradiation after decay-correcting them to the end of the ATR irradiation plus 1 day.

** All actinides were from ECAR-2753 which accounts only for the initial irradiation in ATR.

3. DIMENSIONAL RESULTS FROM COMPACT RADIAL DECONSOLIDATIONS

The compact dimensions were obtained via the analysis of videos taken before and after the deconsolidation of each radial segment of a compact, as described in Section 2.4. In prior work on eight as-irradiated compacts, the pre-deconsolidation diameters determined via contact metrology matched well with the pre-deconsolidation diameters determined from video analyses. For those compacts, +3.5% was the maximum video-based bias, and the rest of the video-based diameters were within ±1.2% of the contact metrology results (Stempien and Cai 2024a). There was no consistent direction to the bias from the video analyses in that study. Here, Table 12 compares the pre-deconsolidation diameters determined via contact metrology (Stempien et al. 2016) to the pre-deconsolidation diameters determined from video analyses of the five compacts in this report. For Compact 8-1, the pre-deconsolidation diameter determined from the video analysis was 5% larger than that from contact metrology. The other compacts had diameter biases ranging from −0.08 to +1.79%. Note that contact metrology was performed on the compacts in the as-irradiated state, but the video analyses were performed after FACS testing. As was the case in the RDLBL study of as-irradiated compacts (Stempien and Cai 2024a), here there is no consistent bias in the pre-deconsolidation diameters, and no attempts were made to adjust the results for a bias.

The bias is potentially inconsistent for the same compact at various points in the radial deconsolidation process as well. The camera and lighting had to be moved out of the way in between every radial segment to allow the hot-cell operator to position the glassware, electrodes, and compact, and recover the thimble and deconsolidation solutions. While all attempts were made to set up the lighting in a consistent manner, variations were noticeable when it came time to process the videos, and FrameGrabber parameters (see Table 6) were frequently adjusted from one radial segment to another. Additionally, the compact surface was moist in between each segment, which increased the reflectivity of the compact, and adjustments to the camera and lighting setup were used to reduce light reflection from the compact.

There is another source of uncertainty in the dimensional analyses. In prior trials with unirradiated compacts, it was observed that the first 2 minutes of a radial deconsolidation can cause the compact diameter to increase by up to 0.4 mm, and a reduction in volume may not be apparent for at least the first 4 minutes (Helmreich 2015). That observation was made by taking video during the entire deconsolidation of unirradiated compacts in a clean (non-radioactive) laboratory environment. In the hot cell environment, it was impossible to collect video suitable for analysis while the deconsolidation progressed. Thus, whether this effect occurred or the extent of this kind of effect could not be determined for the irradiated fuel compacts.

Table 12. Comparison of compact as-irradiated diameter measured by contact metrology and post-FACS diameter measured by video analysis via FrameGrabber.

Compact	Diameter before deconsolidation		Video bias	
	Contact metrology (mm)	Video analysis (mm)	(mm)	(%)
3-2	12.129 ± 0.01	12.119 ± 0.235	-0.010	-0.08%
8-2	12.138 ± 0.006	12.355 ± 0.07	0.217	1.79%
1-2	12.230 ± 0.01	12.115 ± 0.10	-0.115	-0.94%
3-1	12.135 ± 0.02	12.016 ± 0.11	-0.119	-0.98%
8-1	12.142 ± 0.00	12.750 ± 0.16	0.608	5.01%

3.1. Compact 3-2

Compact 3-2 had an as-irradiated diameter of 12.129 mm ± 0.01 mm (Stempien et al. 2016). The diameter before deconsolidation measured by image analysis was 12.119 ± 0.235 mm. Though the result from image analysis had higher standard deviations, the two methods were consistent. After

deconsolidating Segment 1 and collecting video of the rotating compact, the compact accidentally scraped against a white plastic piece of the deconsolidation apparatus. Some dust came off the plastic part and some may have come from the compact itself, but it was unclear if any particles were lost or broken. The compact fell off the rod about 12 minutes into the second segment radial deconsolidation. Figure 7 shows the photos taken after the compact separated from the rod. There was no obvious visual damage on the compact. The compact was re-attached and the videos for the second segment were taken. The third segment deconsolidation went as planned, and the videos were taken afterwards. Figure 8 shows examples of image analysis from videos after each of the three segments had been deconsolidated. Table 13 summarizes the dimensions and volumes of the compact after each segment of the deconsolidation process.
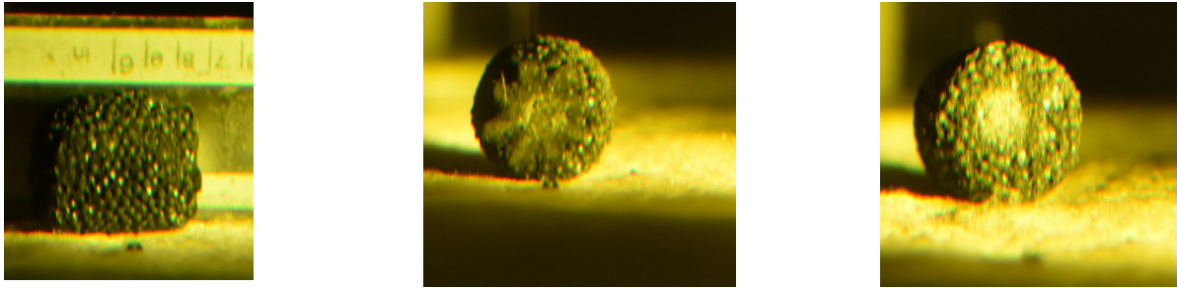
Figure 7. Photos of Compact 3-2 after it fell off the rod during deconsolidation of the second radial segment.
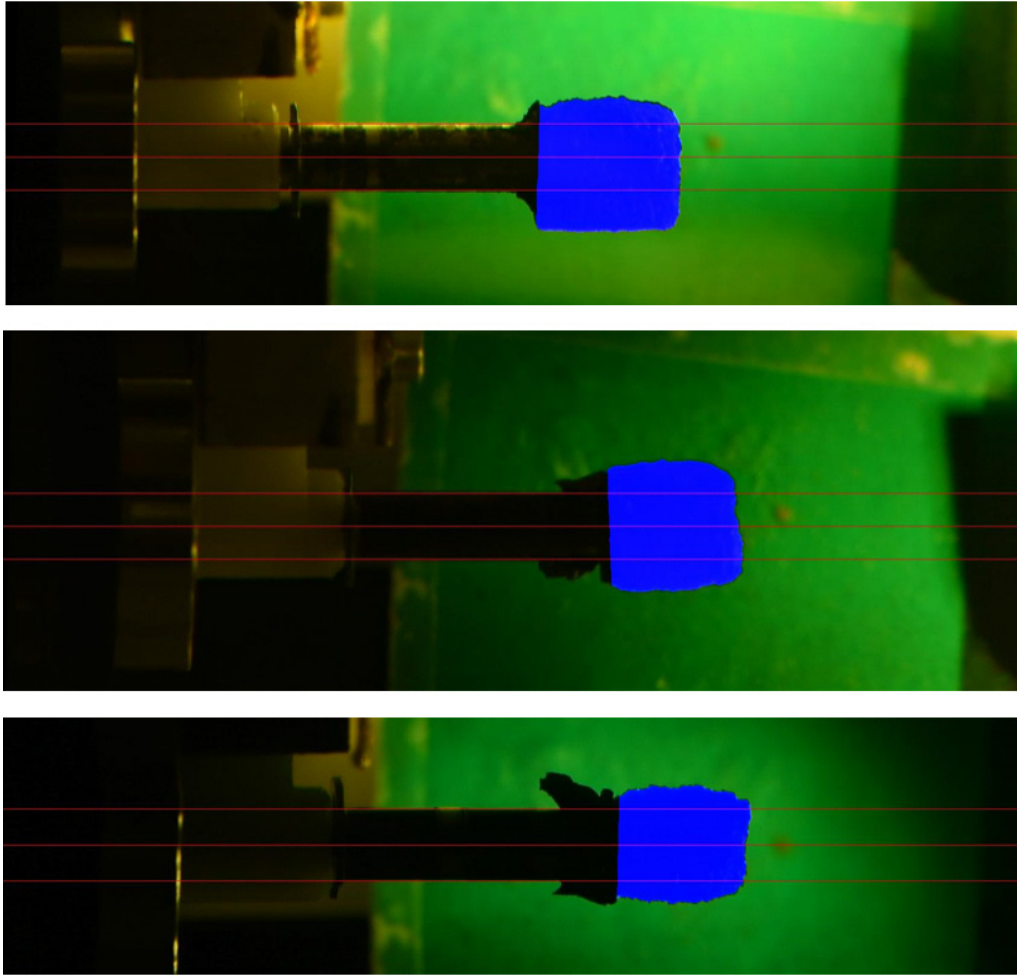
Figure 8. Examples of frames from videos after the first (top), second (middle), and third (bottom) radial segments had been deconsolidated from Compact 3-2.

Table 13. Summary of diameters and volumes of the radial segments of Compact 3-2. The volume of the core remaining after the three segments of radial deconsolidation is also given.

	Segment 1	Segment 2	Segment 3	Core
Radial Deconsolidation Time (min)	21	12	24	—
Diameter Reduction (mm)	0.431	0.463	1.938	—
New Diameter (mm)	11.688	11.225	9.287	—
New Diameter Std Dev	0.300	0.101	0.082	—
Segment Volume (mm3)	99.891	103.297	387.016	839.603
Segment Volume Std Dev	87.944	71.717	26.656	14.881

3.2. Compact 8-2

Compact 8-2 had an as-irradiated diameter of 12.138 mm ± 0.006 mm (Stempien et al. 2016). The diameter before deconsolidation measured using video analysis was 12.355 ± 0.07 mm. The first segment deconsolidation took about 25 minutes. There was initially some uneven removal of material from the compact, but it improved for the last few minutes of the Segment 1 radial deconsolidation. Figure 9 (top) shows an example of a frame analyzed from the video taken after the Segment 1 deconsolidation. In this particular orientation, the top of the compact has an uneven silhouette compared to the bottom. This is evidence of the uneven removal of material during the Segment 1 deconsolidation. Frames from the analysis after the second and third segments had been deconsolidated are shown in the middle and bottom of Figure 9, respectively. The bottom image shows how the compact necks down at the epoxy-compact bond interface. Out of concern that the compact would fall from the deconsolidation rod, the third segment radial deconsolidation was halted as the compact diameter at the epoxy-compact bond was reduced and comparable to the rod diameter. Table 14 summarizes the dimensions and volumes of the compact at each segment of the deconsolidation process.
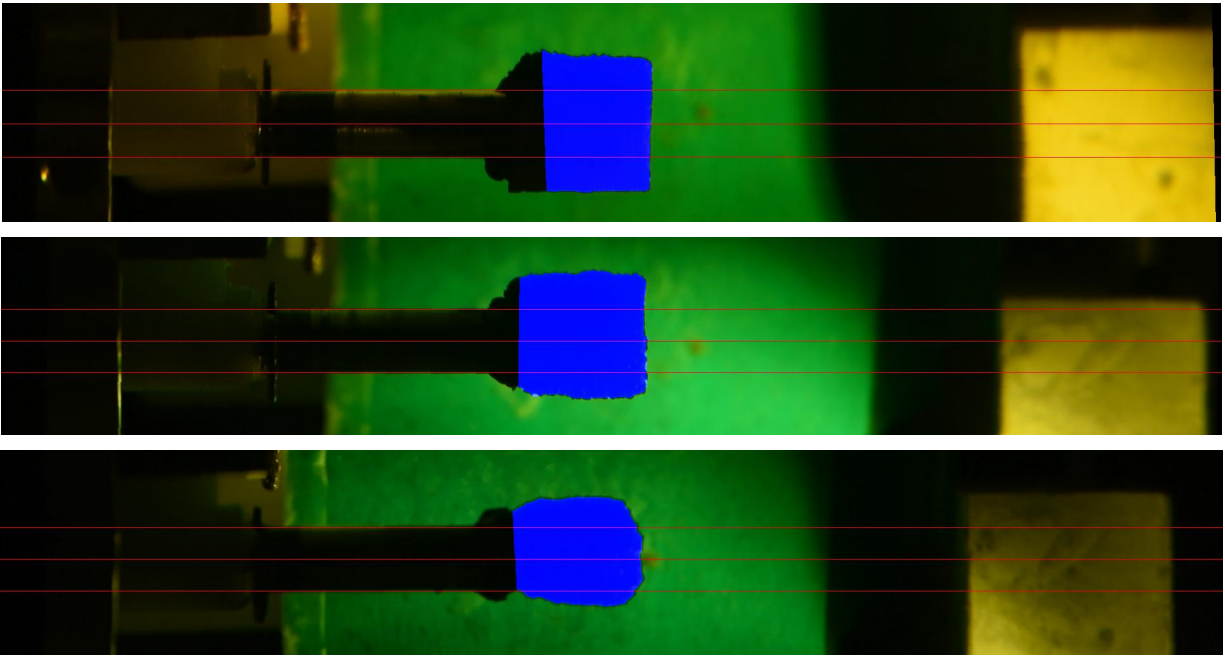
Figure 9. Examples of image analysis from videos after first (top), second (middle), and third (bottom) deconsolidation for Compact 8-2.

Table 14. Summary of Compact 8-2 diameter change, new diameter after each segment of deconsolidation, and the volume of the compact material removed. The volume of the core remaining after the three segments of radial deconsolidation is also given.

Compact 8-2	Segment 1	Segment 2	Segment 3	Core
Deconsolidation Time (min)	25	16	18	—
Diameter Reduction (mm)	0.29	0.43	1.88	—
New Diameter (mm)	12.085	11.655	9.773	—
New Diameter Std Dev	0.117	0.150	0.159	—
Segment Volume (mm3)	64.65	100.02	394.89	935.57
Segment Volume Std Dev	32.33	44.06	45.90	30.52

3.3. Compact 1-2

Compact 1-2 had an as-irradiated diameter of 12.230 ± 0.01 mm (Stempien et al. 2016). To promote more complete epoxy curing, the compact was epoxied to the deconsolidation rod and the assembly was heated at 50°C for 1 h. The pre-deconsolidation diameter from image analysis was 12.115 ± 0.10 mm. This compact was reirradiated at NRAD before being tested at 1400°C in FACS, and the video-based, pre-deconsolidation diameter was determined after those steps had been taken.

With the goal of trying to better preserve the epoxy bond between the compact and the rod, Compacts 1-2, 3-1, and 8-1, were deconsolidated in 6M HNO_3, rather than the 8M HNO_3 used in all the other radial deconsolidations done at INL. The first segment of deconsolidation took about 34 minutes. However, the average diameter from image analysis was 12.123 ± 0.15 mm. This indicates no change in diameter. Comparing images from before (Figure 10a) and after the first segment of deconsolidation (Figure 10b), it was clear that the compact surface was rougher after 34 minutes of deconsolidation. Furthermore, deconsolidated material was collected in the thimble; therefore, material was certainly being removed during this time, despite there being no apparent change in the compact diameter. There was a similar situation during RDLBL of as-irradiated AGR-3/4 Compact 8-3, where the video analysis indicated the diameter after the first segment of deconsolidation increased by 0.17 mm (Stempien and Cai 2024a). Here, because the volume of material removed during the Compact 1-2 Segment 1 deconsolidation could not be determined, the radionuclide contents measured in Segments 1 and 2 were combined, and the volume associated with that material was the difference between the pre-deconsolidation volume and the compact volume after Segment 2 had been deconsolidated.

Figure 10c and d show examples of the image analysis from the videos taken after the second and third radial deconsolidation steps. Some uneven removal of material was observed, and the final shape after three radial deconsolidation steps was like a conical frustum. The third segment of radial deconsolidation was halted, as the compact/screen contact was inconsistent and the compact necked down toward its attachment to the deconsolidation rod. Table 15 summarizes the deconsolidation time as well as dimensions and volumes of the compact at each segment of the deconsolidation process.
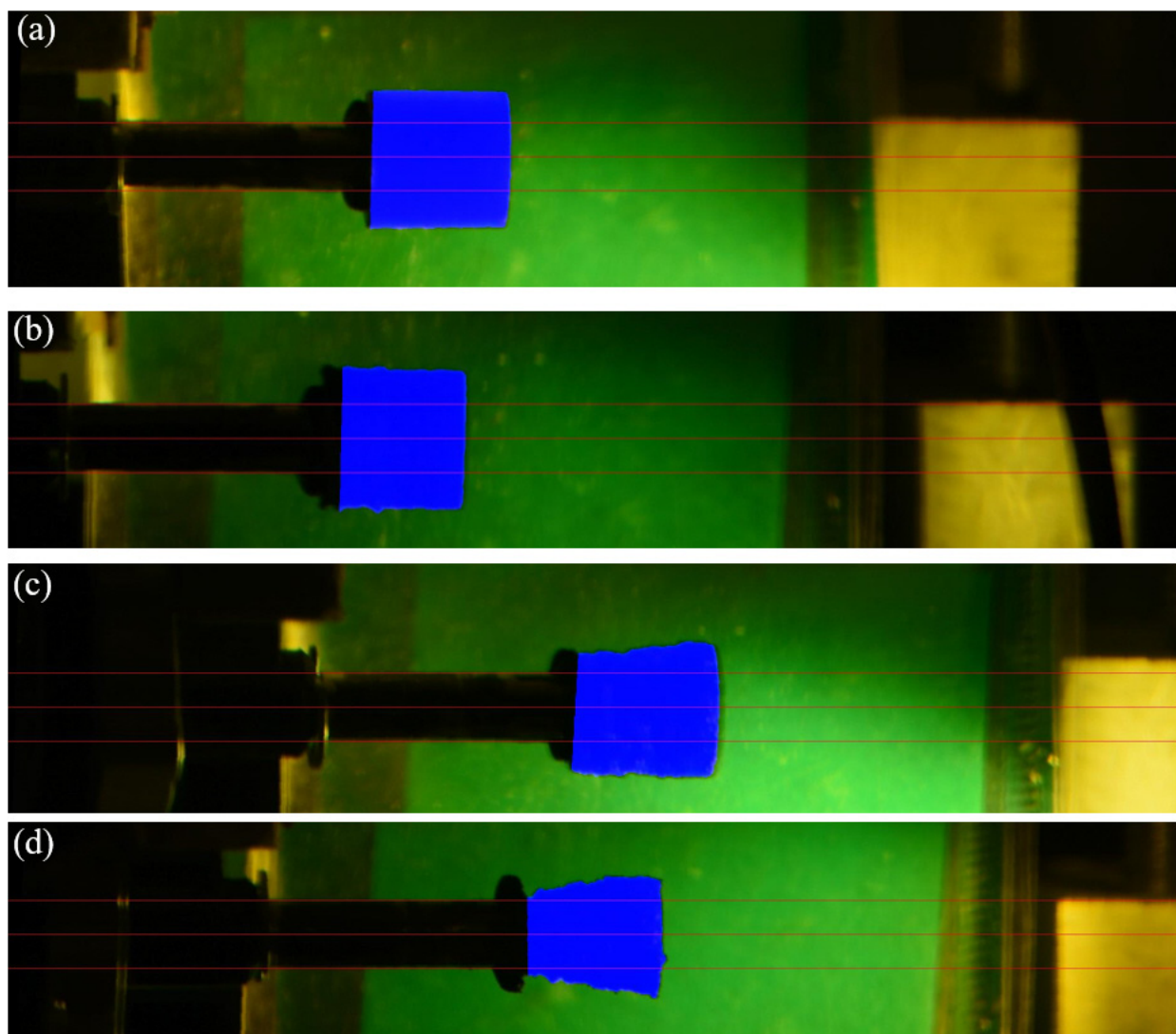
Figure 10. Examples of the image analysis of frames from videos taken before deconsolidation (a) after Segment 1 (b), after Segment 2 (c), and after Segment 3 (d) for Compact 1-2.

Table 15. Summary of Compact 1-2 diameter change, new diameter after a segment of deconsolidation, and the volume of the compact material removed. The volume of the core remaining after the three radial deconsolidation steps is also given.

Compact 1-2	Segment 1 + Segment 2		Segment 3	Core
Radial Deconsolidation Time (min)	34	74	35	—
Diameter Reduction (mm)	1.008		1.255	—
Diameter Reduction Std Dev (± mm)	0.137		0.180	—
New Diameter (mm)	11.108		9.852	—
New Diameter Std Dev (± mm)	0.097		0.151	—
Segment Volume (mm3)	228.288		256.706	946.859
Segment Volume Std Dev (± mm3)	31.116		35.849	29.081

3.4. Compact 3-1

Compact 3-1 was epoxied to the rod three times before radial deconsolidation began. After initially bonding the compact and rod, the assembly was put in a furnace to aid complete epoxy curing. This was done to make accidental debonding less likely during radial deconsolidation. The intended cure temperature was 50°C, but the furnace accidentally went to 700°C for about 20 minutes. As a result, the epoxy was oxidized away. The compact was visually checked, and there was no apparent damage from this incident. This compact was re-epoxied to the rod, and then it again came loose from an accident during handling. The compact was epoxied a third time (as seen in Figure 11). There were some minor scratches on the compact surface, which was not uncommon. However, some chips around the rim of the compact may have been substantial enough to expose some TRISO particles. These are especially visible at the right side of the compact in the photographs shown in Figure 11. To try to better preserve the epoxy bond between the compact and the rod, Compacts 1-2, 3-1, and 8-1 were deconsolidated in 6M HNO_3, rather than the 8M HNO_3 used in all the other radial deconsolidations at INL.

At the start of the first-segment deconsolidation, fines were generated very quickly, which could be a consequence of the accidental exposure at 700°C for about 20 minutes after the first epoxy attempt. It was observed that about half of the compact deconsolidated more rapidly than the other half. After 31 minutes, the electrical continuity was intermittently lost when the compact rotated along the portion that had the most rapid material removal. The process was continued for an additional 13 minutes to give the process a chance to even out the compact. Then, the deconsolidation was stopped for about 3 minutes to add acid. The process ran for an additional 5 minutes, and then the first radial segment of deconsolidation was halted. Figure 12 shows an example from the image analysis following completion of the first radial segment.

The second-segment deconsolidation lasted about 12 minutes before the compact fell off the rod. Uneven material removal was noted during this period as well. Figure 13 shows the detached compact and some of its matrix and particles apparently still bonded to the rod. To enable image analysis of the remaining compact diameter, the compact was placed on a beaker and roughly aligned with the rod while video of the stationary (non-rotating) compact was recorded. A frame from one of these videos is shown in Figure 14. A reflection of the compact on the beaker made it difficult for FrameGrabber to distinguish between the compact edge and the background. Figure 14 shows where a thin, light-blue layer between the compact and beaker was incorrectly identified by FrameGrabber as a part of the compact. The standard deviation of the final diameter was large compared to Compacts 3-2 and 8-2. Table 16 summarizes the dimensions and volumes of the compact at each segment of the deconsolidation process.
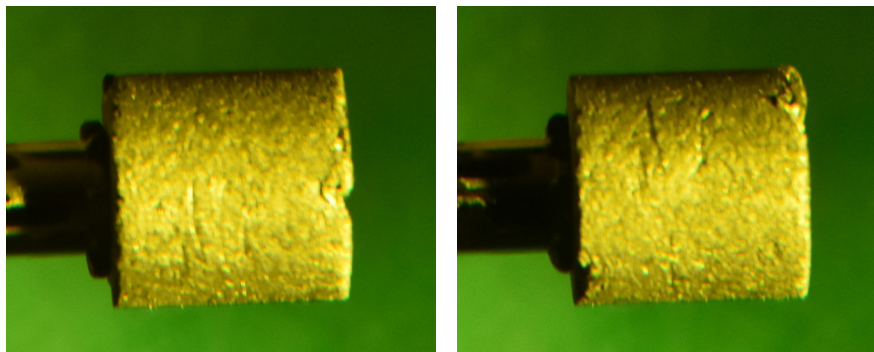
Figure 11. Two images (at two rotational angles to the camera) of Compact 3-1 before deconsolidation.

Figure 12. Analyzed frame from video taken after the first-segment radial deconsolidation was complete.
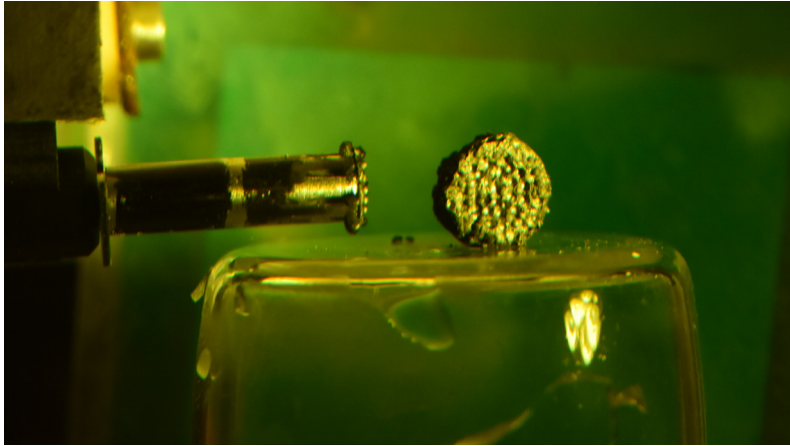
Figure 13. Compact 3-1 fell off the rod during the second radial deconsolidation step.
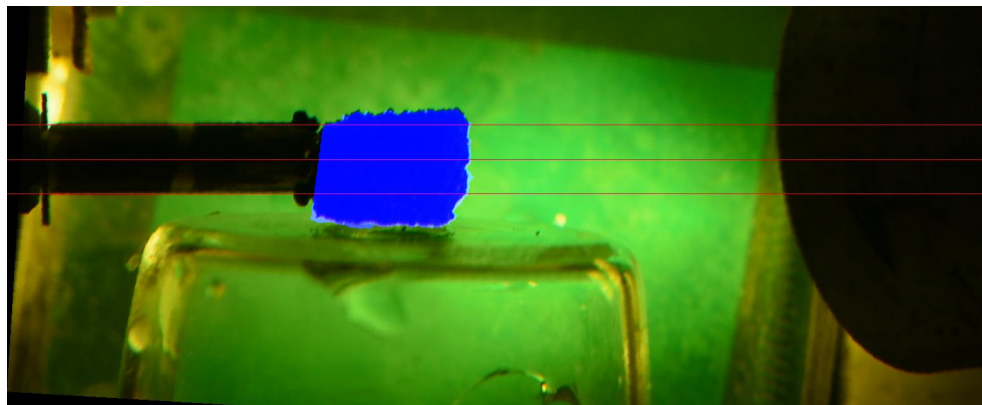
Figure 14. Example of image analysis from a video taken after the second-segment deconsolidation.

Table 16. Summary of Compact 3-1 diameter change, new diameter after a segment of deconsolidation, volume of the compact material removed, and the volume of the core remaining after the three segments of radial deconsolidation.

Compact 3-1	Segment 1	Segment 2	Core
Deconsolidation Time (min)	47	12	—
Diameter Reduction (mm)	0.613	1.359	—
New Diameter (mm)	11.403	10.044	—
New Diameter Std Dev	0.504	0.441	—
Segment Volume (mm^3)	139.8	284.1	983.2
Segment Volume Std Dev	114.8	141.5	86.4

3.5. Compact 8-1

The first-segment deconsolidation of Compact 8-1 took about 120 minutes because the rate of material removal was relatively slow for unknown reasons. To attempt to better preserve the epoxy bond between the compact and the rod, Compacts 1-2, 3-1, and 8-1 were deconsolidated in 6M HNO_3, rather than the 8M HNO_3 used in all the other radial deconsolidations at INL. Slower deconsolidation rates were not noted for Compacts 1-2 and 3-1. Thus, the slower deconsolidation rate for Compact 8-1 Segment 1 is not necessarily related to the acid concentration. After 39 minutes, the process was stopped to adjust the screen, and then the deconsolidation resumed. Uneven removal of material was observed, and the final shape of the compact resembled a conical frustum (see the top image in Figure 15). The second-segment deconsolidation took about 27 minutes because the material removal appeared to be faster than during the first segment. The middle image in Figure 15 is an example of image analysis following the second-segment deconsolidation. The third deconsolidation was halted after about 23 minutes, when pronounced necking of the compact diameter occurred at its bond to the rod (see the bottom image in Figure 15). It is not clear why the compacts in this study experienced this necking phenomenon more than as-irradiated compacts in Stempien and Cai (2024a). Figure 16 summarizes the dimensions and volumes of the compact at each segment of the deconsolidation process.
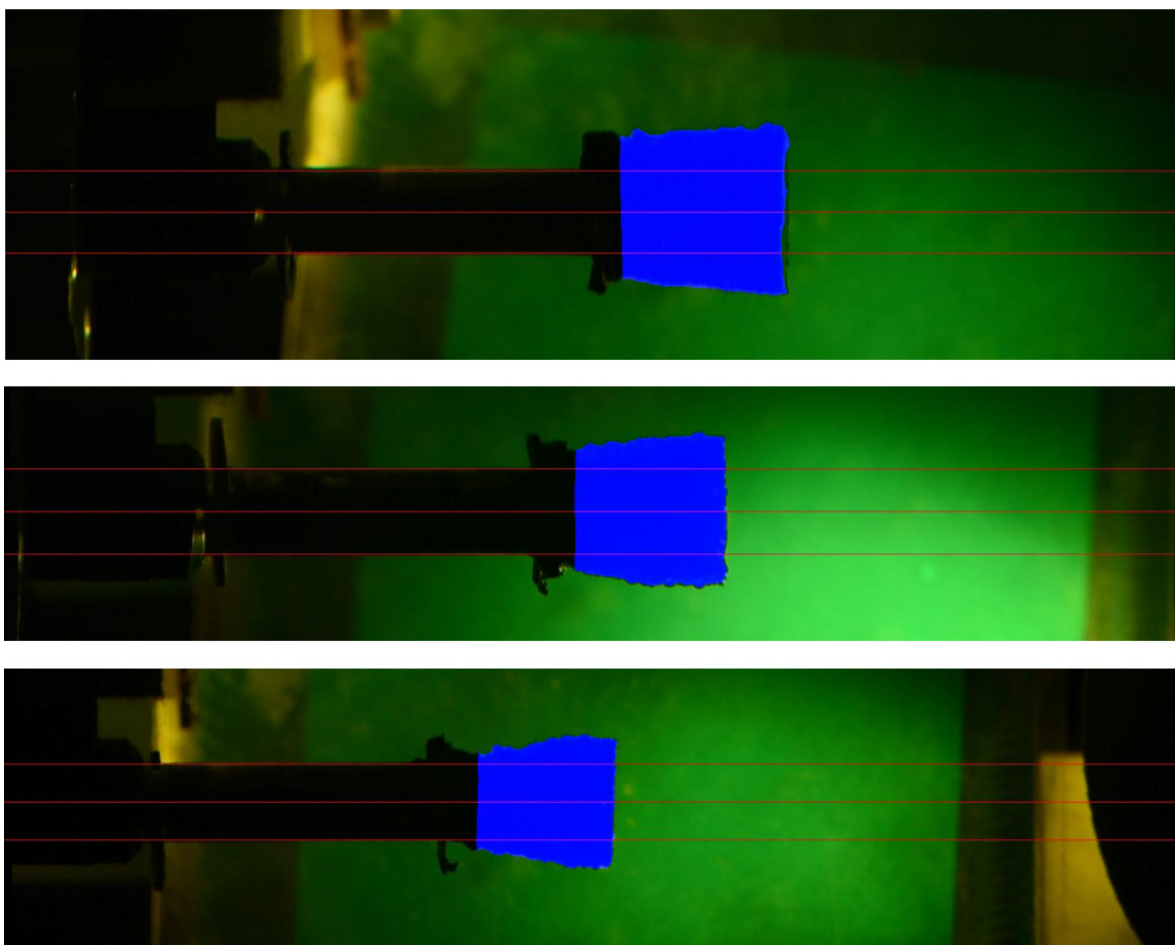
Figure 15. Examples of video frames analyzed after first (top), second (middle), and third (bottom) segments of radial deconsolidation for Compact 8-1

Table 17. Summary of Compact 8-1 diameters and volumes.

Compact 8-1	Segment 1	Segment 2	Segment 3	Core
Deconsolidation Time (min)	120	27	23	—
Diameter Reduction (mm)	1.089	1.616	0.418	—
New Diameter (mm)	11.661	10.045	9.627	—
New Diameter Std Dev	0.137	0.149	0.084	—
Segment Volume (mm^3)	261	344	81	910
Segment Volume Std Dev	51	43	33	16

4. RESULTS FROM RDLBL SOLUTIONS ANALYSES

Radial deconsolidation generates a deconsolidation solution, two pre-burn leach solutions, and two post-burn leach solutions for each radial segment and the compact core that remains after the radial segments have been taken. Each of these solutions was analyzed by gamma spectrometry, strontium separation and gas proportional counting, and ICP-MS. Triplicate analyses of each solution were typically (though not always) performed. For each segment or core, a separate blank sample was measured to monitor any possible contamination. Aside from the RDLBL solutions, 30 TRISO-coated driver particles from each segment of a radial deconsolidation from each compact were picked at random and gamma counted. Those results are not included in this report, but they will be the subject of a future report.

To reiterate what was stated earlier in Section 2.3: the actinides and fission products quantified via RDLBL include those that (a) had migrated through intact SiC coatings of the TRISO-coated driver particles, but were still retained within the compact, (b) were related to uranium contamination present in the compact matrix and/or OPyC at the time the compact was fabricated, (c) were externally introduced by contamination from sources present in the hot cell, (d) were from TRISO-coated driver particles with compromised SiC (with or without the presences of concurrent compromised PyC coatings), (e) were retained in the DTF particles specific to AGR-3/4, and (f) migrated out of the DTF kernels and into the surrounding compact matrix.

To investigate the migration of fission products that originated in the DTF particles, corrections will be applied to exclude the effects of damaged driver particles, if there are indications that there are any such particles. Potential sources of damaged driver particles include in-pile failure, as-fabricated defects, and those accidentally damaged by the RDLBL process. When appropriate, the corrections will be based on the assumption that very little uranium or cerium leaves the DTF kernels, which were aligned approximately along the compact radial centerline and will be a part of the compact "core" inventory, determined after the radial segments have been analyzed. Generally, a determination on the number of damaged driver particles f (an integer) was made based on the quantities of U and Ce, and at what point in the RDLBL process these quantities were detected. In some cases, other nuclides were also considered in the enumeration of damaged driver particles. If the inventory i of a given nuclide in the step of the process that was found to have damaged driver particles was $\geq f$ particle equivalents, f particle equivalents were subtracted from that inventory to give a corrected inventory $i_c = i - f$. If the inventory of a given nuclide in the step where the damaged particles were determined was $<f$ particle equivalents, then the corrected inventory i_c was set to zero. Each instance where a correction was made is discussed in detail in the sections that follow.

Because each of these fuel compacts was subjected to heating in the FACS furnace prior to RDLBL (and some of these were reirradiated prior to the FACS tests), those post-irradiation heating tests and the measurements of fission product release from the FACS tests are germane to the RDLBL results. Preliminary results from the FACS testing of several AGR-3/4 compacts (3-2, 10-2, and 10-4) were prepared in a conference paper (Stempien et al. 2018a). A subsequent test of Compact 8-2 was conducted in the FACS furnace at 1400°C, but was not completed in time for inclusion in the aforementioned 2018 conference paper. The results from these "as-irradiated" FACS tests have been compiled and refined in a recent report (Stempien and Cai 2024b). A report on the results from the reirradiation-FACS tests, including any updated or refined results, will be prepared at a later date.

4.1. Compact 3-2 RDLBL Results

Compact 3-2 was heated in the FACS furnace at 1600 and 1700°C (Stempien and Cai 2024b), but it was not reirradiated in NRAD. The FACS temperature program was discussed in Section 2.2. Three radial segments in addition to the core were obtained from RDLBL of this compact, but the compact had to be re-epoxied to the deconsolidation rod in between the second and third radial segments.

4.1.1. Compact 3-2 Gamma-emitter and Sr-90 Results

The total amounts of key gamma-emitting fission products and beta-emitting Sr-90 measured in the compact outside of the driver fuel SiC layer for each segment of the radial deconsolidation are summarized in Table 18 in terms of the number of particle equivalent inventories. Additional results in units of activity and in terms of the fraction of the compact inventory of fission products can be found in Table 51 and Table 52 of Appendix A-1, Compact 3-2. Table 19 gives the relative error for these results. Section 2.5 described how the measurement errors were determined. Values denoted by "<" are derived from MDAs and should be considered an upper bound on the activity of a given nuclide. No corrections for driver particle damage were applied to MDAs. In summations, MDAs were set equal to zero.

Table 18. Particle-equivalent inventories measured in the solutions from the radial deconsolidation of Compact 3-2. All values were decay-corrected to EOI + 1 day.

Particle Equivalents		Ag-110m	Ce-144	Cs-134	Cs-137	Eu-154	Eu-155	Ru-106	Sb-125	Sr-90
Segment #1	Decon	<1E+01	3.80E-02	7.80E-03	2.34E-02	2.91E-01	3.21E-01	4.55E-01	<4E-02	1.88E-01
	Pre-burn leach 1	<1E+01	<2E-02	1.98E-03	3.37E-03	1.02E-01	1.21E-01	1.30E-01	<4E-02	3.46E-02
	Pre-burn leach 2	<1E+01	<2E-02	1.63E-03	2.22E-03	1.82E-02	<4E-02	5.26E-02	<4E-02	7.92E-03
	Post-burn leach 1	<1E+01	<4E-02	<2E-03	1.07E-03	6.26E-01	7.94E-01	<4E-02	<4E-02	2.50E-01
	Post-burn leach 2	<1E+01	1.33E-02	<8E-04	1.15E-03	9.10E-03	<4E-02	2.51E-02	<4E-02	9.41E-03
	SUM (MDA = 0)	0	5.13E-02	1.14E-02	3.12E-02	1.05E+00	1.24E+00	6.62E-01	0	4.90E-01
Segment #2	Decon	<2E+01	4.75E-02	1.68E-02	4.31E-02	1.90E-01	2.11E-01	3.94E-01	<8E-02	1.07E-01
	Pre-burn leach 1	<1E+01	1.64E-02	<2E-03	5.99E-03	9.48E-02	1.19E-01	1.63E-01	<4E-02	3.71E-02
	Pre-burn leach 2	<1E+01	<2E-02	<2E-03	9.79E-04	<2E-02	<4E-02	<4E-02	<4E-02	6.46E-03
	Post-burn leach 1	<2E+01	<4E-02	<2E-03	9.15E-04	7.68E-01	9.34E-01	<8E-02	<4E-02	3.65E-01
	Post-burn leach 2	<1E+01	<2E-02	<2E-03	<2E-04	<2E-02	<4E-02	<4E-02	<4E-02	6.47E-04
	SUM (MDA = 0)	0	6.40E-02	1.68E-02	5.10E-02	1.05E+00	1.26E+00	5.57E-01	0	5.16E-01
Segment #3	Decon	<4E+01	4.03E-02	4.03E-02	9.85E-02	3.93E-01	4.12E-01	4.18E-01	<1E-01	2.29E-01
	Pre-burn leach 1	<2E+01	<4E-02	<2E-03	1.62E-03	1.47E-01	1.79E-01	2.57E-01	<4E-02	5.58E-02
	Pre-burn leach 2	<2E+01	<4E-02	<2E-03	4.65E-04	1.24E-02	1.20E-02	<8E-02	<4E-02	5.89E-03
	Post-burn leach 1	<8E+01	1.07E+00	6.74E-01	7.51E-01	2.46E+00	2.58E+00	<4E-01	<6E-01	2.00E+00
	Post-burn leach 1 Correction	<8E+01	7.27E-02	0	0	1.46E+00	1.58E+00	<4E-01	<6E-01	1.00E+00
	Post-burn leach 2	<1E+01	<2E-02	3.37E-03	5.44E-03	3.75E-02	5.31E-02	<8E-02	<4E-02	5.87E-04
	SUM (MDA = 0)	0	1.11E+00	7.18E-01	8.57E-01	3.05E+00	3.24E+00	6.75E-01	0	2.29E+00
	SUM (MDA = 0) Corrected	0	1.13E-01	4.37E-02	1.06E-01	2.05E+00	2.24E+00	6.75E-01	0	1.29E+00
Core	Decon	<2E+01	2.20E+00	5.72E-01	1.38E+00	5.30E-01	5.73E-01	3.25E+00	<2E-01	3.82E-01
	Pre-burn leach 1	<6E+01	2.78E+00	5.91E-01	1.37E+00	8.61E-01	9.83E-01	6.65E+00	<4E-01	8.77E-01
	Pre-burn leach 2	<2E+01	1.81E-01	2.36E-02	4.92E-02	4.46E-02	<1E-01	2.50E-01	6.01E-02	1.62E-02
	Post-burn leach 1	<8E+01	1.57E+01	4.50E-01	5.58E-01	3.95E+00	4.24E+00	1.18E+00	1.07E+00	1.96E+00
	Post-burn leach 2	<2E+01	4.21E-02	1.98E-02	3.25E-02	<2E-02	<1E-01	5.87E-01	9.45E-02	3.85E-03
	SUM (MDA = 0)	0	2.09E+01	1.66E+00	3.38E+00	5.38E+00	5.79E+00	1.19E+01	1.22E+00	3.24E+00
Compact TOTAL (MDA = 0)		0	22.13	2.40	4.32	10.53	11.53	13.80	1.22	6.54
Compact TOTAL Corrected (MDA = 0)		0	21.13	1.73	3.57	9.53	10.53	13.80	1.22	5.54

Table 19. Relative error on the Compact 3-2 RDLBL results given in the preceding tables. The errors in the "sum" rows were computed by propagating the measurement error from all the RDLBL steps making up the sum. No attempts to alter the error were made when the inventories were corrected for driver-particle particle damage.

	Uncertainty	Ag-110m	Ce-144	Cs-134	Cs-137	Eu-154	Eu-155	Ru-106	Sb-125	Sr-90
Segment #1	Decon	N/A	18.8%	6.0%	3.0%	3.4%	6.6%	5.0%	N/A	2.0%
	Pre-burn leach 1	N/A	N/A	9.2%	4.3%	3.0%	10.6%	10.9%	N/A	2.0%
	Pre-burn leach 2	N/A	N/A	11.7%	5.6%	19.2%	N/A	24.5%	N/A	2.0%
	Post-burn leach 1	N/A	N/A	N/A	10.3%	3.0%	4.0%	N/A	N/A	2.0%
	Post-burn leach 2	N/A	32.5%	N/A	7.4%	32.3%	N/A	31.4%	N/A	2.0%
	SUM (MDA = 0)	N/A	16.2%	4.7%	2.4%	2.1%	3.3%	4.6%	N/A	1.3%
Segment #2	Decon	N/A	17.1%	5.6%	3.0%	5.5%	10.6%	8.5%	N/A	2.0%
	Pre-burn leach 1	N/A	27.1%	N/A	3.0%	3.9%	9.9%	8.5%	N/A	2.0%
	Pre-burn leach 2	N/A	N/A	N/A	9.0%	N/A	N/A	N/A	N/A	2.6%
	Post-burn leach 1	N/A	N/A	N/A	14.6%	3.0%	4.0%	N/A	N/A	2.0%
	Post-burn leach 2	N/A	N/A	N/A	N/A	N/A	N/A	N/A	N/A	9.2%
	SUM (MDA = 0)	N/A	14.5%	5.6%	2.6%	2.4%	3.6%	6.5%	N/A	1.5%
Segment #3	Decon	N/A	32.0%	4.8%	3.0%	5.2%	12.3%	18.4%	N/A	2.0%
	Pre-burn leach 1	N/A	N/A	N/A	16.4%	7.7%	11.0%	17.0%	N/A	2.0%
	Pre-burn leach 2	N/A	N/A	N/A	23.1%	26.0%	28.0%	N/A	N/A	3.1%
	Post-burn leach 1	N/A	12.2%	3.0%	3.0%	3.7%	8.4%	N/A	N/A	2.0%
	Post-burn leach 2	N/A	N/A	10.9%	4.0%	8.2%	22.7%	N/A	N/A	2.0%
	SUM (MDA = 0)	N/A	11.8%	2.8%	2.7%	3.1%	6.9%	13.1%	N/A	1.8%
Core	Decon	N/A	6.1%	3.0%	3.0%	3.0%	6.0%	3.0%	N/A	2.0%
	Pre-burn leach 1	N/A	7.0%	3.0%	3.0%	6.0%	13.2%	4.1%	N/A	2.0%
	Pre-burn leach 2	N/A	7.7%	3.4%	3.0%	4.0%	N/A	10.7%	41.7%	2.0%
	Post-burn leach 1	N/A	5.0%	3.0%	3.0%	3.0%	4.7%	16.2%	17.4%	2.0%
	Post-burn leach 2	N/A	20.8%	3.3%	3.1%	N/A	N/A	4.6%	13.2%	3.3%
	SUM (MDA = 0)	N/A	3.9%	1.7%	1.8%	2.4%	4.1%	2.9%	15.3%	1.3%
Compact TOTAL (MDA = 0)		N/A	3.8%	1.4%	1.5%	1.6%	2.9%	2.6%	15.3%	0.9%

4.1.2. Compact 3-2 ICP-MS Results

ICP-MS was used to measure actinides in the RDLBL solutions. Intact TRISO particles will retain all actinides, but exposed kernels, such as in the DTF particles or in damaged TRISO-coated particles, will be subject to leaching during the DLBL process. Table 20 summarizes the actinide content measured from the RDLBL of Compact 3-2, and Table 21 gives the relative error in the measurement values. A description of the measurement error was given in Section 2.5. Additional tables (Table 53 and Table 54) in Appendix A-1 provide these results in units of mass and compact fraction.

Table 20. Particle equivalents for select actinides from ICP-MS of solutions from Compact 3-2 RDLBL.

Compact 3-2		Pu-239	Pu-240	U-234	U-235	U-236	U-238
Particle Equivalents		Pu-239	Pu-240	U-234	U-235	U-236	U-238
Segment #1	Decon	8.96E-02	7.99E-02	4.34E-01	4.64E-01	4.24E-01	4.35E-01
	Pre-burn leach 1	1.70E-02	<4E-02	<1E-01	3.53E-03	<6E-03	3.30E-03
	Pre-burn leach 2	<1E-02	<4E-02	<1E-01	<2E-03	<6E-03	1.24E-03
	Post-burn leach 1	6.92E-02	8.39E-02	<8E-02	1.29E-02	9.19E-03	1.14E-02
	Post-burn leach 2	1.73E-02	<2E-02	<8E-02	1.05E-02	1.36E-02	1.30E-02
	SUM (MDA = 0)	1.93E-01	1.64E-01	4.34E-01	4.91E-01	4.47E-01	4.64E-01
Segment #2	Decon	9.96E-02	9.84E-02	7.86E-01	8.27E-01	7.70E-01	7.72E-01
	Pre-burn leach 1	2.88E-02	<2E-02	<8E-02	6.63E-02	5.71E-02	6.21E-02
	Pre-burn leach 2	<1E-02	<4E-02	<1E-01	2.79E-03	<6E-03	2.89E-03
	Post-burn leach 1	8.83E-02	1.26E-01	<1E-01	1.71E-02	1.67E-02	1.70E-02
	Post-burn leach 2	<1E-02	<4E-02	<1E-01	<2E-03	<6E-03	<6E-04
	SUM (MDA = 0)	2.17E-01	2.24E-01	7.86E-01	9.13E-01	8.44E-01	8.54E-01
Segment #3	Decon	8.58E-02	8.66E-02	9.73E-01	9.95E-01	9.37E-01	9.41E-01
	Pre-burn leach 1	<1E-02	<2E-02	<8E-02	1.11E-02	9.19E-03	9.88E-03
	Pre-burn leach 2	<1E-02	<4E-02	<1E-01	<2E-03	<6E-03	<4E-04
	Post-burn leach 1	1.17E+00	1.28E+00	1.16E+00	1.15E+00	1.16E+00	1.13E+00
	Post-burn leach 1 Corrected	1.72E-01	2.81E-01	1.57E-01	1.55E-01	1.60E-01	1.33E-01
	Post-burn leach 2	1.16E-02	<4E-02	<1E-01	4.33E-03	<6E-03	3.59E-03
	SUM (MDA = 0)	1.27E+00	1.37E+00	2.13E+00	2.17E+00	2.11E+00	2.09E+00
	SUM (MDA = 0) Corrected	2.70E-01	3.68E-01	1.13E+00	1.17E+00	1.11E+00	1.09E+00
Core	Decon	2.91E+00	2.99E+00	9.85E+00	1.00E+01	9.70E+00	9.13E+00
	Pre-burn leach 1	3.47E+00	3.47E+00	9.73E+00	9.95E+00	9.49E+00	9.17E+00
	Pre-burn leach 2	1.75E-01	1.76E-01	<2E-01	1.67E-02	1.23E-02	1.46E-02
	Post-burn leach 1	1.38E+01	1.46E+01	1.25E+00	1.20E+00	1.13E+00	1.14E+00
	Post-burn leach 2	7.62E-02	7.51E-02	<1E-01	4.53E-03	<6E-03	3.99E-03
	SUM (MDA = 0)	2.04E+01	2.13E+01	2.08E+01	2.12E+01	2.03E+01	1.95E+01
Compact TOTAL (MDA = 0)		22.07	23.04	24.18	24.77	23.73	22.87
Compact TOTAL (MDA = 0) Corrected		21.07	22.04	23.18	23.77	22.73	21.87

Table 21. Relative error in the Compact 3-2 ICP-MS results that were summarized in Table 20. No attempts to alter the error were made when the inventories were corrected for driver-particle particle damage.

Error (%)		Pu-239	Pu-240	U-234	U-235	U-236	U-238
Segment #1	Decon	5%	10%	10%	5%	5%	5%
	Pre-burn leach 1	15%	N/A	N/A	21%	N/A	7%
	Pre-burn leach 2	N/A	N/A	N/A	N/A	N/A	14%
	Post-burn leach 1	14%	14%	N/A	16%	19%	9%
	Post-burn leach 2	24%	N/A	N/A	14%	19%	7%
	SUM (MDA = 0)	6%	9%	10%	5%	5%	5%
Segment #2	Decon	7%	13%	7%	5%	5%	5%
	Pre-burn leach 1	21%	N/A	N/A	5%	11%	5%
	Pre-burn leach 2	N/A	N/A	N/A	24%	N/A	10%
	Post-burn leach 1	16%	13%	N/A	17%	17%	5%
	Post-burn leach 2	N/A	N/A	N/A	N/A	N/A	N/A
	SUM (MDA = 0)	8%	9%	7%	5%	5%	5%
Segment #3	Decon	9%	12%	9%	5%	5%	5%
	Pre-burn leach 1	N/A	N/A	N/A	12%	23%	7%
	Pre-burn leach 2	N/A	N/A	N/A	N/A	N/A	N/A
	Post-burn leach 1	7%	11%	10%	5%	5%	5%
	Post-burn leach 2	20%	N/A	N/A	20%	N/A	7%
	SUM (MDA = 0)	7%	10%	7%	4%	4%	4%
Core	Decon	5%	5%	5%	5%	5%	5%
	Pre-burn leach 1	5%	5%	7%	5%	5%	5%
	Pre-burn leach 2	7%	14%	N/A	18%	25%	9%
	Post-burn leach 1	5%	5%	13%	5%	5%	5%
	Post-burn leach 2	14%	20%	N/A	19%	N/A	9%
	SUM (MDA = 0)	4%	4%	4%	3%	3%	3%
Compact TOTAL (MDA = 0)		3%	3%	4%	3%	3%	3%

4.1.3. Compact 3-2 Discussion

Segments 1 and 2 had 0.4 and 0.7 particle equivalents of U-238, respectively, in their deconsolidation solutions. However, the Ce-144 inventories in Segments 1 and 2 were only 0.05 and 0.06 particle equivalents, respectively, and the total Cs inventories in each of these segments were even smaller than the Ce inventories. If these segments each had a TRISO-coated driver particle that was broken by the deconsolidation process, the Ce, U, and Cs inventories would be similar. Furthermore, the U, and especially the Ce, should be present in values much closer to one. That is not the case here; therefore, Segments 1 and 2 do not appear to have any TRISO particles that were broken by the RDLBL process.

If Segments 1 and 2 had TRISO particles that had failed in-pile, the Cs retained in such particles should be low; however, the Ce and U inventories would be similar, and likely closer to one. That is not the case either, and Segments 1 and 2 do not appear to have TRISO particles that failed in-pile. If Segments 1 and 2 each had a particle with a failed SiC layer that occurred during the 1600/1700°C FACS test that preceded RDLBL, the amount of Cs measured on the FACS condensation plates should correlate to these failures, but it does not (Stempien and Cai 2024b). TRISO failures can also be ruled out because the 0.3 particle equivalents of Kr-85 measured in the first 300 h at 1600°C were too small and accrued too gradually over that time (Stempien and Cai 2024b). It was not released in a rapid fashion characteristic of an acute particle failure. (See Demkowicz et al. [2015a] for some examples of Kr-85 release from particle failure.)

These Segment 1 and 2 inventories are not believed to be from failed or damaged TRISO-coated driver particles. Instead, the U and Ce inventories in Segments 1 and 2 are believed to have originated in the DTF particles. It appears that the 1600/1700°C FACS test of this compact drove significant U, and a little Ce, into these two outer segments. In the RDLBL exam of Compact 10-4 (Hunn et al. 2020), which had been subjected to a 1400°C FACS test (Stempien and Cai 2024b), there were no indications of damaged particles, and the amounts of Ce and U in its first and second segments were similar to those in Segments 1 and 2 from Compact 3-2. It was also noteworthy in that study that the amounts of U in these segments were considerably higher than the amounts of Ce, just as they are here for Compact 3-2. The same effects appear to be dominating in the deconsolidation phase of Segment 3 as well.

Ideally, the ATR irradiation, the FACS test, and the radial deconsolidation process would not damage the fuel compact or its TRISO particles. With no damaged TRISO particles, the DTF particles are the only major sources of Cs, Ce, and actinides (for example) in the RDLBLs. Based on the results from RDLBL of as-irradiated AGR-3/4 compacts, no radial segments outside the compact core had a single DLBL step where the actinide and Ce-144 quantities were simultaneously greater than about 0.2 particle equivalents, unless failure of the SiC layer or the entire TRISO coating had occurred, either accidentally during RDLBL or in-pile prior to RDLBL (Stempien and Cai 2024a). In Table 18 and Table 20, there are elevated quantities of Ce-144 (1.07 particle equivalents) and actinides (~1.15 particle equivalents) in the Segment 3 post-burn leach 1. This is indicative of a driver particle that was leached in that step. When a kernel is leached in the first post-burn leach, that suggests the particle had an in-pile or in-safety-test (if applicable) SiC failure (Hunn et al. 2016; Demkowicz et al. 2015b; Stempien et al. 2021a). In a report on RDLBLs of as-irradiated fuel compacts (Stempien and Cai 2024a), it was argued that because AGR-3/4 TRISO particles are of the same specification as AGR-1, which saw very low rates of in-pile SiC (Demkowicz et al. 2015b), it is extremely unlikely that in-pile SiC failure contributed to this. If the SiC failure rates observed in AGR-1 were applied to AGR-3/4, the probability of an in-pile SiC failure here would be low (≤3.1E-5 at 95% confidence), though not impossible. After 21 total RDLBLs in AGR-3/4, one in-pile SiC failure would give an observed SiC failure rate in AGR-3/4 of about 2.5E-5, which is about what the AGR-1 SiC in-pile failure rate was at 95% confidence.

However, this compact was not in the as-irradiated state at the time of its RDLBL. It had been heated in the FACS furnace (Stempien and Cai 2024b) for 300 h at 1600°C before the temperature was raised to 1700°C for the final 48 h of the test (see Figure 3). Considering that only about 0.3 particle equivalents of Cs-134 were released during the prior 300 h at 1600°C, the release of an additional 0.60 particle equivalents of Cs-134 over the 48 h at 1700°C represents a rapid release rate (Stempien and Cai 2024b). Some of this could be additional release from Cs-134 that originated in the DTF particles or the surrounding compact matrix, but some of it might be attributable to the damaged particle leached in this first post-burn leach of Segment 3. The amount of Kr-85 measured during the stage at 1700°C only increased by 0.06 particle equivalents; therefore, a full TRISO failure did not occur (Stempien and Cai 2024b). Given that the Cs-134 measured in the first post-burn leach of Segment 3 equated to ~0.7 particle equivalents, this particle could not have contributed more than about 0.3 of the 0.6 particle equivalents of Cs-134 released in the FACS furnace during the period of time at 1700°C. With 0.7 particle equivalents remaining in the particle (which is relatively high, though not impossibly high, if the particle had a failed SiC coating and was releasing Cs-134 either in-pile or in FACS), the final possibility is that this particle was intact until it was accidentally broken during the first post-burn leach of Segment 3, and the increased Cs release at 1700°C during the FACS test would then be attributable to inventory that originated in the DTF particles.

It is not possible to identify the cause of this particle damage in Segment 3 with 100% certainty, but on the basis that there is insufficient evidence to categorize this particle as having an in-pile or in-FACS SiC failure, the Segment 3 RDLBL results should be corrected for it to attempt to minimize its effect on the results that represent fission products that originated with the DTF particles. A correction for the broken or failed SiC particle in Segment 3 was applied following the methods employed previously (Stempien and Cai 2024a) and described at the top of Section 4. If the inventory of a given nuclide in the first burn-leach in Segment 3 was ≥1 particle equivalent, a single particle equivalent was subtracted from that inventory. If the inventory of a given nuclide in the first burn-leach in Segment 3 was <1 particle equivalent, that value was set to zero. Table 18 and Table 20 contain results both with and without a correction for one damaged particle in Segment 3.

In the core segment, there were 21.2 and 19.5 particle equivalents of U-235 and U-238, respectively. In that segment there were also 20.9 particle equivalents of Ce-144. This gave total measured values for these nuclides (meaning the sums of the inventories from all the segments of the compact) that were a little higher than usual. The average total RDLBL inventories of Ce-144 and U-235 from all the as-irradiated RDLBLs were about 19.4 particle equivalents. However, there were six as-irradiated compacts where the Ce-144 and/or the U-235 recoveries exceeded 20 particle equivalents. These compacts were 1-4, 1-3, 5-4, 7-3, 8-3 and 12-3. Among that group, four had Ce-144 values >20 that ranged from 20.39-21.66 particle equivalents. The total Ce-144 in Compact 3-2 (after correcting for a particle damaged in the RDLBL) was 21.13 particle equivalents—not unreasonable. Among that group of six compacts, four had U-235 values >20 that ranged from 20.09-21.8 particle equivalents. From that group, only Compacts 5-4 and 7-3 had both Ce-144 and Eu-154 values that exceeded 20 particle equivalents. The total U-235 in Compact 3-2 (after correcting for a particle damaged in the RDLBL) was a bit more at 23.77 particle equivalents. This is nearly 2 particle equivalents more than the next nearest value from an as-irradiated compact. With reasonable values for Ce-144 and U-238, there was no strong evidence that any driver particles were damaged here, and no corrections were made.

Figure 16 shows a summary of the total fission product inventories measured from the FACS test and subsequent RDLBL of Compact 3-2. The average in-pile release of fission products from a Capsule 3 compact are also given in Figure 16. To compute this average in-pile release from a compact, the Capsule 3 fission product mass balance, which represents the fission products measured on the capsule components outside of the fuel (Stempien et al. 2018b), was divided by four, the number of compacts in each AGR-3/4 irradiation capsule. Capsule 3 components include the hardware (foils, felts, spacers, and through tubes) and graphite rings (inner, outer, and sink ring). This has limitations in the event that a

complete mass balance was not obtained. The AGR-3/4 stainless-steel capsule shells could not be leached, and some data suggest it is possible that Ag or Cs may have migrated beyond the sink rings and onto the shells (Stempien et al. 2018b).

There was no Ag-110m measured via RDLBL, which was consistent with all previous as-irradiated AGR-3/4 RDLBLs (Hunn et al. 2020; Helmreich et al. 2021; Helmreich et al. 2022; Stempien and Cai 2024a). Two factors have made it impossible to quantify Ag-110m in these RDLBLs. By comparing the Ag-110m M/C for a compact with the Ag-110m measured from DLBL of that compact, it is apparent that generally very little of the Ag-110m released through intact TRISO coatings (and presumably from DTF particles as well) is retained in the compact matrix, where it can be measured via DLBL (Demkowicz et al. 2015b; Stempien et al. 2021a). Instead, Ag-110m that diffused out of particles is mostly released from the compact altogether. Comparing the Ag-110m mass balance for Capsule 3 in Figure 16 to the Ag-110m inventories measured from FACS testing also supports this assertion. Additionally, Ag-110m had decayed through many of its 249-d half-lives between the end of the AGR-3/4 irradiation (in 2014) and the dates of these RDLBL exams.

As stated earlier, even after a correction was made for a damaged TRISO particle in Segment 3, the total Ce-144 inventory from the Compact 3-2 DLBL is a little higher than expected from 20 DTF particles. Perhaps this could be attributed to a damaged TRISO particle among the DTF particles in the compact core, but there is insufficient evidence to conclude that. Whether a driver particle was damaged in the core or not, the Ce-144 inventory measured in the post-FACS DLBL of Compact 3-2 demonstrates that Ce-144 was well retained in the DTF kernels and the matrix surrounding them. Accordingly, Figure 16 shows that the mass balance of Ce-144 outside of the fuel in Capsule 3 equates to a low average compact-release of 0.01 particle equivalents of Ce-144. Furthermore, Ce-144 was well retained even after FACS testing at 1600 and 1700°C, where only 3×10^{-3} particle equivalents of Ce-144 were measured (Stempien and Cai 2024b).

Like Ce-144, Ru-106 appears to be well retained despite only about 13 particle equivalents being measured in the RDLBL. No Ru-106 release was detected from the FACS tests of Compact 3-2, and none was measured outside of the fuel in AGR-3/4 Capsule 3. This led to the conclusion that the recovery of Ru-106 from the RDLBL operations was often noticeably low relative to the actinide and Ce-144 recoveries, which has been noted previously (Stempien et al. 2021a [Table 11]; Helmreich et al. 2022; Stempien and Cai 2024a).

Figure 16 shows that each Capsule 3 compact released an average of about nine particle equivalents of Cs-134, 45% of the DTF-particle inventory of this nuclide. In the AGR-3/4 mass balance report (Stempien et al. 2018b), a couple possible explanations were discussed for why less than 100% of the DTF inventory of Cs was measured outside of the fuel in all capsules. One explanation was that the DTF particles or the compact matrix retained significant Cs. A report on the as-irradiated RDLBL of AGR-3/4 compacts (Stempien and Cai 2024a) shows that as-irradiated AGR-3/4 compacts may retain from about 7 to 15 particle equivalents (35-75% of the DTF inventory) for time-average volume-average (TAVA) irradiation temperatures from about 850 to 959°C. From about 1000°C to 1400°C, the Cs-134 retained in the as-irradiated compacts and measured via RDLBL ranged from 5-20% of the DTF inventory. In AGR-1, in-pile cesium release from particles with failed SiC layers was found to vary widely, from about 27% to 96%, based on gamma counting of individual particles with failed SiC recovered from deconsolidated compacts (Hunn et al. 2016). Inversely, this finding from AGR-1 suggests that Cs retention in a particle with a failed SiC layer (similar to the DTF particles in AGR-3/4) can range from about 4% to 73% (subject to biases in calculations and uncertainties in the measurements). Based solely on the mass balance, then, an average Capsule 3 compact retains about 55% of the DTF-particle inventory of Cs. The total Cs measured via RDLBL of Compact 3-2 (1.7 particle equivalents), plus that released during the FACS test (0.9 particle equivalents), plus the estimated ~11 particle equivalents of Cs-134 released from the compact to the capsule components during irradiation amounts to about 13.6 particle equivalents (68% of the DTF inventory); therefore, the amount of Cs-134 measured in and released from

Compact 3-2 is significantly below 20 particle-equivalent inventories. This could be the result of one of several factors (or a combination of factors), one being that the Cs FACS collection efficiency may not be perfectly constant from one test to another, and the efficiency that is applied was determined over the course of tens of un-fueled trials.

Another possible effect that could contribute to the difference in the amount of Cs measured via the mass balance and the amount of Cs apparently retained in the compact outside of the TRISO-coated driver particles is that some Cs could have transported beyond the sink ring to the capsule shell, where it could not be quantified. The shells were not analyzed because they were too radioactive to transfer to the AL, and it was anticipated that the relatively cold (typically 600°C or less) sink rings would quantitatively capture key fission products that migrated out of the outer ring. The sink rings in Capsules 3, 7, and 10 were found to have more Cs than the inner and outer rings in those capsules, and the Capsule 3 sink ring contained 68% of all the Cs-134 measured outside of the fuel compacts in that capsule (Stempien et al. 2018b). It is possible that some Cs migrated beyond the sink ring, making the Cs mass balance incomplete (low) and making the low apparent retention of Cs in Compact 3-2 seem more reasonable.

To further inform conclusions on the Cs retention or release in Capsule 3 compacts, the results from the as-irradiated RDLBL of AGR-3/4 Compact 3-3 could be considered (Stempien and Cai 2024a). There was evidence that, based on the U-235 and U-238, 13-14 TRISO-coated driver particles were accidentally damaged during RDLBL of Compact 3-3. The Ce-144 content in that compact suggested about 8 driver particles were damaged. With no corrections made for that accidental damage, there were 7.8 particle equivalents of Cs-134 (39% of the DTF inventory) and 14.4 particle equivalents of Cs-137 (72% of the DTF inventory). If any correction were applied (whether for 8 or 14 accidentally broken particles) the result would indicate there was little or no remaining Cs in Compact 3-3. This would force other conclusions for Compact 3-3 as well. First, more Cs was driven out of the compact during irradiation and, Compact 3-3 would have released in-pile more than the "average" 11 particle equivalents estimated by dividing the mass balance by four. Second, the mass balance itself is incomplete and biased low. Given the proximity and similar irradiation histories between Compact 3-3 (AI RDLBL) and Compact 3-2 (post-FACS RDLBL), it is reasonable to conclude that Compact 3-2 truly had little DTF Cs remaining (roughly 2.6 particle equivalents or 13% of the DTF inventory) after irradiation for measurement during the FACS test and subsequent RDLBL.

During the preceding FACS test (Stempien and Cai 2024b), about 15 and 16 particle equivalents of Eu-154 and Sr-90 were released, respectively. The FACS test releases would have been from some combination of the release of residual post-ATR DTF and matrix inventory and some (perhaps small) amount of additional diffusion through intact coatings and out of the compact during the FACS test. In the subsequent RDLBL of Compact 3-2, inventories of 9.5 and 5.5 particle equivalents of Eu-154 and Sr-90 were measured, respectively. The RDLBL of Compact 3-2 gives the quantity of Eu-154 and Sr-90 that was retained after irradiation in the compact outside of the intact SiC coatings that remained in the compact after the FACS test, plus any additional Eu-154 and Sr-90 that may have diffused through intact TRISO coatings to be retained in the compact matrix after the FACS test.

In total, the Capsule 3 mass balance found 35.3 and an estimated 33.7 particle equivalents of Eu-154 and Sr-90, respectively, outside of the fuel. This equates to an average of about 9.0 and 8.0 particle equivalents being contributed from each Capsule 3 compact. If the mass-balance, plus the RDLBL, plus the FACS release are added, it is estimated that 33.5 and 29.5 particle equivalents of Eu-154 and Sr-90 were present in this compact outside of the driver particle SiC layers or were released from the compact during FACS testing. With only 20 DTF particles in this compact, the additional 13.5 and 9.5 particle equivalents of Eu and Sr, respectively, came from diffusion through intact TRISO coatings. However, it is not obvious exactly when some of this could have diffused through the coatings (e.g., whether or how much was from the initial irradiation in ATR or how much was from FACS testing alone).
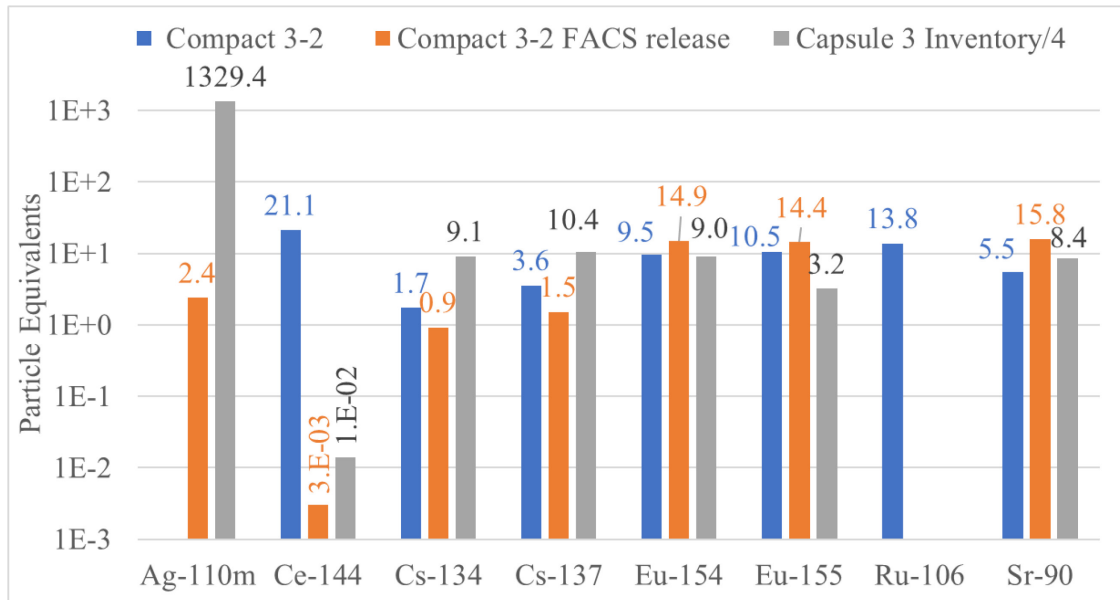
Figure 16. Fission product release during FACS testing at 1600/1700°C, fission product inventories in Compact 3-2 from RDLBL (graphite matrix, OPyC, and DTF), and average in-pile compact release. Values used here include the correction for one TRISO particle leached in Segment 3.

4.2. Compact 8-2 RDLBL Results

Compact 8-2 was heated in the FACS furnace at 1400°C for 300 h, but it was not reirradiated in NRAD. Three radial segments in addition to the core of this compact were obtained from RDLBL. There were no major difficulties encountered during the RDLBL (see Section 3.2).

4.2.1. Compact 8-2 Gamma-emitter and Sr-90 Results

Table 22 summarizes the inventories of selected fission products measured at each step of the RDLBL of Compact 8-2. Results are presented here in units of particle equivalents. Additional results in units of activity and the fraction of the compact inventory can be found in Table 55 and Table 56 of Appendix A-2, Compact 8-2. Table 23 gives the relative error for these results. Section 2.5 described how the measurement errors were determined. Values denoted by "<" are derived from MDAs and should be considered an upper bound on the activity of a given nuclide. In summations, MDAs were set equal to zero. Both corrected and uncorrected values are given for the first post-burn leach of Segment 3, where two unexpected driver particle kernels were leached. The reasoning behind that correction and its implementation are discussed in Section 4.2.3; however, it is ultimately concluded that the uncorrected results may be more accurate.

36

Table 22. Particle-equivalent inventories measured in the solutions from the radial deconsolidation of Compact 8-2. All values were decay-corrected to EOI + 1 day. The uncorrected Segment 3 values will reflect what are believed to be real in-pile SiC failures.

		Ag-110m	Ce-144	Cs-134	Cs-137	Eu-154	Eu-155	Ru-106	Sb-125	Sr-90
						Compact 8-2				
Particle Equivalents		Ag-110m	Ce-144	Cs-134	Cs-137	Eu-154	Eu-155	Ru-106	Sb-125	Sr-90
Segment #1	Decon	<1E+01	<2E-02	<2E-03	9.91E-04	5.40E-01	5.48E-01	<6E-02	<4E-02	6.08E-01
	Pre-burn leach 1	<2E+01	<6E-02	<4E-03	2.88E-03	3.13E-01	3.48E-01	<1E-01	<8E-02	1.87E-01
	Pre-burn leach 2	<6E+00	<2E-02	<6E-04	1.30E-03	1.72E-02	<4E-02	2.75E-02	<2E-02	1.63E-02
	Post-burn leach 1	<2E+01	<6E-02	<8E-03	2.32E-03	1.55E+00	1.59E+00	1.09E-01	<1E-01	1.19E+00
	Post-burn leach 2	<6E+00	<2E-02	<6E-04	6.48E-04	1.32E-02	2.20E-02	1.92E-02	<2E-02	3.92E-03
	SUM (MDA = 0)	0	0	0	8.13E-03	2.43E+00	2.51E+00	1.56E-01	0	2.01E+00
Segment #2	Decon	<1E+01	<4E-02	<2E-03	1.06E-03	7.50E-01	7.56E-01	<6E-02	<6E-02	7.71E-01
	Pre-burn leach 1	<2E+01	<4E-02	8.22E-04	1.91E-03	4.90E-01	5.47E-01	<8E-02	<6E-02	3.56E-01
	Pre-burn leach 2	<4E+00	<6E-03	2.34E-04	5.00E-04	2.18E-02	2.43E-02	4.01E-03	<8E-03	2.32E-02
	Post-burn leach 1	<2E+01	1.08E-01	1.01E-03	2.04E-03	3.65E+00	4.13E+00	<8E-02	5.73E-02	3.21E+00
	Post-burn leach 2	<2E+01	<4E-02	1.14E-04	3.91E-04	2.91E-03	3.50E-03	<6E-02	5.35E-03	3.08E-03
	SUM (MDA = 0)	0	1.08E-01	2.18E-03	5.90E-03	4.91E+00	5.46E+00	4.01E-03	6.27E-02	4.37E+00
Segment #3	Decon	<4E+01	<6E-02	4.12E-03	1.27E-02	1.64E+00	1.71E+00	<1E-01	4.29E-02	1.76E+00
	Pre-burn leach 1	<4E+01	<6E-02	1.70E-03	3.15E-03	9.73E-01	1.14E+00	<2E-01	<1E-01	6.93E-01
	Pre-burn leach 2	<1E+01	<2E-02	<2E-03	4.65E-04	5.11E-02	5.58E-02	<6E-02	<4E-02	3.95E-02
	Post-burn leach 1	<6E+01	1.94E+00	2.43E-01	3.80E-01	8.38E+00	9.62E+00	1.10E+00	7.36E-01	7.59E+00
	Post-burn leach 1 Corrected	<6E+01	0	0	0	6.38E+00	7.62E+00	0	0	5.59E+00
	Post-burn leach 2[a]	<2E+01	6.53E-02	2.29E-01	3.03E-01	6.09E-02	7.70E-02	1.09E-01	<1E-01	1.41E-01
	SUM (MDA = 0)	0	2.00E+00	4.78E-01	6.99E-01	1.11E+01	1.26E+01	1.21E+00	7.79E-01	1.02E+01
	SUM (MDA = 0) Corrected	0	6.53E-02	2.35E-01	3.19E-01	9.11E+00	1.06E+01	7.25E-02	4.29E-02	8.22E+00
Core	Decon	<4E+01	3.80E+00	5.30E-01	1.45E+00	4.38E+00	4.89E+00	5.17E+00	4.90E-01	5.55E+00
	Pre-burn leach 1	<1E+02	5.98E+00	8.02E-01	2.16E+00	4.43E+00	5.40E+00	8.06E+00	<8E-01	6.14E+00
	Pre-burn leach 2	<1E+02	1.85E-01	2.35E-01	2.88E-01	2.71E-01	3.36E-01	<6E-01	<4E-01	4.81E-01
	Post-burn leach 1	<2E+02	1.30E+01	6.14E-01	8.06E-01	2.54E+01	2.73E+01	1.01E+00	2.50E+00	2.33E+01
	Post-burn leach 2	<6E+01	3.46E-01	1.84E-01	2.57E-01	2.10E-01	2.42E-01	2.91E-01	<4E-01	3.76E-01
	SUM (MDA = 0)	0	2.33E+01	2.37E+00	4.96E+00	3.47E+01	3.81E+01	1.45E+01	2.99E+00	3.58E+01
Compact TOTAL (MDA = 0)		0	25.44	2.85	5.68	53.19	58.70	15.90	3.83	52.43
Compact TOTAL (MDA = 0) Corrected		0	23.50	2.60	5.30	51.19	56.70	13.91	3.10	50.43

a. There might be some holdover from Segment 3's post-burn leach 1 into post-burn leach 2, but no corrections were made.

37

Table 23. Relative error for the results given for Compact 8-2 in Table 22. No attempts to alter the error were made when the inventories were corrected for driver-particle particle damage.

Compact 8-2										
Uncertainty		Ag-110m	Ce-144	Cs-134	Cs-137	Eu-154	Eu-155	Ru-106	Sb-125	Sr-90
Segment #1	Decon	N/A	N/A	N/A	15.7%	3.4%	5.4%	N/A	N/A	2.0%
	Pre-burn leach 1	N/A	N/A	N/A	21.0%	10.5%	11.1%	N/A	N/A	2.0%
	Pre-burn leach 2	N/A	N/A	N/A	6.1%	14.2%	N/A	24.1%	N/A	4.6%
	Post-burn leach 1	N/A	N/A	N/A	22.8%	3.8%	5.3%	36.0%	N/A	2.0%
	Post-burn leach 2	N/A	N/A	N/A	9.3%	15.5%	31.0%	39.0%	N/A	9.9%
	SUM (MDA = 0)	N/A	N/A	N/A	10.1%	2.9%	3.9%	26.0%	N/A	1.3%
Segment #2	Decon	N/A	N/A	N/A	21.2%	3.3%	5.4%	N/A	N/A	2.0%
	Pre-burn leach 1	N/A	N/A	20.0%	13.3%	3.3%	8.4%	N/A	N/A	2.0%
	Pre-burn leach 2	N/A	N/A	11.0%	8.1%	8.0%	24.5%	16.0%	N/A	2.0%
	Post-burn leach 1	N/A	16.0%	15.0%	8.6%	3.0%	3.4%	N/A	14.0%	2.4%
	Post-burn leach 2	N/A	N/A	15.0%	4.0%	8.0%	11.0%	N/A	10.0%	3.5%
	SUM (MDA = 0)	N/A	16.0%	10.4%	6.5%	2.3%	2.8%	16.0%	12.8%	1.8%
Segment #3	Decon	N/A	N/A	10.5%	4.2%	3.0%	4.8%	N/A	32.0%	2.0%
	Pre-burn leach 1	N/A	N/A	8.0%	15.5%	3.0%	7.2%	N/A	N/A	2.0%
	Pre-burn leach 2	N/A	N/A	N/A	12.2%	15.7%	8.0%	N/A	N/A	2.8%
	Post-burn leach 1	N/A	22.7%	3.0%	3.0%	3.0%	3.0%	15.2%	14.4%	2.0%
	Post-burn leach 2	N/A	20.9%	3.0%	3.0%	5.4%	12.7%	18.7%	N/A	2.0%
	SUM (MDA = 0)	N/A	22.0%	2.1%	2.1%	2.3%	2.5%	13.9%	13.7%	1.5%
Core	Decon	N/A	7.2%	3.0%	3.0%	3.0%	3.7%	3.4%	14.0%	2.0%
	Pre-burn leach 1	N/A	9.4%	3.0%	3.0%	3.4%	5.0%	7.0%	N/A	2.0%
	Pre-burn leach 2	N/A	33.1%	3.5%	3.0%	13.2%	14.5%	N/A	N/A	2.0%
	Post-burn leach 1	N/A	14.5%	3.0%	3.0%	3.0%	3.7%	14.0%	11.5%	2.0%
	Post-burn leach 2	N/A	21.6%	3.0%	3.0%	11.8%	23.7%	22.3%	N/A	2.0%
	SUM (MDA = 0)	N/A	8.5%	1.5%	1.7%	2.3%	2.8%	4.2%	9.9%	1.4%
Compact TOTAL (MDA = 0)		N/A	8.0%	1.3%	1.5%	1.6%	1.9%	4.1%	8.2%	1.0%

4.2.2. Compact 8-2 ICP-MS Results

ICP-MS was used to measure actinides in the RDLBL solutions. Intact TRISO particles will retain all actinides, but exposed kernels, such as in the DTF particles or in damaged TRISO-coated particles, will be subject to leaching during the DLBL process. Table 24 summarizes the actinide content measured from the RDLBL of Compact 8-2, and Table 25 gives the relative error in the measurement values, including the error propagated to the summations. Additional tables (Table 57 and Table 58) in Appendix A-2 provide these results in units of mass and compact fraction. A correction for two damaged particles was applied to the first post-burn leach of Segment 3. The reasoning behind that correction and its implementation is discussed in Section 4.2.3, where it is concluded that the uncorrected values may be more accurate.

Table 24. Particle equivalents for select actinides from ICP-MS of solutions from Compact 8-2. The uncorrected Segment 3 values will reflect what are believed to be real in-pile SiC failures.

Particle Equivalents		Pu-239	Pu-240	U-234	U-235	U-236	U-238
Segment #1	Decon	7.09E-03	<1E-02	<4E-02	8.78E-03	4.05E-03	5.82E-03
	Pre-burn leach 1	<2E-02	<2E-02	<2E-01	7.77E-03	<6E-03	4.89E-03
	Pre-burn leach 2	<1E-02	<1E-02	<1E-01	<6E-03	<4E-03	5.38E-04
	Post-burn leach 1	4.28E-02	7.59E-02	<2E-01	7.19E-03	6.35E-03	6.18E-03
	Post-burn leach 2	<2E-02	<2E-02	<2E-01	<6E-03	<6E-03	<1E-03
	SUM (MDA = 0)	4.99E-02	7.59E-02	0.00E+00	2.37E-02	1.04E-02	1.74E-02
Segment #2	Decon	<8E-03	<1E-02	<4E-02	<4E-03	<4E-03	2.01E-03
	Pre-burn leach 1	<4E-02	<2E-02	<2E-01	<8E-03	<6E-03	<2E-03
	Pre-burn leach 2	<4E-02	<4E-02	<2E-01	<8E-03	<6E-03	<2E-03
	Post-burn leach 1	1.63E-01	2.92E-01	<2E-01	5.18E-02	2.70E-02	6.37E-02
	Post-burn leach 2	<4E-02	<2E-02	<2E-01	<8E-03	<6E-03	<2E-03
	SUM (MDA = 0)	1.63E-01	2.92E-01	0.00E+00	5.18E-02	2.70E-02	6.57E-02
Segment #3	Decon	<8E-03	<1E-02	<4E-02	1.83E-02	1.47E-02	1.63E-02
	Pre-burn leach 1	<2E-02	<2E-02	<2E-01	<6E-03	<6E-03	1.77E-03
	Pre-burn leach 2	<4E-02	<4E-02	<2E-01	<8E-03	<6E-03	<2E-03
	Post-burn leach 1	1.89E+00	2.17E+00	1.91E+00	1.89E+00	1.84E+00	1.82E+00
	Post-burn leach 1 Correction	0	1.70E-01	0	0	0	0
	Post-burn leach 2[a]	1.75E-01	1.88E-01	<2E-01	1.68E-01	1.59E-01	1.62E-01
	SUM (MDA = 0)	2.06E+00	2.36E+00	1.91E+00	2.08E+00	2.02E+00	2.00E+00
	SUM (MDA = 0) Correction	1.75E-01	3.58E-01	0	1.86E-01	1.74E-01	1.80E-01
Core	Decon	5.91E+00	5.19E+00	9.42E+00	9.77E+00	9.25E+00	8.66E+00
	Pre-burn leach 1	9.42E+00	9.10E+00	1.23E+01	1.26E+01	1.22E+01	1.18E+01
	Pre-burn leach 2	1.29E-01	1.77E-01	<2E-01	1.94E-02	1.88E-02	1.90E-02
	Post-burn leach 1	5.02E+00	7.09E+00	1.98E+00	1.94E+00	1.90E+00	1.86E+00
	Post-burn leach 2	3.79E-01	4.21E-01	3.51E-01	3.40E-01	3.31E-01	3.29E-01
	SUM (MDA = 0)	2.09E+01	2.20E+01	2.40E+01	2.47E+01	2.37E+01	2.27E+01
Compact TOTAL (MDA = 0)		23.13	24.70	25.93	26.86	25.73	24.74
Compact TOTAL (MDA = 0) Correction		21.24	22.70	24.02	24.97	23.88	22.92

a. There might be some holdover from post-burn leach 1 into post-burn leach 2, but no corrections were made.

Table 25. Relative error in the Compact 8-2 ICP-MS results. No attempts to alter the errors were made when the inventories were corrected for driver-particle particle damage in Segment 3.

Error (%)		Pu-239	Pu-240	U-234	U-235	U-236	U-238
				Compact 8-2			
Segment #1	Decon	20%	N/A	N/A	23%	15%	16%
	Pre-burn leach 1	N/A	N/A	N/A	23%	N/A	6%
	Pre-burn leach 2	N/A	N/A	N/A	N/A	N/A	24%
	Post-burn leach 1	10%	25%	N/A	25%	28%	5%
	Post-burn leach 2	N/A	N/A	N/A	N/A	N/A	N/A
	SUM (MDA = 0)	9%	25%	N/A	13%	18%	6%
Segment #2	Decon	N/A	N/A	N/A	N/A	N/A	20%
	Pre-burn leach 1	N/A	N/A	N/A	N/A	N/A	N/A
	Pre-burn leach 2	N/A	N/A	N/A	N/A	N/A	N/A
	Post-burn leach 1	15%	9%	N/A	9%	18%	5%
	Post-burn leach 2	N/A	N/A	N/A	N/A	N/A	N/A
	SUM (MDA = 0)	15%	9%	N/A	9%	18%	5%
Segment #3	Decon	N/A	N/A	N/A	11%	15%	5%
	Pre-burn leach 1	N/A	N/A	N/A	N/A	N/A	15%
	Pre-burn leach 2	N/A	N/A	N/A	N/A	N/A	N/A
	Post-burn leach 1	7%	7%	14%	5%	5%	5%
	Post-burn leach 2	17%	16%	N/A	7%	9%	5%
	SUM (MDA = 0)	7%	7%	14%	5%	5%	5%
Core	Decon	5%	5%	5%	5%	5%	5%
	Pre-burn leach 1	5%	5%	7%	5%	5%	5%
	Pre-burn leach 2	12%	21%	N/A	11%	27%	10%
	Post-burn leach 1	5%	5%	9%	5%	5%	5%
	Post-burn leach 2	11%	12%	25%	7%	7%	5%
	SUM (MDA = 0)	3%	3%	4%	3%	3%	3%
Compact TOTAL (MDA = 0)		4%	3%	5%	4%	4%	4%

4.2.3. Compact 8-2 Discussion

Considering that only 0.27 particle equivalents of Kr-85 were measured from the entire 1400°C test of Compact 8-2, there were no indications that any TRISO-coated driver particles failed during the FACS test (Stempien and Cai 2024b). Furthermore, the Cs-134 quantity measured from that test was accrued gradually and amounted to 0.17 particle equivalents, meaning there was no evidence any driver-particle SiC layers failed during the test. The Eu-154 and Sr-90 releases during the FACS test were also small, at about 0.5 and 0.1 particle equivalents, respectively. If there were any TRISO coatings or SiC layers that had been degraded during the AGR-3/4 irradiation, they were not apparent from the FACS test results.

The RDLBL results were reviewed for signs of driver particle damage that may interfere with the observations of fission product transport specifically originating in the DTF particles. Segments 1 and 2 both had low quantities of Cs, Ce, Ru, Pu, and U; therefore, it is concluded that no driver particles were damaged in those segments. In Segment 3, the amounts of Cs, Ce, Ru, Pu, and U were also low in all the steps before the first post-burn-leach of that segment. However, in the first post-burn leach of Segment 3, about 2 particle equivalents of Ce, U, and Pu were measured. Segment 3 was outside of the compact core where the DTF particles reside; therefore, it appears that two TRISO-coated driver particles were leached in this step.

It is possible that these two particles had been accidentally damaged between the end of the second pre-burn leach and the end of the first post-burn leach. Alternatively, this behavior may indicate that these particles had SiC layer failures in-pile. AGR-1-type TRISO fuel particles (the same type used in AGR-3/4) had low in-pile SiC failure rates of ≤3.1E-5 (at 95% confidence) (Demkowicz et al. 2015b).

However, it appears in-pile SiC failure may well explain the observations from FACS testing and RDLBL of this compact. The average Cs-134 and Cs-137 M/C ratios for intact particles from each segment and the core of Compact 8-2 are listed in Table 26. In each case, the average M/C is 0.93 to 1.02. If two intact TRISO-coated particles were accidentally damaged during a step of the RDLBL process, about 2 particle equivalents of Cs would be detected in the offending step. Instead, about 2 particle equivalents of Ce, U, and Pu were measured with a simultaneously low Cs-134 quantity (about 0.24 particle equivalents) in the first post-burn leach from Segment 3. These relative amounts might be expected from in-pile SiC failures, where most of the Cs-134 from these two particles was released from the compact during irradiation while the Ce and actinides were largely retained. Half of a SiC shell was found among the particles after the second post-burn leach of the Segment 3 material had been completed (see Figure 17). This could be the remains of one of the two particles that might have in-pile SiC failures.

A correction could be made for Segment 3 by subtracting up to 2 particle equivalents from the nuclide inventories measured in the first post-burn leach using the correction methodology described at the top of Section 4. Both corrected and uncorrected values are shown in Table 22 and Table 24. The second post-burn leach in Segment 3 may contain some holdover that originated in these two failed-SiC particles that was not completely leached in the first post-burn leach, but it is impossible to conjecture how much is holdover. If these two particles indeed experienced in-pile SiC failure, the fission product profiles outside of Segment 3 (e.g., Segments 1 and 2) would be influenced by these failures. However, it is not clear to what extent any fission products from these two Segment-3 particles could have migrated to other segments in the compact. By subtracting two particle equivalents from Segment 3, the correction assumes that fission products from these particles remained in Segment 3. Given the evidence presented in the preceding paragraph, it appears in-pile SiC failure may well explain the observations from FACS testing and RDLBL of this compact. On that basis, the uncorrected results in Table 22 and Table 24 are believed to better reflect the true fission product concentration profiles that developed from irradiation and subsequent FACS testing. In that case, the segment 3 inventories will reflect the OPyC and matrix inventories and the kernel inventories of the two failed-SiC particles.

The results from the compact core suggest that some driver particles were leached during RDLBL. It is unclear exactly how many particles were affected, but the U, Pu, and Ce values indicate 1–5 driver particles. About 23 particle equivalents of Ce-144 and about 21 to 25 particle equivalents of various U and Pu isotopes were measured. Additionally, because of the 20 DTF particles (whose contents were also being leached), it is difficult to tell when in the process these driver particles may have been leached and whether they were the result of accidental damage or had another cause. As a result, no corrections have been made in the core. The DLBL results from Compact 8-2 are further discussed in Section 4.5.3 in comparison to Compact 8-1 and other results from the Capsule 8 mass balance.

Table 26. The average ratio of measured individual particle over calculated particle (M/C) Cs values and the standard deviation.

Compact 8-2	# of particles	Cs-134 M/C	Cs-137 M/C
Segment 1	29	0.93 ± 0.25	1.02 ± 0.21
Segment 2	29	0.95 ± 0.08	1.00 ± 0.09
Segment 3	30	0.96 ± 0.07	1.02 ± 0.08
Core	28	0.93 ± 0.18	0.98 ± 0.19
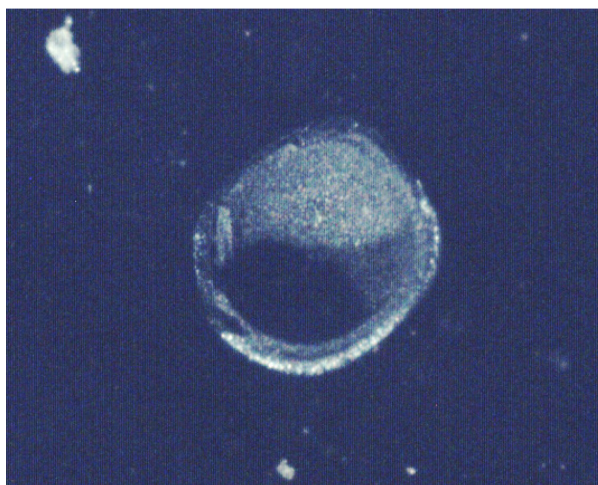
Figure 17. Half of a SiC shell found among the burn-back TRISO particles inspected after the second post-burn leach of the Segment 3 material from Compact 8-2.

4.3. Compact 1-2 RDLBL Results

Compact 1-2 was loaded into a storage rack in the NRAD reactor tank at the same time that Compact 4-3 was loaded into the NRAD C4SW core position. Compact 1-2 remained in this low-flux storage rack while Compact 4-3 was reirradiated. Then, Compact 1-2 was moved from the storage rack and reirradiated in the C4SW position for 120 h (ending on August 7, 2021). The compact was gamma scanned on the PGS, and then it was loaded into the FACS furnace. No unusual challenges were encountered during the RDLBL of this compact (see Section 3.3).

As was the practice with all reirradiated AGR-3/4 compacts, physics calculations were performed to predict the inventory of fission products in Compact 1-2 after reirradiation. The quantities measured in the FACS test and subsequent RDLBL were compared to those predictions to give an estimate of the release/retention of key nuclides. As shall be discussed in the next few sections, the comparisons between the predicted values (from physics calculations) and the values measured from RDLBL gave abnormal results for certain nuclides in the compact core.

4.3.1. Compact 1-2 Gamma-emitter and Sr-90 Results

The total amounts of key fission products measured in Compact 1-2 outside of the driver-fuel SiC layer for each segment of the RDLBL are summarized in Table 27. The measured activities were decay-corrected to the end of the NRAD reirradiation and compared to the predicted inventories in the fuel following the reirradiation. Additional results in units of activity and compact fraction can be found in Table 59 and Table 60 of Appendix A-3. Table 28 gives the relative error for these results. Section 2.5 described how the measurement errors were determined. Values denoted by "<" are derived from MDAs and should be considered an upper bound on the activity of a given nuclide. In summations, the MDAs were set equal to zero. Data points for which the results are most in question (i.e., the core inventories of Ce-144, Eu-154, Eu-155, and Ru-106) are shown in light gray font. The measurement values from the RDLBL experiment and the calculated values were checked and rechecked. The Ce-144, Eu-154, Eu-155, and Ru-106 values in the core appear to be the most abnormal, which suggests the problem lies with the measured values for those nuclides specifically in the core. Furthermore, preliminary results from the FACS test of Compact 1-2 seem reasonable, which would also suggest that it is the measurement values for some of the nuclides in the compact RDLBL core that are the problem.

Table 27. Particle-equivalent inventories measured in the solutions from the radial deconsolidation of Compact 1-2. All values were decay-corrected to the date and time of the end of the NRAD reirradiation and compared to the post-reirradiation inventories calculated in work by Gleicher. Data with abnormal results are in gray font.

Compact 1-2		Ag-110m	Ce-144	Cs-134	Cs-137	Eu-154	Eu-155	Ru-106	Sb-125	Sr-90
Particle Equivalents		**Ag-110m**	**Ce-144**	**Cs-134**	**Cs-137**	**Eu-154**	**Eu-155**	**Ru-106**	**Sb-125**	**Sr-90**
Segment #1	Decon	<2E+1	4.56E-2	4.72E-3	4.47E-3	5.62E-2	4.27E-2	1.40E-1	<2E-3	3.75E-2
	Pre-burn leach 1	<8E+0	<2E-3	2.10E-2	1.04E-2	2.16E-2	<8E-3	3.71E-2	<2E-3	1.22E-2
	Pre-burn leach 2	<1E+1	<4E-3	1.09E-2	4.74E-3	5.61E-3	<2E-2	<2E-2	<2E-3	3.69E-3
	Post-burn leach 1	<1E+1	1.02E-2	1.04E-2	5.27E-3	1.32E-1	8.17E-2	<2E-2	<1E-3	6.08E-2
	Post-burn leach 2	<8E+0	<2E-3	8.29E-3	3.67E-3	<6E-3	4.38E-3	<2E-2	<1E-3	2.84E-3
	SUM (MDA = 0)	0	5.58E-2	5.53E-2	2.85E-2	2.16E-1	1.29E-1	1.77E-1	0.00E+0	1.17E-1
Segment #2	Decon	<4E+1	8.23E-2	9.83E-3	1.17E-2	4.91E-2	2.43E-2	3.46E-1	<8E-3	3.31E-2
	Pre-burn leach 1	<4E+0	<1E-3	9.04E-3	4.66E-3	1.48E-2	1.04E-2	1.95E-2	1.62E-3	6.99E-3
	Pre-burn leach 2	<1E+1	1.21E-2	9.88E-3	5.02E-3	9.47E-2	8.04E-2	<2E-2	<2E-3	4.09E-2
	Post-burn leach 1	<1E+1	<4E-3	1.73E-2	1.03E-2	2.36E-1	1.34E-1	<4E-2	<4E-3	8.72E-2
	Post-burn leach 2	<1E+1	<4E-3	4.12E-2	1.70E-2	<1E-2	<2E-2	<2E-2	<4E-3	3.39E-3
	SUM (MDA = 0)	0	9.44E-2	8.73E-2	4.86E-2	3.95E-1	2.49E-1	3.65E-1	1.62E-3	1.72E-1
Segment #3	Decon	<2E+1	1.19E-1	1.54E-2	1.95E-2	7.59E-2	4.51E-2	2.90E-1	6.43E-3	9.85E-2
	Pre-burn leach 1	<8E+0	<4E-3	1.45E-2	9.71E-3	4.20E-2	2.14E-2	9.03E-2	<2E-3	2.94E-2
	Pre-burn leach 2	<1E+1	<2E-3	8.43E-3	4.85E-3	1.29E-2	8.04E-3	<4E-2	<2E-3	4.75E-3
	Post-burn leach 1	<1E+1	<4E-3	1.40E-2	1.03E-2	3.69E-1	2.18E-1	<2E-2	3.36E-3	2.80E-1
	Post-burn leach 2	<8E+0	<2E-3	5.26E-3	3.14E-3	9.63E-3	<8E-3	1.90E-2	<8E-4	2.94E-3
	SUM (MDA = 0)	0	1.19E-1	5.76E-2	4.75E-2	5.10E-1	2.93E-1	3.99E-1	9.79E-3	4.16E-1
Core	Decon	<4E+1	4.87E+0	8.92E-2	1.11E-1	1.90E+0	1.90E+0	1.16E+0	3.05E-2	3.28E+0
	Pre-burn leach 1	<8E+2	3.24E+1	1.93E+0	2.22E+0	7.08E+0	7.70E+0	8.84E+1	3.30E-1	5.64E+0
	Pre-burn leach 2	<8E+2	1.80E+0	5.59E-1	4.19E-1	7.84E-1	7.57E-1	2.57E+1	1.88E-1	3.55E+0
	Post-burn leach 1	<8E+2	3.66E+1	8.36E-1	9.03E-1	5.66E+1	6.93E+1	7.28E+0	3.58E-1	7.75E-1
	Post-burn leach 2	<2E+2	1.09E+0	1.60E-1	7.35E-2	4.18E-1	4.31E-1	1.08E+1	7.31E-2	3.95E+0
	SUM (MDA = 0)	0	7.67E+1	3.57E+0	3.72E+0	6.67E+1	8.01E+1	1.33E+2	9.79E-1	1.72E+1
Compact TOTAL (MDA = 0)		0	77.02	3.77	3.85	67.86	80.76	134.31	0.99	17.90

Table 28. Relative error for the fission products measured from the RDLBL of Compact 1-2.

	Error	Ag-110m	Ce-144	Cs-134	Cs-137	Eu-154	Eu-155	Ru-106	Sb-125	Sr-90
						Compact 1-2				
Segment #1	Decon	N/A	15.0%	17.2%	4.5%	21.9%	23.0%	18.5%	N/A	2.0%
	Pre-burn leach 1	N/A	N/A	3.0%	3.0%	17.6%	N/A	30.1%	N/A	2.0%
	Pre-burn leach 2	N/A	N/A	6.9%	3.7%	32.0%	N/A	N/A	N/A	2.0%
	Post-burn leach 1	N/A	27.5%	5.7%	4.0%	5.7%	15.7%	N/A	N/A	2.0%
	Post-burn leach 2	N/A	N/A	5.8%	3.7%	N/A	27.0%	N/A	N/A	2.1%
	SUM (MDA = 0)	N/A	13.2%	2.7%	1.7%	7.0%	12.6%	16.0%	N/A	1.2%
Segment #2	Decon	N/A	25.3%	12.7%	3.8%	17.9%	27.9%	16.2%	N/A	2.0%
	Pre-burn leach 1	N/A	N/A	4.0%	3.0%	12.8%	17.8%	32.6%	33.0%	2.0%
	Pre-burn leach 2	N/A	27.8%	5.7%	4.0%	6.8%	16.7%	N/A	N/A	2.4%
	Post-burn leach 1	N/A	N/A	5.3%	4.0%	4.4%	13.4%	N/A	N/A	2.0%
	Post-burn leach 2	N/A	N/A	3.0%	3.0%	N/A	N/A	N/A	N/A	2.0%
	SUM (MDA = 0)	N/A	22.3%	2.4%	1.7%	3.8%	9.4%	15.4%	33.0%	1.2%
Segment #3	Decon	N/A	21.7%	5.4%	3.0%	9.6%	18.2%	11.0%	7.0%	2.0%
	Pre-burn leach 1	N/A	N/A	4.6%	3.0%	10.3%	10.0%	17.6%	N/A	2.0%
	Pre-burn leach 2	N/A	N/A	6.0%	3.4%	27.6%	24.0%	N/A	N/A	2.0%
	Post-burn leach 1	N/A	N/A	4.0%	3.0%	3.0%	9.0%	N/A	25.0%	2.0%
	Post-burn leach 2	N/A	N/A	7.9%	3.7%	36.4%	N/A	35.0%	N/A	2.0%
	SUM (MDA = 0)	N/A	21.7%	2.4%	1.6%	2.9%	7.3%	9.1%	9.7%	1.4%
Core	Decon	N/A	3.7%	4.9%	3.0%	3.8%	8.2%	13.6%	5.0%	2.0%
	Pre-burn leach 1	N/A	3.7%	3.0%	3.0%	5.2%	8.6%	3.0%	19.1%	2.0%
	Pre-burn leach 2	N/A	9.1%	4.9%	3.0%	24.6%	21.8%	4.9%	6.0%	2.0%
	Post-burn leach 1	N/A	3.4%	3.3%	3.0%	3.0%	3.7%	23.9%	11.8%	2.0%
	Post-burn leach 2	N/A	8.9%	6.9%	3.6%	16.9%	24.3%	6.4%	8.0%	2.0%
	SUM (MDA = 0)	N/A	2.3%	2.0%	2.0%	2.6%	3.3%	2.6%	7.9%	1.0%
Compact TOTAL (MDA = 0)		N/A	2.3%	1.9%	1.9%	2.6%	3.3%	2.6%	7.8%	0.9%

4.3.2. Compact 1-2 ICP-MS Results

Table 29 summarizes the actinide content measured from the RDLBL of Compact 1-2, and Table 30 gives the relative error in the measurement values, including the error propagated to the summations. Section 2.5 described the origin of the calculated values and the measurement errors. Additional tables (Table 61 and Table 62) in Appendix A-3 provide these results in units of mass and compact fraction.

Table 29. Summary of ICP-MS results for select actinides from the Compact 1-2 RDLBL.

Compact 1-2							
Particle Equivalents		Pu-239	Pu-240	U-234	U-235	U-236	U-238
Segment #1	Decon	7.95E-2	8.30E-2	3.31E-1	3.26E-1	3.51E-1	3.35E-1
	Pre-burn leach 1	1.21E-2	1.50E-2	<1E-02	8.02E-3	1.73E-2	4.55E-2
	Pre-burn leach 2	<4E-03	<1E-02	<8E-03	5.63E-4	2.83E-4	3.37E-4
	Post-burn leach 1	9.03E-3	<1E-02	<8E-03	2.15E-3	3.81E-3	7.30E-3
	Post-burn leach 2	<4E-03	<1E-02	<8E-03	<2E-04	<2E-04	<2E-04
	SUM (MDA = 0)	1.01E-1	9.80E-2	3.31E-1	3.37E-1	3.72E-1	3.88E-1
Segment #2	Decon	1.60E-1	1.62E-1	6.14E-1	5.94E-1	6.28E-1	5.94E-1
	Pre-burn leach 1	4.74E-3	<8E-03	<8E-03	2.14E-3	2.13E-3	2.23E-3
	Pre-burn leach 2	8.75E-3	<1E-02	<8E-03	1.65E-3	3.39E-3	5.19E-3
	Post-burn leach 1	<6E-03	<1E-02	<1E-02	1.35E-3	2.32E-3	1.61E-3
	Post-burn leach 2	<4E-03	<1E-02	<8E-03	4.61E-4	<8E-04	7.41E-4
	SUM (MDA = 0)	1.74E-1	1.62E-1	6.14E-1	6.00E-1	6.36E-1	6.04E-1
Segment #3	Decon	1.91E-1	1.90E-1	6.44E-1	6.46E-1	6.67E-1	6.30E-1
	Pre-burn leach 1	6.53E-3	3.70E-3	<2E-03	8.68E-4	8.70E-4	1.11E-3
	Pre-burn leach 2	<1E-03	<2E-03	<2E-03	<6E-05	<8E-05	<6E-05
	Post-burn leach 1	1.13E-3	<1E-03	<1E-03	2.41E-4	3.64E-4	2.50E-4
	Post-burn leach 2	<1E-03	<2E-03	<2E-03	<6E-05	<8E-05	<6E-05
	SUM (MDA = 0)	1.99E-1	1.93E-1	6.44E-1	6.47E-1	6.68E-1	6.32E-1
Core	Decon	6.56E+0	6.49E+0	1.12E+1	1.09E+1	1.13E+1	1.10E+1
	Pre-burn leach 1	9.38E+0	9.19E+0	7.54E+0	7.28E+0	7.54E+0	7.28E+0
	Pre-burn leach 2	7.47E-2	7.32E-2	1.79E-2	1.74E-2	1.66E-2	1.93E-2
	Post-burn leach 1	2.46E+0	2.45E+0	2.12E-1	2.09E-1	2.18E-1	2.14E-1
	Post-burn leach 2	1.45E-2	1.66E-2	5.42E-3	3.44E-3	3.21E-3	3.89E-3
	SUM (MDA = 0)	1.85E+1	1.82E+1	1.89E+1	1.84E+1	1.91E+1	1.85E+1
Compact TOTAL (MDA = 0)		18.97	18.67	20.52	20.00	20.74	20.10

Table 30. Relative error in the Compact 1-2 ICP-MS results.

	Compact 1-2						
Error (%)		Pu-239	Pu-240	U-234	U-235	U-236	U-238
Segment #1	Decon	9%	14%	9%	5%	7%	5%
	Pre-burn leach 1	22%	25%	N/A	11%	17%	5%
	Pre-burn leach 2	N/A	N/A	N/A	30%	5%	19%
	Post-burn leach 1	22%	N/A	N/A	11%	20%	9%
	Post-burn leach 2	N/A	N/A	N/A	N/A	N/A	N/A
	SUM (MDA = 0)	8%	12%	9%	5%	7%	4%
Segment #2	Decon	7%	18%	7%	5%	5%	5%
	Pre-burn leach 1	30%	N/A	N/A	17%	15%	9%
	Pre-burn leach 2	23%	N/A	N/A	11%	20%	9%
	Post-burn leach 1	N/A	N/A	N/A	12%	30%	14%
	Post-burn leach 2	N/A	N/A	N/A	16%	N/A	7%
	SUM (MDA = 0)	7%	18%	7%	5%	5%	5%
Segment #3	Decon	9%	9%	7%	7%	7%	7%
	Pre-burn leach 1	21%	24%	N/A	17%	31%	9%
	Pre-burn leach 2	N/A	N/A	N/A	N/A	N/A	N/A
	Post-burn leach 1	20%	N/A	N/A	20%	25%	10%
	Post-burn leach 2	N/A	N/A	N/A	N/A	N/A	N/A
	SUM (MDA = 0)	8%	9%	7%	7%	7%	7%
Core	Decon	5%	5%	5%	5%	5%	5%
	Pre-burn leach 1	5%	5%	5%	7%	5%	5%
	Pre-burn leach 2	12%	17%	20%	7%	19%	5%
	Post-burn leach 1	5%	5%	12%	5%	7%	5%
	Post-burn leach 2	12%	25%	5%	14%	19%	9%
	SUM (MDA = 0)	3%	3%	4%	4%	4%	4%
Compact TOTAL (MDA = 0)		4%	4%	4%	5%	4%	4%

4.3.3.   Compact 1-2 Discussion

Based on the quantities of U and Pu nuclides measured, the RDLBL results do not indicate there were any particles with failed SiC or TRISO coatings in Compact 1-2. In total, 20 particle equivalents of U-235 and U-238 were measured from the Compact 1-2 RDLBL. These amounts are attributable to the 20 DTF particles in this compact. This indicates complete retention of all the U from the DTF particles, and about 92% of all this U was detected in the core. There is good confidence in this conclusion because the long half-lives of these nuclides and the comparatively short reirradiation in NRAD resulted in predicted inventories of these nuclides that varied negligibly between the as-run ATR predictions (Sterbentz 2015) and the post-NRAD prediction performed by Gleicher in work that has not yet been reported.

The uranium and plutonium comparisons were reasonable and self-consistent. However, the Ce-144 and Ru-106, which should generally agree with the U and Pu values, were much different than the U and Pu quantities measured in the core. From the work presented in this report and the work completed previously (Hunn et al. 2020, Helmreich et al. 2021, Helmreich et al. 2022, Stempien and Cai 2024a), the ratios of total particle equivalents (or compact fractions) of Ce-144 to U-238 in AGR-3/4 compacts subjected to RDLBL most often range from about 0.9 to 1.05. For Compact 1-2, the ratio of Ce-144:U-238 detected via RDLBL is 3.8. In prior work (Hunn et al. 2020; Helmreich et al. 2021; Helmreich et al. 2022; Stempien and Cai 2024a), the Ru-106 to U-238 ratios were most often from about 0.6 to 0.9. Here, the Ru-106:U-238 ratio is 6.7. The disparity in relative amounts of Ru and U and Ce suggests something is wrong with the Ce and Ru M/C values.

Like Ce-144 and Ru-106, the total Eu-154 and Eu-155 inventories from RDLBL were also higher than expected. Eu may diffuse to some extent through intact TRISO coatings, so an M/C value significantly greater than 20 particle equivalents does not necessarily indicate an abnormal result. The 68 particle equivalents of Eu-154 measured in Compact 1-2 via RDLBL are higher than what was seen in as-irradiated Capsule 7 and 8 compacts that had much higher average irradiation temperatures. As-irradiated Compacts 8-3, 7-3, and 7-4 were found to have about 50 to 55 particle equivalents of Eu-154 and about 40-48 particle equivalents of Sr-90 (Stempien and Cai 2024a). Like Compact 1-2, Compact 8-2 was also FACS-tested at 1400°C, but Compact 8-2 was found via RDLBL to have about 51 particle equivalents of Eu-154 and 50 particle equivalents of Sr-90. These amounts from Compact 8-2 are similar to what was found in as-irradiated Compact 8-3 and suggest there was little or no additional release of Eu-154 through the intact TRISO coatings in that compact during the 1400°C exposure of Compact 8-2 while in FACS. Perhaps a more telling comparison is that as-irradiated Compacts 1-4 and 1-3 had about 16 and 18 particle equivalents of Eu-154, respectively, and about 24 to 26 particle equivalents of Sr-90, respectively. For Compact 1-2 to have 68 particle equivalents of Eu-154 in it from RDLBL, it would have had to release over 40 particle equivalents of Eu-154 through intact SiC coatings into the OPyC and matrix during the 1400°C FACS test, and that is not credible based on the data collected from other AGR-3/4 compacts and tests. By comparison, the Sr-90 value of 17.9 particle equivalents measured in the Compact 1-2 RDLBL is reasonable. Ordinarily, the Sr and Eu behaviors are very similar; the fact that the Sr-90 inventory is reasonable, but the Eu-154 is not reasonable, is another indication of odd results for the Eu measurements and/or calculations in this compact.

Along with the reasonable Sr-90 M/C value, the Cs-134 and Cs-137 M/Cs were also reasonable at about 3.8 particle equivalents. FACS-tested AGR-3/4 compacts with similar RDLBL totals of Cs-134 and Cs-137 included 8-2 (2.9 and 5.7, respectively), 3-2 (2.4 and 4.3, respectively), and 8-1 (1.7 and 2.9, respectively). From the 1400°C FACS test of Compact 1-2, about 14 particle equivalents of Cs-134 were measured. Adding to that number, the 3.8 particle equivalents measured from the RDLBL, the total comes out to 17.8 particle equivalents of Cs-134 that were measured from this compact. As-irradiated Compacts 1-3 and 1-4 were found via RDLBL to have about 15 particle equivalents of Cs-134 (Hunn et al. 2020; Helmreich et al. 2022). The mass balance in Capsule 1 gives some indication that each Capsule 1 compact released about 1.25 particle equivalents of Cs-134 on average in-pile during irradiation in ATR.

Therefore, the total amount of Cs-134 measured (17.8 particle equivalents) between the FACS test and the post-FACS RDLBL is reasonable for Compact 1-2.

In summary, the RDLBL M/C values for nuclides of U and Pu, Cs-134, Cs-137, and Sr-90 are reasonable, but the Ce-144, Eu-154, Eu-155, and Ru-106 M/Cs are abnormally high. The only place where those M/C values abnormally high is in the RDLBL core, which suggests the problem lies with the measured values for those nuclides in the core only. Supporting this assertion is that the preliminary FACS M/C values results appearing reasonable for all the long-lived nuclides, including Ce-144, Eu-154, Eu-155, and Ru-106. It is not known why these particular measured values are abnormally high, but there is no reasonable physical or phenomenological explanation for it. It appears to be an error in the radiochemistry in the compact core samples. The results from Segments 1–3 are believed to be correct.

4.4.   Compact 3-1 RDLBL Results

Compact 3-1 was reirradiated in NRAD for about 114 h. It was then gamma scanned via PGS and loaded into the FACS furnace. In the FACs furnace, the compact was heated to 1600°C and held for about 200 h. To facilitate the completion of another FACS test, this test was cut short. This compact was then transferred to AL for RDLBL.

Some difficulties were encountered in the RDLBL of Compact 3-1 (see Section 3.4), and several mounting attempts were required before the deconsolidation started. Two radial segments were obtained; however, only 12 minutes of radial deconsolidation were completed before the compact fell off the rod during the second segment. As shall be discussed later, it seems these problems could have damaged some of the particles, particularly in Segment 1.

4.4.1.   Compact 3-1 Gamma-emitter and Sr-90 Results

The total amounts of key fission products measured in Compact 3-1 outside of the driver fuel SiC layers for each segment of the radial deconsolidation are summarized in Table 31. Additional results in units of activity and compact fraction can be found in Table 63 and Table 64 of Appendix A-4, Compact 3-1. Table 32 summarizes the relative errors for these quantities. Section 2.5 described how the measurement errors were determined. Values denoted by "<" are derived from MDAs and should be considered an upper bound on the activity of a given nuclide. In summations, MDAs were set equal to zero.

Table 31. Particle-equivalent inventories measured in the solutions from the radial deconsolidation of Compact 3-1. The measured values were compared to the inventories calculated by Gleicher (not currently referenceable) following reirradiation in NRAD. All values were decay-corrected to ATR EOI + 1 day.

Compact 3-1										
Particle Equivalents		Ag-110m	Ce-144	Cs-134	Cs-137	Eu-154	Eu-155	Ru-106	Sb-125	Sr-90
Segment #1[a]	Decon	<4E+01	1.1E+00	6.7E-02	1.6E-01	7.7E-01	9.0E-01	8.6E-01	4.5E-01	1.0E+00
	Pre-burn leach 1	<6E+01	<6E-02	3.6E-01	4.6E-01	2.2E-01	2.6E-01	9.3E-02	9.3E-02	2.3E-01
	Pre-burn leach 2	<6E+01	<6E-02	1.3E-01	1.7E-01	5.0E-02	5.4E-02	<2E-01	<8E-02	9.5E-02
	Post-burn leach 1	<1E+02	6.1E+00	2.1E+00	2.5E+00	5.2E+00	6.0E+00	4.9E+00	2.6E+00	5.7E+00
	Post-burn leach 2	<6E+01	<1E-01	7.4E-01	9.0E-01	2.1E-01	2.8E-01	2.1E-01	3.0E-01	4.2E-01
	SUM (MDA = 0)	0	7.1E+00	3.4E+00	4.2E+00	6.4E+00	7.5E+00	6.0E+00	3.4E+00	7.5E+00
Segment #2	Decon	<8E+00	4.9E-02	2.3E-02	7.6E-02	2.2E-01	2.5E-01	1.1E-02	<1E-02	4.7E-01
	Pre-burn leach 1	<2E+01	<2E-02	7.3E-03	1.1E-02	2.7E-01	3.4E-01	2.4E-02	2.3E-02	3.8E-01
	Pre-burn leach 2	<2E+01	<2E-02	3.5E-03	3.5E-03	2.2E-02	2.6E-02	<4E-02	1.0E-02	6.1E-02
	Post-burn leach 1	<6E+01	<6E-02	3.6E-03	3.4E-03	2.2E+00	2.5E+00	<1E-01	4.1E-02	2.7E+00
	Post-burn leach 2	<2E+01	<2E-02	2.5E-03	2.5E-03	2.5E-02	3.0E-02	<2E-02	7.8E-03	7.7E-03
	SUM (MDA = 0)	0	4.9E-02	4.0E-02	9.6E-02	2.7E+00	3.1E+00	3.5E-02	8.3E-02	3.6E+00
Core	Decon	<4E+01	1.9E+00	1.6E-01	5.1E-01	8.7E-01	1.1E+00	6.1E-01	<6E-02	1.2E+00
	Pre-burn leach 1	<1E+02	5.4E+00	9.5E-01	1.1E+00	2.8E+00	3.2E+00	4.5E+00	4.6E-01	3.0E+00
	Pre-burn leach 2	<8E+01	1.1E-01	3.2E-01	3.5E-01	8.2E-02	1.4E-01	2.2E-01	1.5E-01	1.6E-01
	Post-burn leach 1	<4E+02	1.4E+01	1.0E+00	1.2E+00	7.5E+00	8.5E+00	7.5E-01	1.1E+00	6.1E+00
	Post-burn leach 2	<2E+01	<4E-02	2.6E-02	3.0E-02	8.7E-02	1.0E-01	2.9E-01	1.2E-01	1.2E-02
	SUM (MDA = 0)	0	2.2E+01	2.5E+00	3.2E+00	1.1E+01	1.3E+01	6.3E+00	1.8E+00	1.0E+01
Compact TOTAL (MDA = 0)		0	29.0	5.9	7.5	20.4	23.6	12.4	5.3	21.4

a. Section 4.4.3 discusses that Segment 1 had up to nine damaged driver particles and that corrections to the quantities in this segment could not be reasonably made.

Table 32. Relative errors for the results given for Compact 3-1 in Table 31. The errors in the "sum" rows were computed by propagating the measurement error from all the RDLBL steps making up the sum.

		Ag-110m	Ce-144	Cs-134	Cs-137	Eu-154	Eu-155	Ru-106	Sb-125	Sr-90
					Compact 3-1					
Segment #1[a]	Decon	N/A	9.9%	3.0%	3.0%	3.0%	3.8%	5.9%	4.3%	2.0%
	Pre-burn leach 1	N/A	N/A	3.0%	3.0%	6.8%	12.7%	20.0%	16.0%	2.0%
	Pre-burn leach 2	N/A	N/A	3.0%	3.0%	7.1%	23.2%	N/A	N/A	2.0%
	Post-burn leach 1	N/A	8.8%	3.0%	3.0%	3.0%	3.8%	4.7%	4.6%	2.0%
	Post-burn leach 2	N/A	N/A	3.0%	3.0%	6.2%	13.0%	34.0%	19.6%	2.0%
	SUM (MDA = 0)	N/A	7.6%	2.0%	1.9%	2.5%	3.2%	4.0%	4.0%	1.6%
Segment #2	Decon	N/A	25.1%	3.0%	3.0%	3.0%	3.7%	27.0%	N/A	2.0%
	Pre-burn leach 1	N/A	N/A	6.5%	3.0%	3.0%	4.0%	30.0%	9.0%	2.0%
	Pre-burn leach 2	N/A	N/A	10.7%	5.0%	12.5%	16.3%	N/A	33.0%	2.0%
	Post-burn leach 1	N/A	N/A	18.8%	7.2%	3.0%	4.1%	N/A	14.0%	2.0%
	Post-burn leach 2	N/A	N/A	14.5%	6.0%	20.4%	9.0%	N/A	21.0%	3.0%
	SUM (MDA = 0)	N/A	25.1%	3.0%	2.4%	2.5%	3.3%	22.3%	8.7%	1.5%
Core	Decon	N/A	6.1%	3.0%	3.0%	3.0%	4.0%	7.8%	N/A	2.0%
	Pre-burn leach 1	N/A	11.0%	3.0%	3.0%	3.0%	5.6%	4.4%	31.0%	2.0%
	Pre-burn leach 2	N/A	35.0%	3.0%	3.0%	23.4%	26.0%	32.0%	22.0%	2.0%
	Post-burn leach 1	N/A	6.4%	3.0%	3.0%	3.0%	3.7%	29.5%	12.6%	2.0%
	Post-burn leach 2	N/A	N/A	4.3%	3.6%	9.1%	20.3%	9.0%	13.9%	2.0%
	SUM (MDA = 0)	N/A	5.1%	1.7%	1.6%	2.1%	2.8%	4.9%	11.1%	1.3%
Compact TOTAL (MDA = 0)		N/A	26.7%	4.0%	3.5%	4.1%	5.4%	23.2%	14.6%	2.6%

a. Section 4.4.3 discusses that Segment 1 had up to nine damaged driver particles and that corrections to the quantities in this segment could not be reasonably made.

4.4.2. Compact 3-1 ICP-MS Results

Table 33 summarizes the actinide content measured from RDLBL of Compact 3-1 via ICP-MS, and Table 34 gives the relative error in these values. A description of the measurement error was given in Section 2.5. Additional tables (Table 65 and Table 66) in Appendix A-4 provide these results in units of mass and compact fraction.

Table 33. Particle equivalents for selected actinides from ICP-MS of solutions from Compact 3-1 RDLBL.

Compact 3-1							
Particle Equivalents		Pu-239	Pu-240	U-234	U-235	U-236	U-238
Segment #1[a]	Decon	1.36E+00	1.41E+00	2.91E+00	2.86E+00	2.93E+00	2.75E+00
	Pre-burn leach 1	4.56E-02	4.49E-02	5.85E-02	5.84E-02	5.92E-02	5.95E-02
	Pre-burn leach 2	5.69E-03	5.45E-03	<8E-03	2.44E-03	2.32E-03	2.31E-03
	Post-burn leach 1	6.19E+00	6.46E+00	5.99E+00	5.82E+00	5.96E+00	5.65E+00
	Post-burn leach 2	1.18E-01	1.20E-01	1.47E-01	1.46E-01	1.50E-01	1.49E-01
	SUM (MDA = 0)	7.72E+00	8.04E+00	9.11E+00	8.88E+00	9.10E+00	8.61E+00
Segment #2	Decon	3.71E-03	3.66E-03	1.84E-02	1.80E-02	1.80E-02	7.60E-01
	Pre-burn leach 1	<2E-03	<8E-04	<4E-03	1.05E-04	9.40E-05	1.00E-04
	Pre-burn leach 2	<2E-03	<1E-03	<4E-03	<1E-04	<1E-06	<4E-05
	Post-burn leach 1	<2E-03	<1E-03	<4E-03	<1E-04	7.40E-05	7.27E-05
	Post-burn leach 2	<2E-03	<8E-04	<4E-03	<1E-04	3.72E-06	<2E-05
	SUM (MDA = 0)	3.71E-03	3.66E-03	1.84E-02	1.81E-02	1.82E-02	7.61E-01
Core	Decon	4.87E+00	4.83E+00	1.43E+01	1.40E+01	1.39E+01	1.38E+01
	Pre-burn leach 1	5.04E+00	5.30E+00	4.52E+00	4.23E+00	4.43E+00	4.29E+00
	Pre-burn leach 2	1.00E-01	1.07E-01	<2E-02	1.30E-02	1.27E-02	1.29E-02
	Post-burn leach 1	9.92E+00	1.09E+01	2.93E-01	2.03E-01	2.05E-01	2.04E-01
	Post-burn leach 2	1.94E-02	2.18E-02	<2E-03	1.35E-03	8.69E-04	1.32E-03
	SUM (MDA = 0)	1.99E+01	2.12E+01	1.91E+01	1.84E+01	1.86E+01	1.83E+01
Compact TOTAL (MDA = 0)		27.67	29.22	28.22	27.32	27.67	27.69

a. Section 4.4.3 discusses that Segment 1 had up to nine damaged driver particles and that corrections to the quantities in this segment could not be reasonably made.

Table 34. Error in the Compact 3-1 ICP-MS results that were summarized in Table 33.

	Compact 3-1						
Error (%)		Pu-239	Pu-240	U-234	U-235	U-236	U-238
Segment #1[a]	Decon	5%	5%	5%	5%	5%	5%
	Pre-burn leach 1	10%	19%	19%	5%	11%	5%
	Pre-burn leach 2	25%	18%	N/A	14%	13%	7%
	Post-burn leach 1	5%	5%	5%	5%	5%	5%
	Post-burn leach 2	7%	7%	17%	5%	7%	5%
	SUM (MDA = 0)	4%	4%	4%	4%	4%	4%
Segment #2	Decon	5%	7%	7%	5%	5%	5%
	Pre-burn leach 1	N/A	N/A	N/A	5%	12%	5%
	Pre-burn leach 2	N/A	N/A	N/A	N/A	N/A	N/A
	Post-burn leach 1	N/A	N/A	N/A	N/A	11%	5%
	Post-burn leach 2	N/A	N/A	N/A	N/A	17%	N/A
	SUM (MDA = 0)	5%	7%	7%	5%	5%	5%
Core	Decon	5%	5%	5%	5%	5%	5%
	Pre-burn leach 1	5%	7%	5%	9%	5%	5%
	Pre-burn leach 2	7%	13%	N/A	7%	16%	5%
	Post-burn leach 1	5%	5%	17%	5%	7%	5%
	Post-burn leach 2	19%	21%	N/A	22%	15%	7%
	SUM (MDA = 0)	3%	3%	4%	4%	4%	4%
Compact TOTAL (MDA = 0)		3%	3%	3%	3%	3%	3%

a. Section 4.4.3 discusses that Segment 1 had up to nine damaged driver particles and that corrections to the quantities in this segment could not be reasonably made.

4.4.3. Compact 3-1 Discussion

After first epoxying the compact to the deconsolidation rod, the assembly was accidentally exposed to 700°C in air for ~20 minutes. It was supposed to have been heated to only 50°C to ensure complete epoxy curing, but the brief high-temperature exposure oxidized away the epoxy and the compact had to be rebonded to the rod. A handling error after the initial rebonding meant the compact had to be rebonded a second time prior to the start of the RDLBL. There were some significant chips around the rim of the compact before RDLBL started. These could have been deep enough to leave a TRISO particle exposed, but it was not visually obvious that any particles were damaged before the RDLBL. The first segment was deconsolidated, albeit with uneven material removal. After about 12 minutes, the deconsolidation of the second segment was stopped when the compact fell from the rod. When the compact came off the rod, it appeared to have fractured within itself, as some particles and matrix remained bonded to the rod.

The numbers of damaged or degraded TRISO particles and the timing of this damage or degradation are difficult to establish for this compact because of all the processes involved in its PIE (e.g., 1600°C FACS test and the preparation for and execution of RDLBL) and the presence of 20 DTF particles.

From prior FACS tests of as-irradiated AGR-3/4 fuel compacts, up to about 0.3 particle equivalents of Kr-85 were released, indicating the DTF kernels retained little of the Kr-85 generated in-pile during irradiation in ATR. About 0.25 particle equivalents of Cs-134 were released after about 40 h from as-irradiated Compact 3-2 during its exposure at 1600°C in FACS (Section 4.1). An additional 0.17 particle equivalents of Cs-134 were released from that compact during the remainder of the time at 1600°C.

About 1.7 particle equivalents were recovered in the post-FACS RDLBL of that compact (see Table 18). Other as-irradiated FACS tests of AGR-3/4 fuel compacts had even lower Cs-134 releases.

During the post-reirradiation FACS test of Compact 3-1, about 0.77 particle equivalents of Cs-134 were released in the first 40 h, and that release started as soon as the temperature ramp from 300 to 1600°C began. An additional 0.11 particle equivalents of Cs-134 were released over the remaining ~165 h of the test (which ended at roughly the 210-h mark). Coinciding with this Cs release was a release of about 1.8 particle equivalents of Kr-85 in the first 40 h. These quantities of Cs-134 and Kr-85 are larger than those observed from as-irradiated Compact 3-2. This suggests that either Compact 3-2 retained more Kr-85 in its DTF kernels and Cs-134 in its DTF kernels and/or compact matrix than Compact 3-1, or a SiC or TRISO failure could have occurred during the FACS test. Given the quantities of Cs-134 and Kr-85, one hypothesis is that there were two particles that had in-pile SiC failures that subsequently developed into TRISO failures at the beginning of the FACS test. These particles would have retained their Kr-85 until failure of any remaining PyC layers in the FACS furnace, and they would have released some Cs in-pile, reducing the amount of Cs that was available for subsequent release in the FACS furnace. Statistically, however, this is very unlikely.

There were 2.86 and 2.75 particle equivalents of U-235 and U-238, respectively, in the Segment 1 deconsolidation solution (Table 33). The Pu inventories measured in this step were lower, at about 1.4 particle equivalents, and the Ce-144 inventory from the first segment deconsolidation was 1.1 particle equivalents (Table 31). In typical deconsolidation solutions from the compact core (where the DTF particles reside), it is common for the Ce-144 quantity to be lower than the U-238 quantity by a factor of 2–5. It is also common for the Pu inventory in the core deconsolidation solution to be lower than the U quantity by a factor of about 1.5–3 in the same core deconsolidation solution. The total Ce, Pu, and U quantities tend to agree more closely in the two post-burn leach solutions. If the U-238 and U-235 quantities are used as indications of the number of particles leached in the Segment 1 deconsolidation process, there were three TRISO-coated particles affected.

It is unclear what caused these kernels to be exposed to the deconsolidation acid, and there are several hypotheses. It could have been accidental damage from the three attempts to epoxy the compact to the rod or from the chips suffered during handling before RDLBL that roughened the rim of the compact. Or some or all of that uranium could be from particles that had some in-pile degradation that was further exacerbated by the FACS test. In the FACS test, it appeared possible that two particles with prior in-pile SiC failure could have had failures of their remaining PyC layers during the test. Those could account for two of leached kernels in Segment 1. Or what was measured in the FACS test was simply the release of residual inventories of fission products unrelated to any damaged driver particles. The third leached kernel could have been damaged at some point during the RDLBL preparation (where the compact had to be repeatedly attached to the deconsolidation rod) or during the Segment 1 radial deconsolidation itself. Conceivably the third kernel might have been an in-pile TRISO failure, but that is unlikely. There is insufficient evidence to conclude on the cause and timing of the coating damage incurred by these three particles.

Compared to the inventories of U and Pu in the Segment 1 deconsolidation solution (about 3 particle equivalents), the inventory of Cs-134 was low, at about 0.06 particle equivalents. This is reasonably consistent with the hypothesis that two particles had in-pile SiC failures that released some Cs in-pile before releasing much of the rest of their Cs during the FACS test. The quantities of Cs-134 recovered from Segment 1's pre-burn leaches 1 and 2 were 0.36 and 0.13 particle equivalents, respectively. Of all the nuclides detected, Cs-134 and Cs-137 were the only ones that increased from the deconsolidation solution to the pre-burn leach 1 solution. It is not clear why the Cs inventory in the pre-burn leach 1 would be higher than that in the deconsolidation solution while all other nuclides were lower in pre-burn-

leach 1 than in the deconsolidation solution.[a] Perhaps additional Cs in the coatings of the leached particles was accessed and dissolved as the debris was further broken up over time in the pre-burn leaches. As will be discussed below, the post-burn leaches suggest additional particles had in-pile SiC layer failures, and if so, perhaps their Cs-134 was contributing to what was recovered in pre-burn leaches 1 and 2 and what was measured in the FACS furnace.

While the explanations posited based on the FACS and RDLBL results appear to be internally consistent, the coating failures assumed in those explanations have very low probabilities. Particle damage during the DLBL processes is not uncommon (Stempien and Cai 2024a), but SiC failures in-pile or TRISO failures in FACS are rare for AGR-1-type particles. AGR-1 fuel experienced a measured in-pile SiC failure rate of 1.3E-5 (4 out of about 298,000 particles) and no in-pile TRISO failures out of 298,000 particles (Demkowicz et al. 2015b). It must be said that AGR-3/4 fuel is different in that the DTF particles contributed some fission products to the compact matrix that might not otherwise be there. Those could conceivably undergo chemical reactions with TRISO-coated driver particles. Additionally, a lot of the AGR-3/4 fuel had higher irradiation temperatures than AGR-1, which may also have stressed the fuel more than in AGR-1.

Everything discussed above referred only to the Segment 1 deconsolidation and pre-burn leaches. Following the burn, the post-burn leaches of Segment 1 material contained about three particle equivalents of Cs and about six particle equivalents of Ce-144, Eu-154, Sr-90, Pu, and U, in addition to what was measured in the deconsolidation and pre-burn leach solutions. The difference in the amounts of Cs and the other fission products and actinides suggests that these six particles released Cs prior to RDLBL, or that these particles were broken during the burn or first post-burn leach and there was lower recovery of Cs from these broken particles. The recovery of Cs from particles that were broken during RDLBL of as-irradiated compacts was often about 70% of a particle equivalent, not 100% (Stempien and Cai 2024a). The amount of Cs measured in the preceding FACS test is too small to make up the difference between three and six particle equivalents; therefore, these do not appear to be failures in the FACS furnace. Another theory is that there were six TRISO-coated particles with SiC layer failures that occurred in-pile (and released Cs there) that survived the FACS test and were not leached until the Segment 1 post-burn leaches. In addition to the two potential in-pile SiC failures mentioned above, these six particles would have contributed some Cs to what was measured in the FACS test, and in the Segment 1 deconsolidation and pre-burn leach solutions as well. However, given the AGR-1 history and the results of as-irradiated AGR-3/4 RDLBL, it seems unlikely that Compact 3-2 had a total of eight or nine in-pile SiC failures.

Whatever the cause of the apparent particle damage in Layer 1, the number of TRISO particles affected here means the contribution of the DTF particles to the inventories measured in Segment 1 cannot be reasonably determined. Thus, no corrections were applied, and no attempts to distinguish the quantity originating with the DTF particles from that originating in the TRISO-coated particles were made in Segment 1.

The fission product and actinide inventories measured in Segment 2 indicate that there were no exposed kernels or coating damage despite the compact falling from the rod during the radial deconsolidation. The radionuclide quantities generally decreased with each successive step of the Segment 2 RDLBL. Most of the actinide quantities were measured in the deconsolidation solution, with little additional recovery of actinides coming in later steps.

---

[a] There were other instances where the Cs inventory in the pre-burn leach 1 was nearly identical to or greater than in the deconsolidation. This was commonly seen in the core of compacts analyzed at INL. Aside from the core, certain radial segments from Compacts 8-2, 1-2, and 8-1 (discussed in this report) and Compacts 3-3, 7-3, 8-3, and 10-2 (from Stempien and Cai 2024a) had higher Cs inventories in pre-burn leach 1 than in the deconsolidation solution. Interestingly, none of the results at ORNL had higher Cs in a pre-burn leach than in a deconsolidation solution.

Similarly, in the core segment, there were no obvious indications that driver particles had been damaged. The core inventories of U and Pu were between 18 and 21 particle equivalents (depending on the isotope), and the core inventory of Ce-144 was about 22 particle equivalents.

Figure 18 shows a summary of fission products detected from RDLBL of Compact 3-1, released during the 1600/1700°C FACS test, and measured outside of the fuel on the Capsule 3 components. The Capsule 3 mass balance (Stempien et al. 2018b) was divided by four to give the fission product quantity outside of the fuel that was contributed from an average Capsule 3 compact (labeled in the plot as "Capsule 3 inventory/4"). The plot only totals the RDLBL results from Segment 2 and the core. Given the uncertainty in the number and cause of apparent driver particle damage, the Segment 1 RDLBL results were not included in the RDLBL totals in this plot. For most RDLBLs, in the absence of driver particle damage, the total inventory of actinides and fission products in Segment 1 is low; therefore, ignoring the Segment 1 inventories will not significantly impact the estimated total of fission products that originated in the DTF particles.

Similar to Compact 3-2 (which was tested in FACS without reirradiation), the total Cs measured from RDLBL of Compact 3-1, plus the Cs mass balance normalized by the number of compacts, and the Cs release from FACS testing all add up to less than 20 particle equivalents for Compact 3-1. A concern is that this might be due to Cs transporting beyond the sink ring to the stainless-steel capsule shell that was not analyzed. Between the RDLBL, the FACS test, and the mass balance, the total Eu and Sr inventories measured outside of driver particles exceeds 20 particle equivalents, indicating that those nuclides diffused through intact TRISO coatings in appreciable amounts. The portion of that Eu and Sr measured in the compact RDLBL is still significant and demonstrates that the matrix retains a substantial portion of any Eu and Sr outside of intact TRISO fuel particles. The Ce data demonstrate once more that Ce will largely remain in kernels (or at least in the compact matrix near the kernels), even for exposed kernels like the DTF particles. Finally, Ag-110m was not measured in the RDLBL or in the FACS test. This was normal for these AGR-3/4 heating tests, which took place years (and multiple Ag-110m half-lives) after the end of the ATR irradiation. The mass balance, on the other hand, shows that on average, Capsule 3 compacts released more than half their Ag-110m during irradiation.

Segment 1 had eight or nine TRISO-coated particles leached for unexplained reasons. If the inventories measured there are neglected, 6.4 particle equivalents of Ru-106 were measured in the rest of Compact 3-1. A little Ru-106 was detected from the FACS test of Compact 3-1 (1.4 particle equivalents), and no Ru-106 was measured outside of the fuel in the Capsule 3 mass balance. This led to the conclusion that the recovery of Ru-106 from the RDLBL operations was noticeably low relative to the actinide and Ce-144 recoveries. This has been noted previously (Stempien et al. 2021a [Table 11]; Helmreich et al. 2022; Stempien and Cai 2024a).
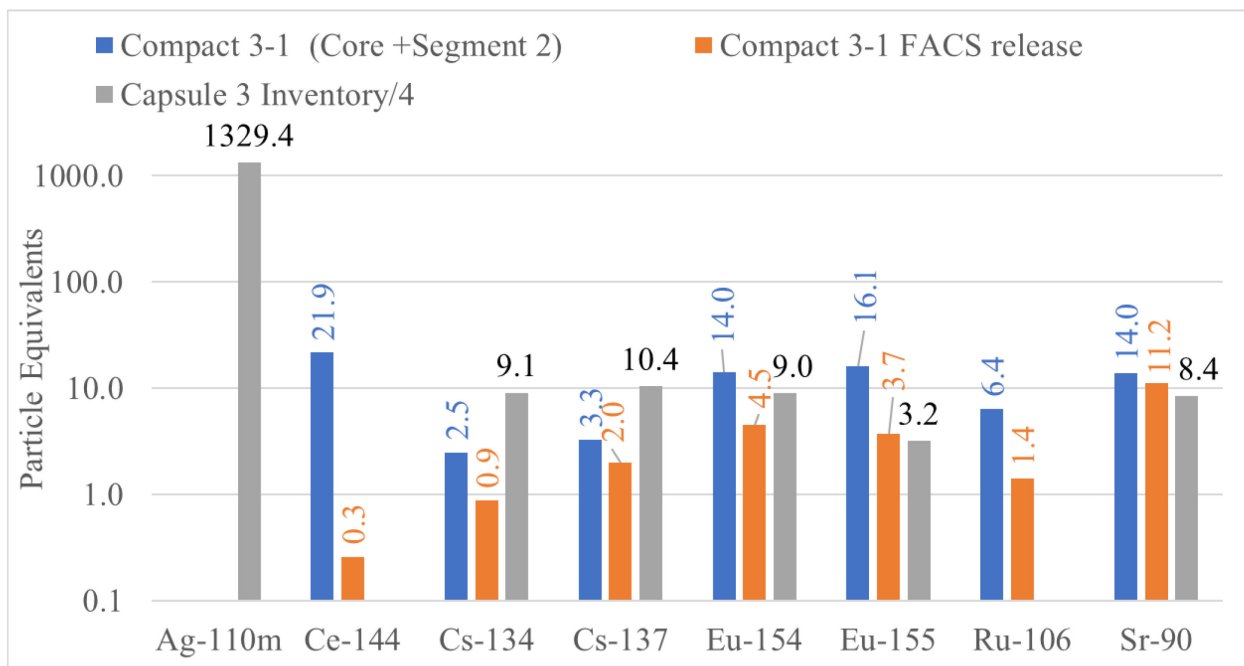
Figure 18. A summary of fission product release during FACS testing at 1600/1700°C, as well as fission product inventories in Compact 3-1 (graphite matrix, OPyC, and DTF of core and Segment 2). A quarter of fission product inventories at Capsule 3 (including foils, felts, spacers, through tubes, inner ring, outer ring, and sink ring) is also included for comparison.

4.5. Compact 8-1 RDLBL Results

Compact 8-1 was reirradiated in NRAD before it was removed and gamma scanned on PGS. It was then loaded into the FACS furnace and heated to 1200°C. Three ramps from near ambient temperature up to 1200°C were performed to see if temperature cycling noticeably affected fission product release. Section 2.2 describes the NRAD and FACS operations in more detail. Section 3.5 described the observations from the RDLBL process, which went well with no apparent problems. No attempts will be made to tie the inventories measured here via RDLBL to possible effects from temperature cycling. Releases from the compact during the FACS test will be discussed in a future report.

4.5.1. Compact 8-1 Gamma-emitter and Sr-90 Results

The total amounts of key fission products measured in Compact 8-1 outside of the driver fuel SiC layers for each segment of the radial deconsolidation are summarized in Table 35. Additional results in units of activity and compact fraction can be found in Table 67 and Table 68 of Appendix A-5, Compact 8-1. Here the measured fission product activities were compared to unreported inventory calculations by Gleicher to account for any additional depletion of the fuel during re-irradiation in NRAD. Note that in Table 35, the Ag-110m result from the Segment 1 post-burn leach 1 was discarded. This solution was measured three times with differing values. In the first measurement, no Ag-110m peaks were identified, and an MDA was reported, just like in the prior steps of the Segment 1 RDLBL. Ag-110m peaks were identified in the second and third measurements with a different detector, but those equated to more than 100 particle equivalents, which is unreasonably high. Given Ag-110m was seldom detected in the RDLBL process for other compacts, no Ag-110m was detected in the deconsolidation and pre-burn leach of Segment 1 of this compact, and the results from different detectors were inconsistent, this Ag-110m value was discarded. Table 36 gives the relative error for these results.

Table 35. Particle-equivalent inventories measured in the solutions from RDLBL of Compact 8-1. The measured values were compared to the inventories calculated by Gleicher following reirradiation in NRAD. All values were decay-corrected back to ATR EOI + 1 day.

Compact 8-1										
Particle Equivalents		Ag-110m	Ce-144	Cs-134	Cs-137	Eu-154	Eu-155	Ru-106	Sb-125	Sr-90
Segment #1	Decon	<2E+01	<6E-02	2.71E-03	9.78E-03	1.23E+00	1.32E+00	<6E-02	5.07E-02	1.30E+00
	Pre-burn leach 1	<1E+01	2.15E-02	2.18E-03	3.19E-03	2.30E-01	2.92E-01	1.09E-02	3.75E-02	2.31E-01
	Pre-burn leach 2	<2E+01	<2E-02	3.44E-04	5.79E-04	6.82E-02	8.96E-02	<8E-02	1.66E-02	3.67E-02
	Post-burn leach 1	Discard	5.54E-02	1.34E-03	1.80E-03	5.60E+00	6.73E+00	1.18E-01	7.95E-02	4.84E+00
	Post-burn leach 2	<6E+00	<2E-02	2.87E-04	3.82E-04	6.35E-03	5.94E-03	<2E-02	1.37E-02	6.88E-03
	SUM (MDA = 0)	0	7.69E-02	6.86E-03	1.57E-02	7.14E+00	8.44E+00	1.29E-01	1.98E-01	6.41E+00
Segment #2	Decon	<2E+01	<4E-02	2.24E-02	8.14E-02	8.45E-01	8.55E-01	8.87E-02	<4E-02	1.06E+00
	Pre-burn leach 1	<2E+01	<4E-02	7.86E-04	3.26E-03	4.86E-01	5.24E-01	<8E-02	1.29E-02	5.35E-01
	Pre-burn leach 2	<1E+01	<2E-02	5.25E-04	4.22E-04	3.82E-02	3.77E-02	<2E-02	4.52E-03	2.91E-02
	Post-burn leach 1	<4E+01	1.46E-01	8.78E-04	1.41E-03	5.62E+00	6.10E+00	1.11E-01	7.86E-02	5.05E+00
	Post-burn leach 2	<1E+01	<2E-02	1.78E-04	2.84E-04	1.54E-02	1.79E-02	<2E-02	1.32E-02	1.19E-02
	SUM (MDA = 0)	0	1.46E-01	2.48E-02	8.68E-02	7.00E+00	7.54E+00	2.00E-01	1.09E-01	6.69E+00
Segment #3	Decon	<1E+01	8.30E-02	2.52E-02	1.07E-01	4.73E-01	5.31E-01	1.35E-01	<4E-02	9.33E-01
	Pre-burn leach 1	<1E+01	<2E-02	7.26E-04	1.90E-03	2.98E-01	2.88E-01	<6E-02	<2E-02	2.77E-01
	Pre-burn leach 2	<1E+01	<2E-02	6.61E-04	1.00E-03	4.29E-02	4.96E-02	<2E-02	<1E-02	3.52E-02
	Post-burn leach 1	<4E+01	1.12E-01	<4E-03	1.60E-03	5.37E+00	5.83E+00	<1E-01	6.90E-02	4.63E+00
	Post-burn leach 2	<2E+01	<2E-02	5.60E-04	8.38E-04	9.41E-03	1.00E-02	<2E-02	7.91E-03	6.31E-03
	SUM (MDA = 0)	0	1.95E-01	2.72E-02	1.12E-01	6.20E+00	6.71E+00	1.35E-01	7.69E-02	5.88E+00
Core	Decon	<4E+01	2.77E+00	2.41E-01	9.31E-01	1.56E+00	1.97E+00	2.73E+00	4.45E-01	2.36E+00
	Pre-burn leach 1	<1E+02	2.49E+00	4.63E-01	7.31E-01	2.00E+00	2.12E+00	8.81E+00	4.75E-01	1.99E+00
	Pre-burn leach 2	<6E+01	1.82E-01	6.79E-02	7.38E-02	2.91E-01	3.02E-01	3.42E-01	1.41E-01	2.93E-01
	Post-burn leach 1	<1E+02	1.28E+01	7.30E-01	8.51E-01	2.87E+01	3.43E+01	1.22E+00	2.48E+00	2.05E+01
	Post-burn leach 2	<4E+01	<1E-01	9.49E-02	1.07E-01	8.40E-02	8.93E-02	5.01E-01	1.84E-01	5.71E-02
	SUM (MDA = 0)	0	1.82E+01	1.60E+00	2.69E+00	3.26E+01	3.88E+01	1.36E+01	3.73E+00	2.52E+01
Compact TOTAL (MDA = 0)		0	18.67	1.66	2.91	52.96	61.49	14.08	4.11	44.17

Table 36. Relative error on the Compact 8-1 RDLBL results given in Table 35. The errors in the "sum" rows were computed by propagating the error from all the RDLBL steps.

		Ag-110m	Ce-144	Cs-134	Cs-137	Eu-154	Eu-155	Ru-106	Sb-125	Sr-90
	Compact 8-1									
Segment #1	Decon	N/A	N/A	11.5%	4.8%	3.0%	4.4%	N/A	12.0%	2.0%
	Pre-burn leach 1	N/A	19.0%	7.9%	3.8%	3.0%	10.3%	19.0%	11.9%	2.0%
	Pre-burn leach 2	N/A	N/A	20.0%	18.7%	5.1%	4.2%	N/A	12.0%	2.0%
	Post-burn leach 1	N/A	39.0%	14.0%	7.2%	3.0%	3.0%	8.5%	12.1%	2.0%
	Post-burn leach 2	N/A	N/A	13.0%	19.3%	9.0%	17.0%	N/A	9.0%	2.0%
	SUM (MDA = 0)	N/A	28.6%	6.0%	3.3%	2.4%	2.5%	7.9%	6.3%	1.6%
Segment #2	Decon	N/A	N/A	4.1%	4.5%	3.0%	5.5%	22.0%	N/A	2.0%
	Pre-burn leach 1	N/A	N/A	10.0%	5.1%	3.0%	5.0%	N/A	16.0%	2.0%
	Pre-burn leach 2	N/A	N/A	9.0%	13.9%	7.0%	19.8%	N/A	22.0%	2.0%
	Post-burn leach 1	N/A	12.0%	22.0%	15.5%	3.0%	3.0%	10.0%	19.1%	2.0%
	Post-burn leach 2	N/A	N/A	18.0%	17.1%	20.3%	14.8%	N/A	8.0%	2.0%
	SUM (MDA = 0)	N/A	12.0%	3.8%	4.2%	2.4%	2.5%	11.3%	14.0%	1.6%
Segment #3	Decon	N/A	25.5%	3.6%	3.6%	3.6%	4.2%	23.5%	N/A	2.0%
	Pre-burn leach 1	N/A	N/A	26.3%	5.9%	3.0%	5.2%	N/A	N/A	2.0%
	Pre-burn leach 2	N/A	N/A	20.6%	6.7%	5.3%	11.1%	N/A	N/A	2.0%
	Post-burn leach 1	N/A	25.0%	N/A	14.3%	3.0%	3.0%	N/A	22.6%	2.0%
	Post-burn leach 2	N/A	N/A	7.0%	11.2%	4.0%	7.0%	N/A	11.0%	3.0%
	SUM (MDA = 0)	N/A	18.0%	3.4%	3.5%	2.6%	2.7%	23.5%	20.3%	1.6%
Core	Decon	N/A	8.0%	3.0%	4.4%	3.0%	5.0%	4.7%	14.6%	2.0%
	Pre-burn leach 1	N/A	6.8%	3.0%	3.0%	3.0%	7.2%	3.0%	20.8%	2.0%
	Pre-burn leach 2	N/A	12.0%	3.7%	3.0%	6.6%	22.3%	10.0%	8.0%	2.0%
	Post-burn leach 1	N/A	4.0%	3.0%	3.0%	3.0%	3.0%	10.5%	4.0%	2.0%
	Post-burn leach 2	N/A	N/A	3.0%	3.0%	4.0%	8.0%	4.0%	15.2%	2.0%
	SUM (MDA = 0)	N/A	3.2%	1.7%	2.0%	2.7%	2.7%	2.4%	4.2%	1.6%
Compact TOTAL (MDA = 0)		N/A	3.1%	1.6%	1.8%	1.7%	1.8%	2.3%	3.9%	1.0%

4.5.2. Compact 8-1 ICP-MS Results

Table 37 summarizes the actinide content measured from RDLBL of Compact 8-1 via ICP-MS, and Table 38 gives the relative error in these values. A description of the measurement error was given in Section 2.5. Additional tables (Table 69 and Table 70) in Appendix A-5 provide these results in units of mass and compact fraction. As a reminder, the actinide activities were not decay-corrected, and the measured values were compared to the predicted values from Sterbentz (2015) to give particle-equivalent inventories. This is appropriate given the long half-lives of these nuclides and the relatively short NRAD reirradiation compared to the irradiation in ATR.

Table 37. Particle equivalents for select actinides from ICP-MS of solutions from Compact 8-1.

Particle Equivalents		Pu-239	Pu-240	U-234	U-235	U-236	U-238
Segment #1	Decon	1.16E-02	7.88E-03	4.90E-02	4.97E-02	4.43E-02	4.58E-02
	Pre-burn leach 1	5.17E-03	5.77E-03	2.41E-02	4.45E-02	4.72E-03	1.32E-02
	Pre-burn leach 2	2.97E-03	<4E-03	<1E-02	7.91E-04	3.52E-04	5.49E-04
	Post-burn leach 1	2.21E-01	3.95E-01	5.05E-02	4.18E-02	4.19E-02	4.00E-02
	Post-burn leach 2	1.18E-02	2.06E-02	<4E-03	4.65E-04	2.86E-04	4.39E-04
	SUM (MDA = 0)	2.53E-01	4.29E-01	1.24E-01	1.37E-01	9.16E-02	1.00E-01
Segment #2	Decon	1.13E-01	8.22E-02	4.83E-01	4.84E-01	4.77E-01	4.70E-01
	Pre-burn leach 1	<2E-02	<2E-02	<1E-01	1.05E-02	9.97E-03	8.92E-03
	Pre-burn leach 2	<8E-03	<2E-02	<1E-01	<2E-03	<4E-03	6.11E-04
	Post-burn leach 1	1.64E-01	2.84E-01	<1E-01	3.13E-02	3.09E-02	2.93E-02
	Post-burn leach 2	8.12E-03	<2E-02	<1E-01	<2E-03	<4E-03	<4E-04
	SUM (MDA = 0)	2.85E-01	3.66E-01	4.83E-01	5.26E-01	5.17E-01	5.09E-01
Segment #3	Decon	1.64E-01	1.20E-01	6.76E-01	6.68E-01	6.49E-01	6.34E-01
	Pre-burn leach 1	<8E-03	<2E-02	<1E-01	1.61E-02	8.81E-03	1.06E-02
	Pre-burn leach 2	<8E-03	<2E-02	<1E-01	<2E-03	<4E-03	2.05E-04
	Post-burn leach 1	1.53E-01	2.63E-01	<1E-01	3.10E-02	2.94E-02	2.82E-02
	Post-burn leach 2	<1E-02	<2E-02	<1E-01	<2E-03	<6E-03	<2E-04
	SUM (MDA = 0)	3.17E-01	3.83E-01	6.76E-01	7.15E-01	6.87E-01	6.73E-01
Core	Decon	5.56E+00	4.80E+00	9.25E+00	8.97E+00	8.63E+00	8.22E+00
	Pre-burn leach 1	2.56E+00	2.64E+00	2.76E+00	2.62E+00	2.54E+00	2.32E+00
	Pre-burn leach 2	7.07E-02	1.10E-01	<2E-02	9.23E-03	8.02E-03	8.54E-03
	Post-burn leach 1	4.90E+00	7.02E+00	1.55E+00	1.33E+00	1.33E+00	1.24E+00
	Post-burn leach 2	2.25E-02	2.81E-02	1.12E-02	9.08E-03	8.06E-03	8.24E-03
	SUM (MDA = 0)	1.31E+01	1.46E+01	1.36E+01	1.29E+01	1.25E+01	1.18E+01
Compact TOTAL (MDA = 0)		13.97	15.78	14.85	14.32	13.82	13.08

Table 38. Relative error in ICP-MS of solutions from Compact 8-1.

Error (%)		Pu-239	Pu-240	U-234	U-235	U-236	U-238
Segment #1	Decon	12%	17%	15%	5%	5%	5%
	Pre-burn leach 1	18%	24%	32%	7%	20%	5%
	Pre-burn leach 2	27%	N/A	N/A	13%	35%	19%
	Post-burn leach 1	7%	5%	26%	5%	7%	5%
	Post-burn leach 2	22%	20%	N/A	32%	25%	13%
	SUM (MDA = 0)	6%	5%	14%	3%	4%	3%
Segment #2	Decon	5%	5%	5%	5%	5%	5%
	Pre-burn leach 1	N/A	N/A	N/A	5%	5%	5%
	Pre-burn leach 2	N/A	N/A	N/A	N/A	N/A	5%
	Post-burn leach 1	5%	5%	N/A	5%	5%	5%
	Post-burn leach 2	5%	N/A	N/A	N/A	N/A	N/A
	SUM (MDA = 0)	3%	4%	5%	5%	5%	5%
Segment #3	Decon	5%	5%	5%	5%	5%	5%
	Pre-burn leach 1	N/A	N/A	N/A	5%	5%	5%
	Pre-burn leach 2	N/A	N/A	N/A	N/A	N/A	5%
	Post-burn leach 1	5%	5%	N/A	5%	5%	5%
	Post-burn leach 2	N/A	N/A	N/A	N/A	N/A	N/A
	SUM (MDA = 0)	4%	4%	5%	5%	5%	5%
Core	Decon	5%	5%	7%	5%	5%	5%
	Pre-burn leach 1	5%	7%	7%	5%	5%	5%
	Pre-burn leach 2	10%	15%	N/A	12%	20%	7%
	Post-burn leach 1	5%	5%	7%	5%	5%	5%
	Post-burn leach 2	10%	30%	35%	14%	26%	5%
	SUM (MDA = 0)	3%	3%	5%	4%	4%	4%
Compact TOTAL (MDA = 0)		3%	4%	5%	3%	3%	3%

4.5.3. Compact 8-1 Discussion

Compact 8-1 was reirradiated in NRAD prior to FACS testing at 1200°C, and Section 2.2 described those operations with some more detail. The FACS test showed no signs of SiC or TRISO failure, and the RDLBL results corroborate this, meaning the only kernels that were leached during RDLBL were in the core where the DTF kernels resided. The total amount of Ce-144 measured in the Compact 8-1 RDLBL was 18.7 particle equivalents. This amount is normal for AGR-3/4 compacts that had no damaged TRISO particles (Hunn et al. 2020; Helmreich et al. 2021; Helmreich et al. 2022; Stempien and Cai 2024a). The amount of U and Pu measured are on the low side (~14 particle equivalents). It is not clear why the U and Pu quantities are noticeably less than those of Ce-144.

The three other Capsule 8 compacts were also subjected to RDLBL. Compacts 8-3 (Stempien and Cai 2024a) and 8-4 (Helmreich et al. 2021) underwent as-irradiated RDLBL, and Compact 8-2 underwent RDLBL after FACS testing at 1400°C (see Section 4.2). For all Capsule 8 compacts, Figure 19 summarizes the RDLBL inventories, the inventories released in FACS (if applicable), and the average release from a Capsule 8 compact computed by taking the mass balance (Stempien et al. 2018b) and dividing it by four. This is a complicated representation because of the different irradiation histories, whether and at what temperature the compacts were FACS tested, and if any TRISO-coated driver particles were leached during RDLBL. For each of these compacts, Table 39 summarizes the ATR-irradiation history, reirradiation history, FACS temperature, and whether any TRISO-coated driver particles were leached during RDLBL. Furthermore, the Compact 8-1 FACS test maintained 1200°C for a total of about 272 h before a series of intentional temperature cycles were performed. The values in Figure 19 represent the total release from Compact 8-1 while in FACS. This includes the heating cycles performed following the isothermal hold at 1200°C.

Despite there being no measurable Ag-110m in the RDLBLs, Figure 19 shows significant Ag-110m was released in the two FACS tests, with Compact 8-1 releasing more Ag-110m at 1200°C than Compact 8-2 at 1400°C. This is consistent with prior observations showing that Ag-110m release rates through intact TRISO SiC layers during post-irradiation heating tests peak from approximately 1100 to 1300°C (Hunn et al. 2015). The mass balance shows that an average Capsule 8 compact released about 88% of its Ag-110m through intact SiC coatings in-pile. The as-irradiated gamma scans of these compacts are generally consistent with this and show compact M/C values around 0.15 (Harp et al. 2021), which equates to an estimated in-pile release of about 85%. Any Ag-110m released during FACS testing is in addition to that released in-pile.

Less than 0.02 particle equivalents of Ce-144 were detected outside of the fuel in Capsule 8. This is about 5,000 times less than the amount of Cs-134 measured outside of the fuel and demonstrates that nearly all Ce-144 is retained in the fuel compacts, despite each compact having 20 DTF kernels. The amount of Ce-144 released during the two FACS-tested compacts was even less. As a result, Ce-144 is a useful indicator of how many exposed kernels were leached in various steps of the RDLBL processes. Compacts 8-1 (tested in NRAD and FACS before RDLBL) and 8-4 (which underwent as-irradiated RDLBL) had very similar amounts of Ce-144 recovered from RDLBL: roughly 18.5 particle equivalents. Compacts 8-2 and 8-3 had some suspected TRISO particle damage, and more Ce-144 was reported even after attempts were made to correct the final values for accidental damage in Compact 8-3 that occurred in the second pre-burn leach of Segment 2.

Intact TRISO particles retain Cs; therefore, in AGR-3/4 compacts with no SiC or TRISO damage, the only source of Cs (aside from small amounts of dispersed uranium contamination from fabrication) that could be released to the capsule components, released during FACS testing, or recovered during RDLBL was the DTF particles. The mass balance indicates that each Capsule 8 compact released an average of about 13.3 particle equivalents of Cs-134 in-pile. This equates to 67% of the Cs-134 inventory from the 20 DTF particles. In the FACS tests of Compacts 8-1 (1200°C) and 8-2 (1400°C), 0.1 and 0.2 particle equivalents of Cs-134 were released, respectively. From those same compacts, an additional 1.7 and 2.8 particle equivalents of Cs-134 were recovered from RDLBL. This means the 1200 and 1400°C tests had insufficient temperature and duration to mobilize most of the Cs that remained in the compacts outside of fully intact TRISO particles after irradiation in ATR. For each compact, taking the amount of Cs-134 recovered from RDLBL, plus any Cs-134 measured in FACS, plus the Cs-134 measured in the mass balance accounts for about 15 particle equivalents per compact. This is a reasonable mass balance given the use of multiple methods (i.e., RDLBL, FACS, and capsule-component mass balance) and the uncertainties involved in each.

Figure 19 shows that the average Eu-154 release from a Capsule 8 compact to the capsule components was 2.8 particle equivalents. Little Eu-154 was released during FACS testing of Compacts 8-1 and 8-2 (≤0.1 particle equivalents), but about 39 to 56 particle equivalents were recovered from RDLBL of each of the four Capsule 8 compacts. A lesser amount of Eu-154 (~39 particle equivalents) was measured in the matrix of Compact 8-4. This could be because it had a lower irradiation temperature than Compact 8-3 (the other Capsule 8 to undergo AI RDLB), and it was not heated in the FACS furnace like Compacts 8-2 and 8-1. This reveals two things about Eu behavior in this system. First, the compact retains the vast majority of the Eu from the DTF particles. Second, intact driver particles may allow some Eu to diffuse out of their SiC coatings; however, the majority of this is still retained in the OPyC and compact graphitic matrix. Similar behavior was observed for Sr-90. It is also worth mentioning that Figure 19 shows that the release of Eu-154 and Sr-90 from the 1400°C test was a factor of 10 higher than it was at 1200°C.

No Ru-106 was measured outside the fuel in the mass balance or on condensation plates from FACS tests. The amounts of Ru-106 recovered from the RDLBL of these four Capsule 8 compacts ranged from 11.3 to 15.3. These amounts are consistent with what was observed previously, and under-recovery of Ru-106 from the RDLBL is typical (Stempien and Cai 2024a).
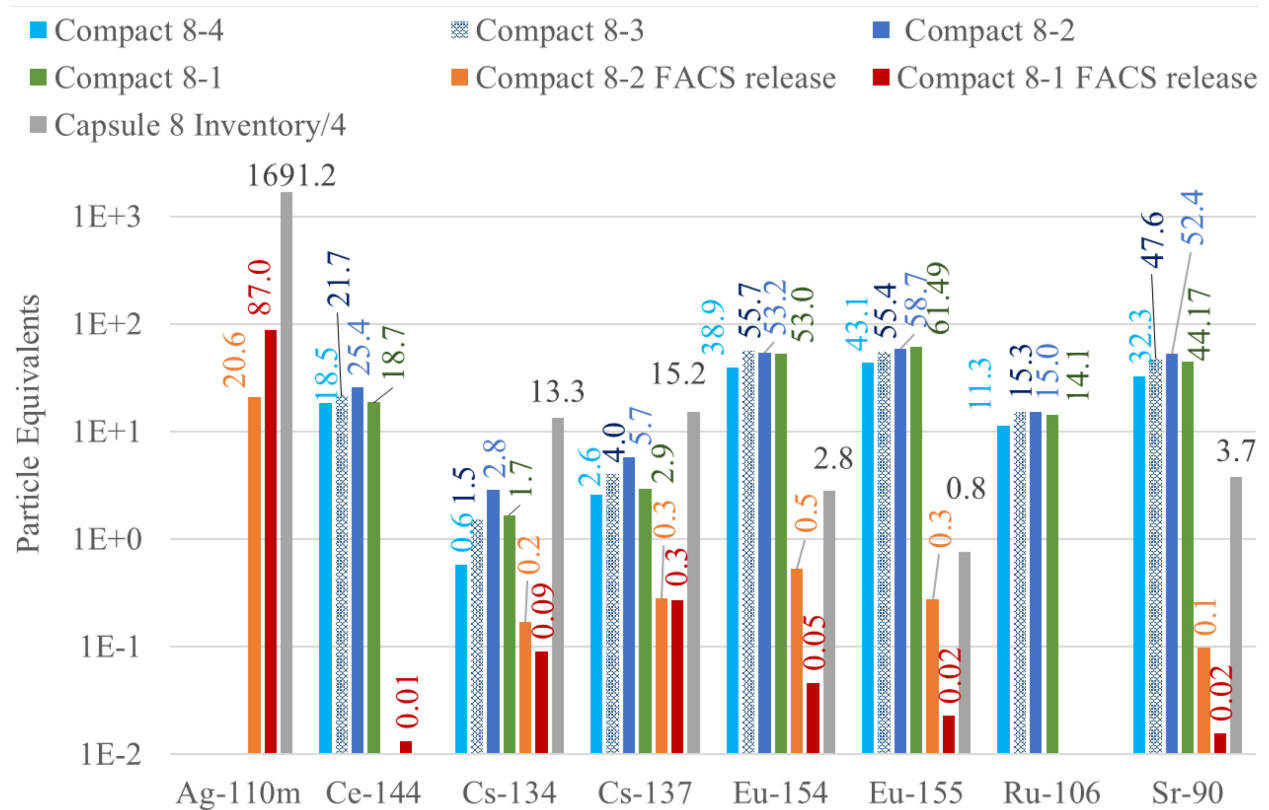
Figure 19. A summary of fission product inventory for Compacts 8-1 to 8-4. The fission release during FACS testing at 1400°C for Compact 8-2 as well as FACS testing 1200°C for Compact 8-1 are included. A quarter of fission product inventories at Capsule 8 (including foils, felts, spacers, through tubes, inner ring, outer ring, and sink ring) is also included for comparison.

Table 39. A comparison of irradiation conditions among Compacts 8-4, 8-3, 8-2, and 8-1.

	Burnup[a]	Neutron Fluence[b]	TAVA Temp[c]	TA Min Temp[c]	TA Peak Temp[c]	NRAD?	FACS Temp[c]	Suspected damage to TRISO?
8-4	14.4	5.02	1169	1068	1242	No	N/A	None
8-3	14.5	5.07	1213	1171	1257	No	N/A	Segment 2, pre-burn leach 2: 1 particle corrected
8-2	14.6	5.11	1213	1171	1257	No	1400	Two particles in Segment 3. 1-5 particles in the core with no corrections made for the core. Uncorrected values used in Figure 19
8-1	14.5	5.13	1165	1063	1242	Yes	1200[d]	None

a. % FIMA

b. 10^{25} n/m^2, E>0.18 MeV

c. °C

d. 272 h at 1200°C, then three rounds of temperature cycling

5.   RADIAL URANIUM AND FISSION PRODUCT CONCENTRATION PROFILES

The radial deconsolidation process allows the determination of the fission product content within specific segments and volumes of the fuel compact. Uneven radial material removal or variations in material removal along the compact length was noted for at least one step of the RDLBL of Compacts 3-1, 8-2, 1-2, and 8-1; however, azimuthally uniform removal of material was assumed (i.e., that the cylinder was always perfectly circular) when calculating the volume of material removed in each segment and when placing a point for the concentration at the middle radius of each segment. The volumes and average radial locations of the segments were presented in Section 3. The fission product inventories in each of the segments were presented for each compact in Section 4. In this section, the fission product inventories were normalized by the segment volumes to give volumetric concentrations. In the figures that follow, these concentrations will be plotted at the radial middle of each segment. The concentration profiles are presented in units of compact fraction/mm^3, particle equivalents/mm^3, and Bq/mm^3. With units of fraction/mm^3 and particle equivalents/mm^3, easy comparisons of the relative amounts of different isotopes can be made. Results given in units of Bq/mm^3 are included for easier comparison to some earlier AGR-3/4 reports and papers (Stempien 2021; Humrickhouse et al. 2016; Humrickhouse et al. 2018; Riet 2022).

In some cases, damaged TRISO particles were encountered either from some degree of failure prior to RDLB or accidental damage incurred during RDLBL. When possible, corrections for TRISO particles accidentally damaged during RDLBL were performed to prevent the kernel inventory from these particles from biasing the results and artificially inflating the amount of fission products and actinides at a given step of the RDLBL. When the exact number of TRISO particles damaged in RDLBL could not be determined (typically because there were more than a few such particles), corrections might not be possible. There appeared to be cases where a TRISO particle had a SiC failure in-pile. It is possible to attempt to correct for that leached particle. However, just because some damage can be corrected does not necessarily mean it should be corrected. If the intent is to construct a fission product concentration profile of the compact as it was during RDLBL, then the inventory contributed from that failed-SiC particle is part of that. If the intent is to focus on fission products contributed from the DTF particles only (and to minimize the impacts from driver particles), then a correction might be appropriate.

For each compact, Table 40 summarizes whether and to what extent TRISO particle damage was encountered and whether corrections could or should be made. For Compacts 3-2 and 8-2, corrections could be made, but because it could not be determined with certainty if the leached kernels were the result

of accidental damage during RDLBL or the result of some degradation during FACS testing or irradiation in ATR, it is debatable whether a correction should be made. If the goal is to know the concentration profiles resulting from only fission products produced in the DTF particles, then a correction may help, especially a correction for suspected accidental damage that occurred during RDLBL. However, a correction applied for a particle that, for example, was suspected of having a SiC failure in-pile or during FACS testing may overcorrect the fission product content in the segment in which it was found and leave uncorrected the other segments in the compact that could have been affected by fission products from this particle.

Table 40. List of FACS-tested AGR-3/4 compacts analyzed via RDLBL at INL and whether corrections could be and/or should be applied to their results to account for accidental particle damage or SiC/particle failure.

Compact	TRISO-coated Kernel Leached in RDLBL?	Corrections?
3-2	Segment 3: 1 TRISO particle leached in post-burn leach 1. Insufficient evidence to conclude it was in-pile or in-FACS SiC failure. Assumption is it was a TRISO particle broken during post-burn leach 1.	Yes, a correction is recommended and was applied. Uncorrected values are also given for comparison.
8-2	Segment 3: 2 TRISO particles leached in post-burn leach 1. Evidence suggests these were two particles with in-pile failed SiC. Core: evidence suggests 1–5 TRISO particles were leached at some point in the DLBL of the core.	Segment 3: a correction is possible but generally was not recommended because these may be legitimate in-pile SiC failures. Both uncorrected and corrected values are included for comparison. Core: a correction is not possible given the uncertainty in the number of affected TRISO particles.
1-2	None	N/Aᵃ
3-1	Segment 1: 9 TRISO particles were leached at various stages of the Segment 1 RDLBL. Two of these could legitimately be in-pile SiC failures that developed into TRISO failure in FACS and were leached in RDLBL. The others are from unknown origins.	A correction is not possible. The Segment-1 concentrations will be overwhelmed by the inventories from these damaged or failed particles.
8-1	None	N/Aᵃ

a. Not applicable.

5.1. Compact 3-2 Radial Fission Product Profiles

The RDLBL process for Compact 3-2 (which was tested in FACS at 1600/1700°C) generated fission product inventories for three radial segments and the core of the compact. Table 41 gives the concentrations for select fission products and U-238 within each segment of the compact. Table 42 gives the relative error on the concentration by accounting for the measurement error on the compact's dimensions and the measurement error of the fission product activities and U-238 masses. The dimensions and radial locations of each segment were given in Section 3.1.

Figure 20 and Figure 21 give the radial concentration profiles for selected fission products in Compact 3-2 in units of particle equivalents/mm³ and Bq/mm³, respectively. Figure 22 presents the concentration profiles of Ce-144 and U-238. A correction is recommended for what is believed to be one TRISO particle that was accidentally damaged in the Segment 3 RDLBL. The figures include the corrected and uncorrected concentrations in Segment 3 for comparison. The uncorrected points are shown as solid symbols that are placed on either side of the center of Segment 3 to make them easier to see on the plots. When corrected for the leached TRISO particle in Segment 3, the Ce-144, Ru-106, Cs-134, and U-238 concentrations in Segment 3 were lower than those of the core. The uncorrected Cs-134 and Eu-154 concentrations in Segment 3 are about the same as they are in the core. All the corrected Segment 3 concentrations shown in Figure 20 through Figure 22 are lower than those in Segments 2 and 1. (There is one exception where the corrected Segment 3 concentration of Cs-134 is about identical to that in

Segment 1.) In the as-irradiated fuel compacts (Stempien and Cai 2024a), profiles where outer segments (like Segments 1 and 2) had similar or higher concentrations than the inner segments (like Segment 3 and the core) were only consistently seen in the hottest three compacts examined, which had TAVA temperatures of 1213, 1319, and 1376°C. In those compacts, relatively flat concentration profiles and profiles with higher concentrations in the peripheral segments than the inner segments were attributed to the enhanced transport driven by the higher irradiation temperatures. Here Compact 3-2 had a lower TAVA temperature of 1196°C, but it was heated for extended periods of time at 1600 and 1700°C in the FACS furnace prior to RDLBL, which would have promoted outward radial transport. As for Eu-154 and Sr-90, the core and the outer segments had similar concentrations (with substantial error bars for Segments 1 and 2). The observed releases of both Eu-154 and Sr-90 from the compact during irradiation and FACS testing were similar between the two nuclides (Figure 16).

Table 41. Radial fission product concentrations expressed in three different units for Compact 3-2.

	Segment	Ag-110m	Ce-144	Cs-134	Cs-137	Eu-154	Eu-155	Ru-106	Sb-125	Sr-90	U-238
Bq/mm^3	1	N/A	2.56E+4	4.02E+2	1.02E+3	1.19E+3	9.55E+2	6.79E+4	N/A	1.40E+4	
	2	N/A	3.08E+4	5.72E+2	1.61E+3	1.16E+3	9.44E+2	5.52E+4	N/A	1.43E+4	
	3	N/A	1.43E+5	6.53E+3	7.24E+3	8.99E+2	6.46E+2	1.78E+4	N/A	1.69E+4	N/A
	3*	N/A	1.45E+4	3.97E+2	8.95E+2	6.05E+2	4.46E+2	1.78E+4	N/A	9.55E+3	
	core	N/A	1.24E+6	6.94E+3	1.32E+4	7.31E+2	5.32E+2	1.45E+5	3.67E+2	1.10E+4	
Fraction/mm^3	1	N/A	2.68E-7	5.96E-8	1.63E-7	5.46E-6	6.45E-6	3.46E-6	N/A	2.56E-6	2.42E-6
	2	N/A	3.23E-7	8.47E-8	2.57E-7	5.31E-6	6.38E-6	2.81E-6	N/A	2.60E-6	4.31E-6
	3	N/A	1.50E-6	9.67E-7	1.15E-6	4.11E-6	4.36E-6	9.09E-7	N/A	3.09E-6	2.81E-6
	3*	N/A	1.52E-7	5.89E-8	1.43E-7	2.77E-6	3.01E-6	9.09E-7	N/A	1.74E-6	1.47E-6
	core	N/A	1.30E-5	1.03E-6	2.10E-6	3.34E-6	3.60E-6	7.40E-6	7.61E-7	2.01E-6	1.21E-5
Particle Equivalents /mm^3	1	N/A	5.14E-4	1.14E-4	3.13E-4	1.05E-2	1.24E-2	6.63E-3	N/A	4.91E-3	4.64E-3
	2	N/A	6.19E-4	1.63E-4	4.94E-4	1.02E-2	1.22E-2	5.39E-3	N/A	4.99E-3	8.26E-3
	3	N/A	2.88E-3	1.85E-3	2.21E-3	7.89E-3	8.37E-3	1.74E-3	N/A	5.92E-3	5.39E-3
	3*	N/A	2.92E-4	1.13E-4	2.74E-4	5.30E-3	5.78E-3	1.74E-3	N/A	3.34E-3	2.81E-3
	core	N/A	2.49E-2	1.97E-3	4.03E-3	6.41E-3	6.90E-3	1.42E-2	1.46E-3	3.85E-3	2.32E-2

*Corrected for one possible damaged (or possibly failed) SiC coating.

Table 42. Relative error for the Compact 3-2 fission product concentrations given in Table 41.

Segment	Ag-110m	Ce-144	Cs-134	Cs-137	Eu-154	Eu-155	Ru-106	Sb-125	Sr-90	U-238
1	N/A	90%	88%	88%	88%	88%	88%	N/A	88%	88%
2	N/A	71%	70%	69%	69%	70%	70%	N/A	69%	70%
3	N/A	15%	8%	7%	7%	9%	15%	N/A	7%	9%
core	N/A	4%	2%	2%	2%	3%	3%	15%	2%	10%
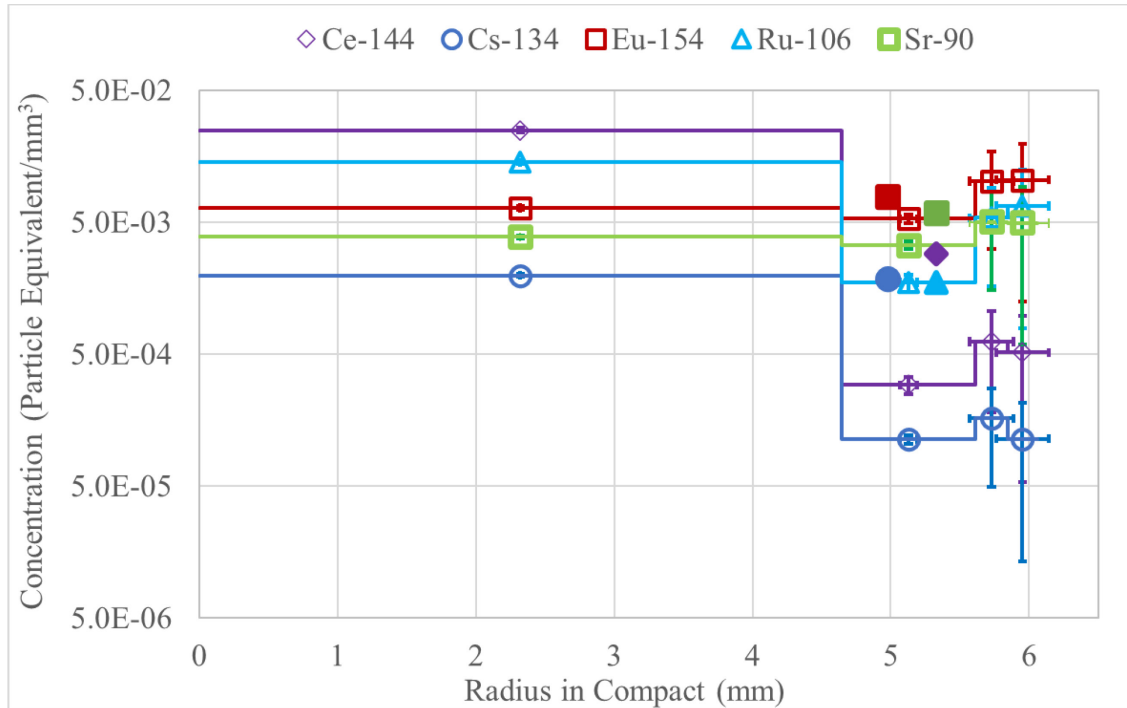
Figure 20. Compact 3-2 fission product radial concentration profiles in units of particle equivalents/mm³. Solid symbols show the uncorrected concentrations. On the x-axis, these were offset on either side of the center of the segment to aid the visibility of all the Segment 3 points.
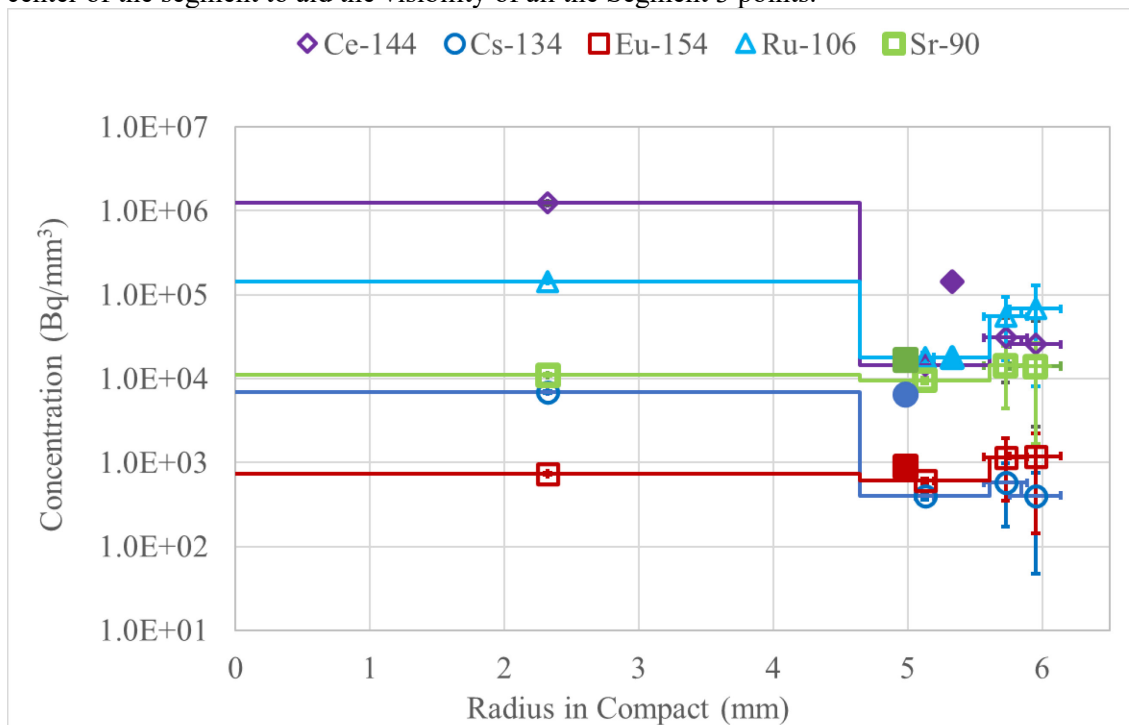
Figure 21. Compact 3-2 fission product radial concentration profiles (Bq/mm³). Solid symbols show the uncorrected concentrations in Segment 3. These were offset on either side of the center of the segment to aid visibility of the points.

68

Figure 22. Comparison of U-238 and Ce-144 radial concentration profiles in Compact 3-2. Solid symbols show the uncorrected concentrations in Segment 3. These were offset from the center of the segment to aid visibility of the points.

5.2. Compact 8-2 Radial Fission Product Profiles

The radial deconsolidation process for Compact 8-2 generated fission product inventories for three radial segments and the core of the compact. Table 43 gives the concentrations for select fission products within each segment of the compact. Table 44 gives the error on the concentration by accounting for the measurement error on the compact's dimensions and the measurement error of the fission product activity. The dimensions and radial locations of each segment were given in Section 3.2, and the total nuclide inventories in each segment were given in Section 4.2. Figure 23 and Figure 24 give the radial concentration profiles for selected fission products in Compact 8-2 in units of particle equivalent/mm^3 and Bq/mm^3, respectively. Figure 25 compares the concentration profile of Ce-144 to that of U-238.

In Section 4.2.3, it was stated that two TRISO-coated driver particles were leached in the post-burn leach of Segment 3. It was not clear if these could be the result of failed SiC layers or if they were caused by accidental damage during RDLBL. Both corrected and uncorrected values are given for the Segment 3 concentrations. The evidence (see Section 4.2.3) suggests that these two particles could be in-pile failed SiC particles, and in that case, the uncorrected values might be preferred over the corrected values. Additionally, in the compact core, there was evidence of 1 to 5 damaged driver particles, depending on which nuclide one considers in the RDLBL results. Because of the 20 DTF particles (whose contents were also being leached), it is not known when in the process these driver particles may have been leached and whether they were the result of accidental damage. No corrections were made for leached TRISO particles in the compact core.

Several behaviors of Eu and Sr are observable when considering the concentration profiles, the total RDLBL inventories, and the releases of these nuclides during FACS testing. The Eu-154 and Sr-90 concentration profiles in Compact 8-2 are relatively flat (within the error bars). The only as-irradiated compacts with relatively flat Eu and Sr profiles were those with TAVA irradiation temperatures ranging

69

from 1169 to 1376°C (Helmreich et al. 2021; Stempien and Cai 2024a). Compact 8-2 had a TAVA of 1213°C, and given that its Eu and Sr profiles are very similar to those of the as-irradiated compacts with similar irradiation temperatures, it is not apparent that the 1400°C test significantly altered these profiles.

The total Eu-154 and Sr-90 inventories measured from the post-FACS RDLBL of Compact 8-2 were about 51 and 50 particle equivalents, respectively, after correcting for suspected particle damage (Table 22). These quantities indicate that in addition to Eu and Sr coming from the 20 DTF particles, some of the Eu and Sr produced in intact TRISO particles diffused through those coatings into the OPyC and compact matrix where it was retained. Similarly, as-irradiated Compact 8-3 was found to have about 56 and 48 particle equivalents of Eu-154 and Sr-90, respectively (Stempien and Cai 2024a). Thus, these two compacts had similar EOI burnups, irradiation temperatures, and similar inventories of Eu-154 and Sr-90 measured via RDLBL. This is despite the post-irradiation FACS testing of Compact 8-2 at 1400°C. The fact that Compact 8-2 released <0.1 particle equivalents of Eu-154 and Sr-90 during FACS testing, a very small quantity compared to its RDLBL inventory, demonstrates that most of the Eu and Sr in the DTF particles, OPyC, and matrix at the start of the test is retained in the compact even after exposure at 1400°C for 300 h.

The concentrations of Cs-134 in Compact 8-2 after FACS testing were low compared to other nuclides in Compact 8-2 because the majority of the Cs-134 was driven out of the DTF particles and out of the compact altogether during irradiation, before the FACS test even started. There are two indirect sources of evidence that the Cs-134 inventory in the compact outside of intact particles was low in Compact 8-2 going into the FACS test. One is from the mass balance, which showed a Cs-134 inventory on the capsule components equivalent to 13 particles from each compact, which equates to 65% of the DTF inventory of that nuclide (Stempien et al. 2018b). As stated earlier, this value may underestimate the Cs-134 release from the compacts if the mass balance was incomplete. It would be incomplete, for example, if some of the Cs had transported to the capsule shells, which could not be analyzed.

The second indirect indication that Compact 8-2 probably had a low Cs-134 inventory outside of the driver particles when the FACS test started is that only about 1.5 and 0.6 particle equivalents of Cs-134 were measured in total from the RDLBL of as-irradiated Compacts 8-3 (Stempien and Cai 2024a) and 8-4 (Helmreich et al. 2021), respectively, which had similar EOI burnups and TAVA temperatures to Compact 8-2. The shape of the Cs-134 profile in Compact 8-2 is common among both as-irradiated and FACS-tested compacts (where it decreases with increasing radius). The difference here is that the core and Segment 3 concentrations of Cs-134 in Compact 8-2 are at the low end of the range compared to as-irradiated compacts, and this is despite evidence of one to five damaged particles in the core that could not be corrected and the leaching of two kernels in Segment 3, which could be corrected. The Cs-134 concentration in Compact 8-2 Segment 1 was below detection. The only as-irradiated compact without detectable Cs-134 in Segment 1 was Compact 7-4 (Helmreich et al. 2021; Stempien and Cai 2024a), which had a TAVA irradiation temperature of 1319°C. The Cs-134 concentration in Compact 8-2 Segment 2 was 2.18E-5 particle equivalents/mm^3, which is about 3x lower than the nearest Cs-134 concentration in an as-irradiated compact (8-4) (Helmreich et al. 2021; Stempien and Cai 2024a), and lower than all other Capsule 8 compacts (see Figure 36). The notably low Cs-134 concentrations in Compact 8-2 Segments 1 and 2 are because of the additional release of Cs-134 (0.17 particle equivalents) from its outer periphery during the 1400°C FACS test (Stempien and Cai 2024b). This 0.17 particle equivalents is greater than the Cs-134 inventories of Segments 1 (below detection) and 2 (2.18E-3 particle equivalents) and a little smaller than the Cs-134 inventory in Segment 3 (0.235 particle equivalents) (Table 22).

In as-irradiated compacts (Hunn et al. 2020; Helmreich et al. 2021; Helmreich et al. 2022; Stempien and Cai 2024a), the Ce-144 and U-238 concentrations generally decreased with increasing radius. In those samples, the concentration adjacent to the core segment was lower than the core concentration by one or two orders of magnitude, and that was the largest concentration difference between any neighboring segments. A similar decrease in the U and Ce concentrations from the core to Segment 3 is apparent in

Figure 25 for Compact 8-2. A correction was applied to the Segment 3 values to account for two particles that were leached in post-burn leach 1. With the available data, it is unclear if these two particles were in-pile failed-SiC particles or if they could have been damaged during the RDLBL process. Without the correction to Segment 3 (see the solid symbols in Figure 25), the concentration profile decreases steadily from the inside out. With the correction, the Segment 3 U-238 concentration is similar to that in Segment 2, and the Ce-144 concentration in Segment 3 is lower than in Segment 2. The lowest U-238 concentration in this compact was measured in the outermost segment, where there was no detectable Ce-144.

The only as-irradiated compacts with local maxima in Ce or U outside of the compact core were Compacts 7-4, 7-3, and 12-1 (see Figures 47 and 48 in Stempien and Cai [2024a]). Compacts 7-3 and 7-4 were the two as-irradiated compacts with the highest irradiation temperatures (>1300°C), and Compact 12-1 had some particle damage in the segment with the local concentration maximum. It is not clear if, hypothetically, local maxima in the U and Ce concentration profiles could be related to the higher irradiation temperatures, promoting a wave of U and Ce transport radially outward in the Capsule 7 compacts and in the 1400°C safety test that Compact 8-2 underwent. The leaching of particles in Compact 8-2 Segment 3 that had exposed kernels from unknown causes (evidence suggests these could have been two particles with in-pile failed SiC layers) increases the uncertainty in the Segment 3 values, meaning it is possible the correction applied to Segment 3 (seen also Table 40 and Section 4.2) produces an artificial local maximum in Ce and U at Segment 2. The situation with Ru-106 is similar, except that it shows a local maximum in the outermost segment (Segment 1), which showed no signs of being affected by driver particle damage. This suggests this Ru-106 local maximum is genuine.

Table 43. Radial fission product concentrations expressed in three different units for each segment of Compact 8-2. The uncorrected Segment 3 values are recommended because they will reflect what are believed to be real in-pile SiC failures.

Concentration	Segment	Ag-110m	Ce-144	Cs-134	Cs-137	Eu-154	Eu-155	Ru-106	Sb-125	Sr-90	U-238
Bq/mm³	1	N/A	N/A	N/A	4.80E+2	5.79E+3	3.93E+3	1.44E+4	N/A	1.02E+5	N/A
	2	N/A	6.13E+4	1.08E+2	2.25E+2	7.55E+3	5.53E+3	1.77E+2	1.90E+2	1.43E+5	
	3	N/A	2.89E+5	5.97E+3	6.76E+3	4.32E+3	3.23E+3	3.93E+4	5.97E+2	8.48E+4	
	3*	N/A	9.41E+3	2.93E+3	3.09E+3	3.55E+3	2.72E+3	2.43E+3	3.28E+1	6.82E+4	
	core	N/A	1.42E+6	1.25E+4	2.03E+4	5.71E+3	4.13E+3	1.95E+5	9.67E+2	1.25E+5	
Fraction/mm³	1	N/A	N/A	N/A	6.56E-8	1.96E-5	2.02E-5	5.67E-7	N/A	1.62E-5	1.41E-7
	2	N/A	5.62E-7	1.14E-8	3.08E-8	2.56E-5	2.84E-5	6.97E-9	3.27E-7	2.28E-5	3.42E-7
	3	N/A	2.65E-6	6.31E-7	9.23E-7	1.47E-5	1.66E-5	1.55E-6	1.03E-6	1.35E-5	2.63E-6
	3*	N/A	8.63E-8	3.10E-7	4.21E-7	1.20E-5	1.40E-5	9.57E-8	5.66E-8	1.09E-5	2.38E-7
	core	N/A	1.30E-5	1.32E-6	2.77E-6	1.94E-5	2.13E-5	7.67E-6	1.67E-6	2.00E-5	1.26E-5
Particle Equivalents /mm³	1	N/A	N/A	N/A	1.26E-4	3.77E-2	3.88E-2	1.09E-3	N/A	3.10E-2	2.70E-4
	2	N/A	1.08E-3	2.18E-5	5.90E-5	4.91E-2	5.46E-2	1.34E-5	6.27E-4	4.37E-2	6.57E-4
	3	N/A	5.08E-3	1.21E-3	1.77E-3	2.81E-2	3.19E-2	2.97E-3	1.97E-3	2.59E-2	5.05E-3
	3*	N/A	1.65E-4	5.95E-4	8.08E-4	2.31E-2	2.68E-2	1.84E-4	1.09E-4	2.08E-2	4.56E-4
	core	N/A	2.49E-2	2.53E-3	5.30E-3	3.71E-2	4.08E-2	1.47E-2	3.20E-3	3.83E-2	2.42E-2

* Corrected for two possible SiC failures.

Table 44. Error in the Compact 8-2 radial fission product concentrations given in Table 43.

Uncertainty of Concentrations	Ag-110m	Ce-144	Cs-134	Cs-137	Eu-154	Eu-155	Ru-106	Sb-125	Sr-90	U-238
1	N/A	N/A	N/A	51%	50%	50%	61%	N/A	50%	50%
2	N/A	47%	45%	45%	44%	44%	52%	46%	44%	44%
3	N/A	25%	12%	12%	12%	12%	18%	18%	12%	12%
Core	N/A	9%	4%	4%	4%	4%	5%	10%	4%	5%
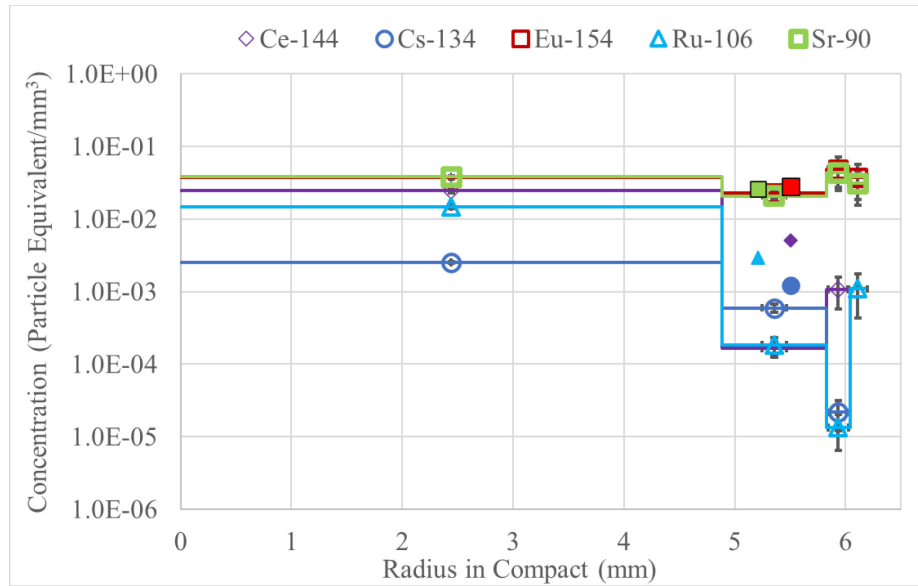
Figure 23. Radial concentrations of fission products in Compact 8-2 in units of particle equivalents per mm³. Solid symbols show the uncorrected concentrations in Segment 3. These were offset fro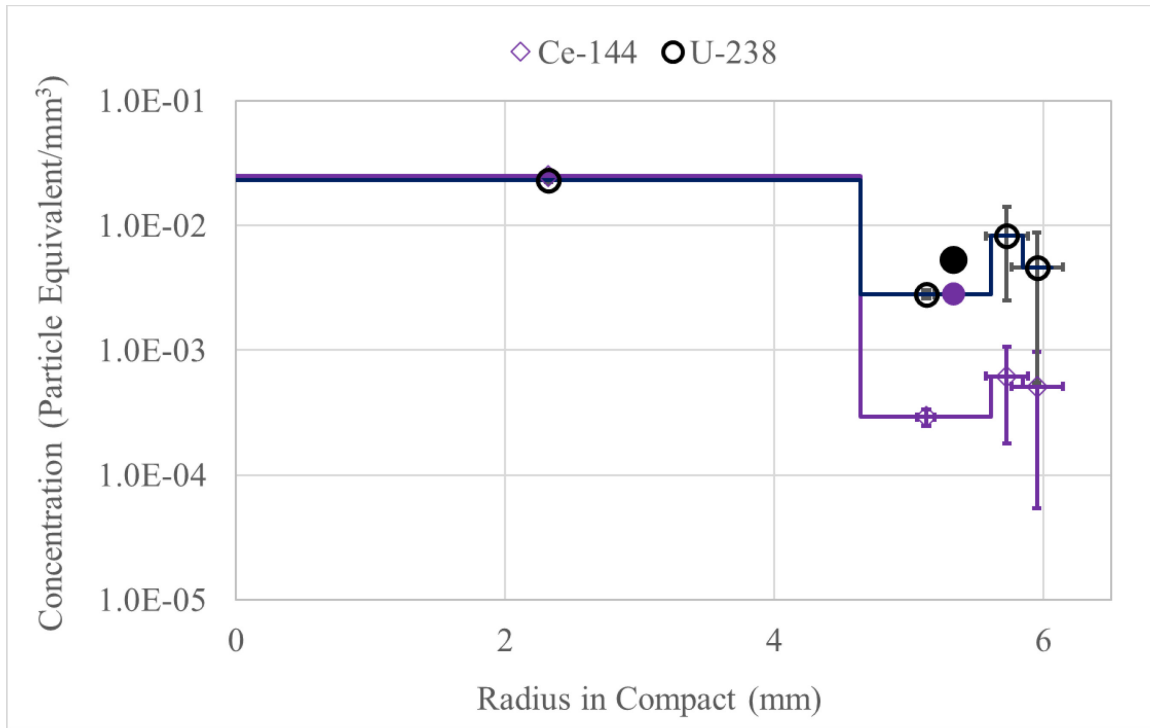m the center of the segment to aid visibility of the points. These uncorrected Segment 3 values are recommended because they will reflect what are believed to be real in-pile SiC failures.
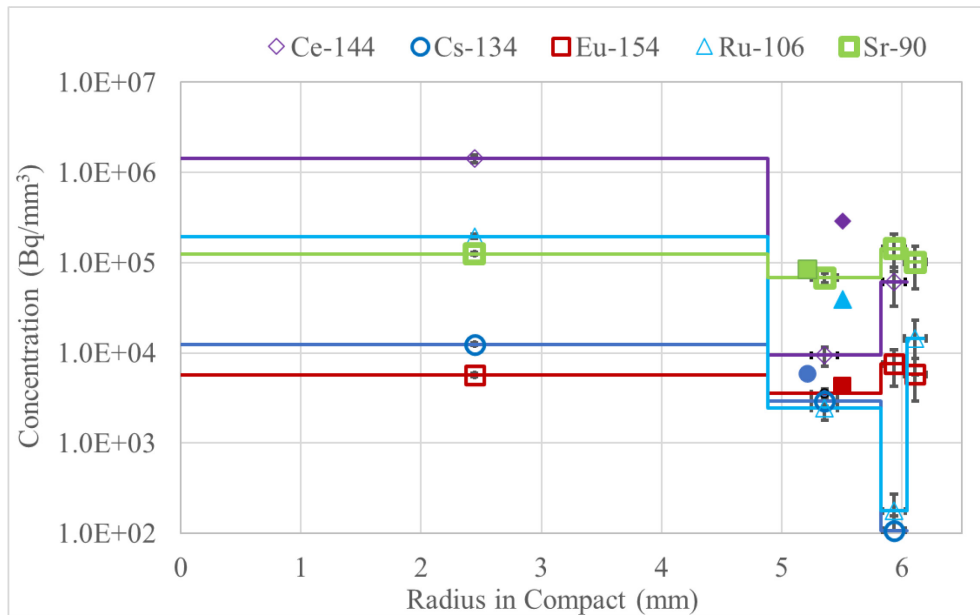
Figure 24. Radial concentrations of fission products in Compact 8-2 in units of Bq per mm³. Offset to either side of the center of the segment, solid symbols show the uncorrected concentrations in Segment 3. These uncorrected Segment 3 values are recommended because they will reflect what are believed to be real in-pile SiC failures.
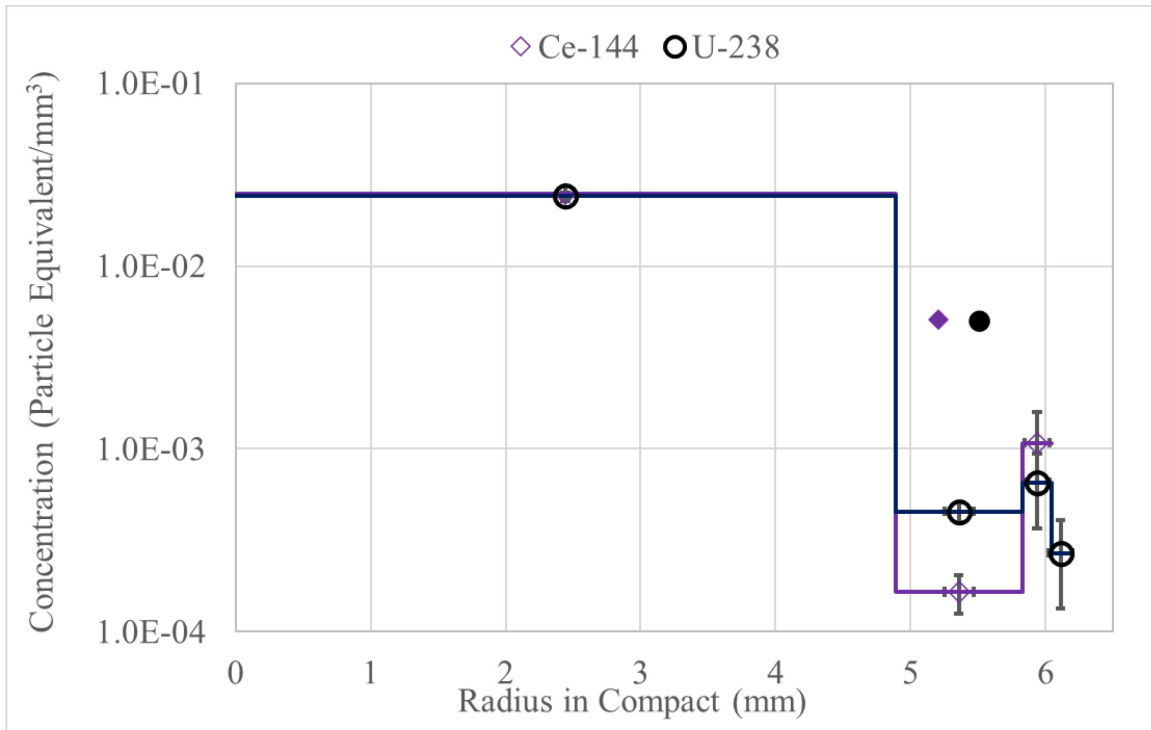
Figure 25. Comparison of Ce-144 and U-238 radial concentration profiles in Compact 8-2. Solid symbols show the uncorrected concentrations in Segment 3. These were offset on either side of the center of Segment 3 to aid visibility of the points. These uncorrected Segment 3 values are recommended because they will reflect what are believed to be real in-pile SiC failures.

5.3. Compact 1-2 Radial Fission Product Profiles

Compact 1-2 was reirradiated in NRAD for 120 h. Following reirradiation and gamma scanning via PGS, Compact 1-2 was loaded into the FACS furnace and heated to 1400°C. As Figure 3 showed, this test was interrupted so the FGMS traps could be baked out. Because of this interruption, only about 250 h were spent at 1400°C. No unusual challenges were encountered during the RDLBL of this compact (see Section 3.3).

Here, because the volume of material removed during the deconsolidation of Segment 1 from Compact 1-2 could not be determined (the post-Segment 1 diameter was not noticeably different from the pre-deconsolidation diameter), the radionuclide contents measured in Segments 1 and 2 were combined, and the volume associated with that material was taken as the difference between the pre-deconsolidation volume and the compact volume after Segment 2 had been deconsolidated. Accordingly, volumetric concentrations are only given for two radial volumes and the compact core.

The radial fission-product concentrations are listed in Table 45, and Table 46 gives the error on the concentration by accounting for the measurement error on the compact's dimensions and the measurement error of the fission product activity. Figure 26 and Figure 27 give the radial concentration profiles for selected fission products in Compact 1-2 in units of particle equivalents/mm^3 and Bq/mm^3, respectively. Figure 28 compares the concentration profiles of Ce-144 and U-238.

The M/Cs and volumetric concentrations of Ce-144, Eu-154, Eu-155, and Ru-106 in the core are abnormally high (see Section 4.3 for more discussion). This issue seems to be confined to only these specific nuclides in the compact core. Multiple rounds of data checks from multiple subject matter experts did not uncover errors in the radiochemistry, however. Thus, the reason for the discrepancy is unknown at this time. These questionable data points are denoted by gray font in Table 45 and Table 46. In Figure 26 through Figure 28, the nuclides with erroneous core concentrations are plotted in gray. The results for other nuclides in the core (i.e., U, Pu, Cs-134, Cs-137, and Sr-90) were reasonable, and the results for all key nuclides (including Ce-144, Eu-154, Eu-155, and Ru-106) in Segments 1–3 were also reasonable.

Compact 1-3 had an EOI burnup and TAVA temperature similar to Compact 1-2, and Compact 1-3 underwent as-irradiated RDLBL at ORNL (Helmreich et al. 2022), making it a suitable sample for comparison with the reirradiated and FACS-tested Compact 1-2. The core concentration of Ce-144 in Compact 1-2 is about 2.7 times higher than in as-irradiated Compact 1-3 (Helmreich et al. 2022), but the concentration in Compact 1-2 Segment 1+2 is very similar to Segment 2 from Compact 1-3. Similarly, the Eu-154 concentration in the core of Compact 1-2 is 3.2 times higher than in as-irradiated Compact 1-3 (Helmreich et al. 2022), but Compact 1-2 Segment 3 is very similar to Compact 1-3 Segment 2. The concentrations for Eu and Ce outside of the core of Compact 1-2 are reasonable, and that would suggest the problem with the Eu and Ce values in the core is related to the radiochemical measurements in the core specifically.

The shapes of the U and Sr-90 profiles are similar between Compacts 1-2 and 1-3. The Compact 1-2 Cs profile is similar in shape to that of Compact 1-3; however, the concentrations of Cs-134 in Compact 1-2 are lower than in Compact 1-3. This is attributed to the fact that Compact 1-2 was exposed to 1400°C in the FACS furnace and Compact 1-3 was in its as-irradiated state when it was deconsolidated. Indeed, the preliminary results from the FACS test of Compact 1-2 show that about 14 particle equivalents of Cs-134 were released during the FACS test, which explains the lower concentrations of Cs-134 in Compact 1-2 relative to Compact 1-3.

Table 45. Radial fission product concentrations expressed in three different units for each segment of Compact 1-2. Abnormal data points in the compact core are shown in gray font.

Concentration	Segment	Ag-110m	Ce-144	Cs-134	Cs-137	Eu-154	Eu-155	Ru-106	Sb-125	Sr-90	U-238
Bq/mm³	1+2	N/A	1.15E+2	3.61E+1	4.40E+2	3.34E+1	1.53E+1	8.62E+1	7.44E-1	1.52E+3	N/A
	3	N/A	8.11E+1	1.30E+1	2.41E+2	2.48E+1	1.06E+1	5.64E+1	4.00E+0	1.95E+3	
	core	N/A	1.41E+4	2.18E+2	5.12E+3	8.79E+2	7.82E+2	5.11E+3	1.08E+2	2.19E+4	
Fraction/mm³	1+2	N/A	3.43E-7	3.26E-7	1.76E-7	1.39E-6	8.64E-7	1.24E-6	3.70E-9	6.59E-7	1.38E-6
	3	N/A	2.42E-7	1.17E-7	9.65E-8	1.04E-6	5.95E-7	8.10E-7	1.99E-8	8.44E-7	1.28E-6
	core	N/A	4.23E-5	1.97E-6	2.05E-6	3.68E-5	4.41E-5	7.34E-5	5.39E-7	9.47E-6	1.02E-5
Particle Equivalents/ mm³	1+2	N/A	6.58E-4	6.25E-4	3.38E-4	2.67E-3	1.66E-3	2.38E-3	7.09E-6	1.26E-3	2.64E-3
	3	N/A	4.65E-4	2.24E-4	1.85E-4	1.99E-3	1.14E-3	1.55E-3	3.81E-5	1.62E-3	2.46E-3
	core	N/A	8.11E-2	3.77E-3	3.93E-3	7.05E-2	8.46E-2	1.41E-1	1.03E-3	1.82E-2	1.95E-2

Table 46. Relative error in the Compact 1-2 radial fission product concentrations given in Table 45. Abnormal data points in the compact core are shown in gray font.

| Segment	Ag-110m	Ce-144	Cs-134	Cs-137	Eu-154	Eu-155	Ru-106	Sb-125	Sr-90	U-238
1 + 2	N/A	29%	14%	14%	16%	21%	26%	36%	14%	14%
3	N/A	26%	14%	14%	14%	16%	17%	17%	14%	16%
core	N/A	4%	4%	4%	4%	5%	4%	8%	3%	5%
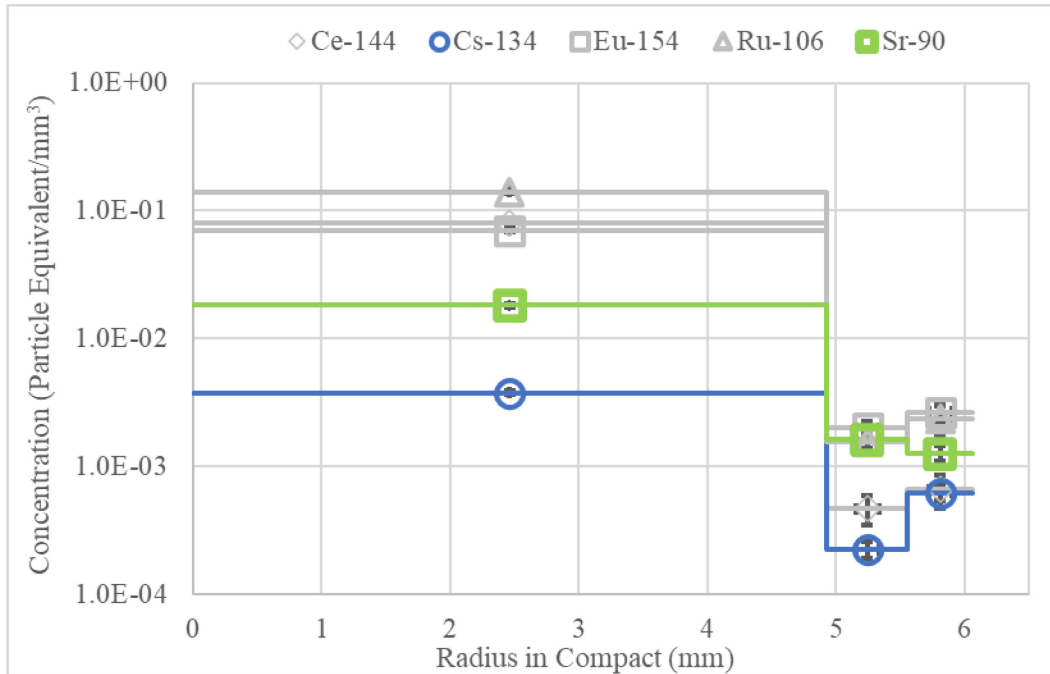
Figure 26. Radial concentrations of fission products in Compact 1-2 in units of particle equivalents per mm^3. The core concentrations of the data series shown in gray are deemed unreliable.
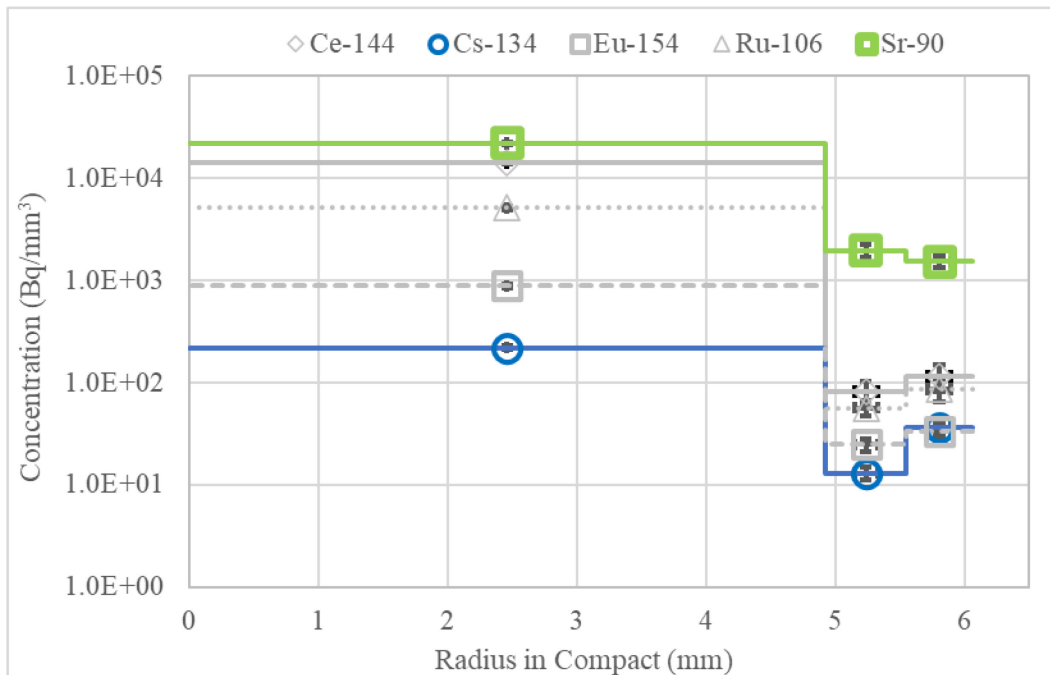
Figure 27. Radial concentrations of fission products in Compact 1-2 in units of Bq per mm^3. The core concentrations of the data series shown in gray are deemed unreliable.
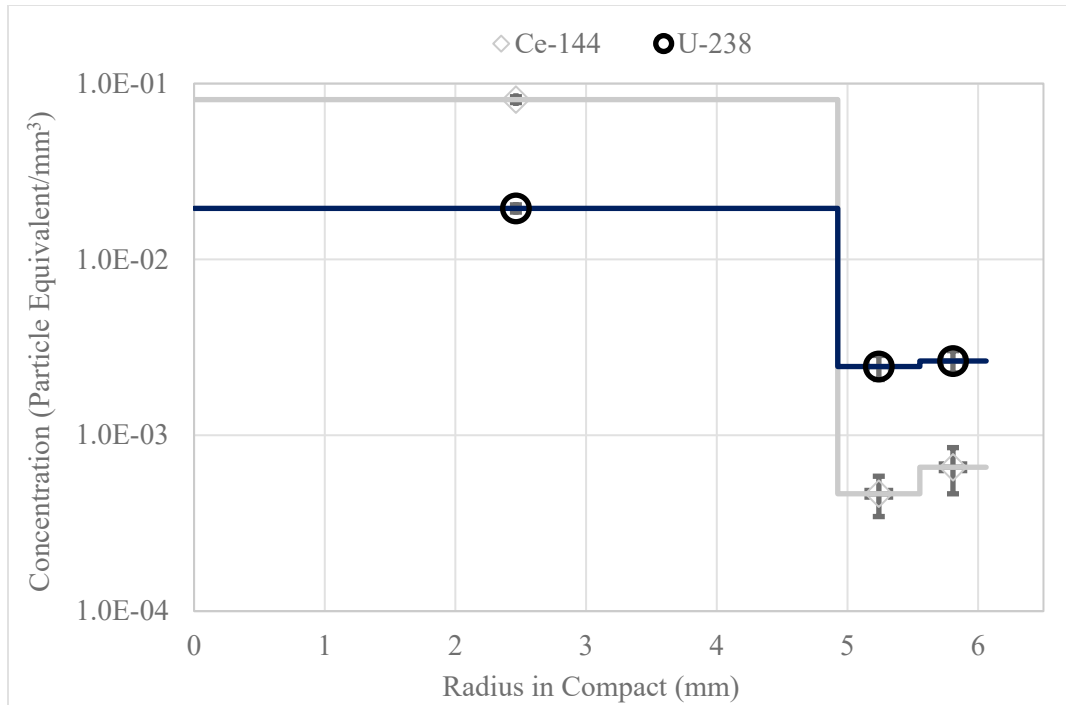
Figure 28. Comparison of U-238 and Ce-144 radial concentration profiles in Compact 1-2. The Ce-144 core concentration is unreasonably high, but the Ce-144 concentrations in the radial segments are trusted.

5.4.   Compact 3-1 Radial Fission Product Profiles

Compact 3-1 (TAVA 1138°C) was reirradiated in NRAD and then heated in the FACS furnace at 1600°C for about 200 h before it was subjected to RDLBL. The EOI TAVA irradiation temperature and burnup for Compact 3-1 are like those for other Capsule 3 and Capsule 8 compacts.[b] Some of those compacts underwent as-irradiated RDLBL (Stempien and Cai 2024a; Helmreich et al. 2021). Others underwent RDLBL following FACS testing and are reported here.

Sections 3.4 and 4.4.3 described the several difficulties encountered during the RDLBL of Compact 3-1. In short, the compact was mounted and remounted to the deconsolidation rod a couple times before it detached from the rod for the final time during radial deconsolidation of Segment 2. The RDLBL inventories indicated that about nine particles were damaged in Segment 1. This is too many particles to reasonably correct the Segment 1 inventories, and concentrations in Segment 1 will not be plotted here. There were no degraded TRISO particles in Segment 2, and there were no obvious signs of damaged TRISO particles in the core segment. The radial concentrations of select fission products and U-238 are listed in Table 47 and Table 48 and plotted in Figure 29, Figure 30, and Figure 31.

The Eu-154 and Sr-90 profiles from the core to Segment 2 in Compact 3-1 are relatively flat (within the error bars). As-irradiated Compacts 8-4, 8-3, 7-4, and 7-3 (TAVA 1169, 1213, 1319, and 1376°C, respectively) also had similar behavior between their cores and their next outer segments (Helmreich et al. 2021; Stempien and Cai 2024a). FACS-tested Compacts 3-2 and 8-2 (Figure 20 and Figure 23) had similar Eu and Sr profiles from their cores to their adjacent radial segments.

There may be a further bifurcation in the Eu and Sr behavior among these compacts. As-irradiated Compacts 7-3, 7-4, and 8-3 (Helmreich et al. 2021; Stempien and Cai 2024a) and FACS-tested Compacts

---

[b] Capsule 3 had a steady volume-average fuel temperature of ~1200°C throughout the irradiation, but the Capsule 8 temperatures were less consistent, starting a little above 1200°C, dropping to ~1100°C at the mid-point of the ATR irradiation, and then reaching as high as 1350°C toward the end. These time variations may affect the interpretation of the results.

3-2 and 8-2 had Eu and Sr profiles (Figure 20 and Figure 23) that were flat or slightly increasing with radius, but Compact 8-4 (Helmreich et al. 2021), which had a little lower TAVA irradiation temperature and was not tested in FACS, decreased slightly between the core and the three radial segments. Compact 3-1 had a similar irradiation temperature to Compact 8-4; however, it was heated at 1600°C. Because the accidental particle damage affected the outer segment concentrations of Compact 3-1, it is not known if the Eu and Sr profiles toward the surface resembled as-irradiated Compact 8-4, which had a slightly decreasing concentration with increasing radius, or Compacts 7-3, 7-4, 8-3, 3-2, and 8-2, which had higher irradiation temperatures or were FACS-tested and all showed flat or increasing concentrations with increasing radius.

From the compact core to the adjacent radial segment, concentrations of Ce-144, Cs-134, U-238, and Ru-106 in Compact 3-1 drop substantially. The magnitudes of these drops are most similar to those seen in Compact 3-2 (Figure 20), which was heated in the FACS furnace at 1600 and 1700°C. Reirradiated and FACS-tested Compact 8-2 exhibited a similar drop in these isotopic concentrations as well with the exception of the Cs-134 concentration, which did not drop as much from the core to the next segment (Figure 23). Perhaps this difference is due to the lower FACS temperature used in the test of Compact 8-2, which caused less radial transport of residual Cs-134 than the 1600°C test used for Compact 3-1.

Table 47. Radial fission product concentrations for Compact 3-1 (reirradiated and FACS-tested at 1600°C). As discussed in 4.4.3, Segment 1 was discarded due to multiple particles damaged during RDLBL.

Concentration	Segment	Ag-110m	Ce-144	Cs-134	Cs-137	Eu-154	Eu-155	Ru-106	Sb-125	Sr-90	U-238
Bq/mm³	2	N/A	9.82E+3	4.60E+2	1.07E+3	1.04E+3	8.44E+2	1.25E+3	7.29E+1	3.53E+4	
	Core	N/A	1.26E+6	8.23E+3	1.03E+4	1.26E+3	1.02E+3	6.54E+4	4.65E+2	2.95E+4	N/A
Fraction/mm³	2	N/A	8.99E-8	7.28E-8	1.76E-7	4.97E-6	5.70E-6	6.42E-8	1.52E-7	6.59E-6	1.40E-6
	Core	N/A	1.16E-5	1.30E-6	1.68E-6	6.00E-6	6.90E-6	3.36E-6	9.67E-7	5.51E-6	9.72E-6
Particle Equivalents /mm³	2	N/A	1.73E-4	1.40E-4	3.37E-4	9.53E-3	1.09E-2	1.23E-4	2.91E-4	1.26E-2	2.68E-3
	Core	N/A	2.22E-2	2.50E-3	3.22E-3	1.15E-2	1.32E-2	6.44E-3	1.85E-3	1.06E-2	1.86E-2

Table 48. Uncertainty for the Compact 3-1 fission product concentrations given in Table 47.

Segment	Ag-110m	Ce-144	Cs-134	Cs-137	Eu-154	Eu-155	Ru-106	Sb-125	Sr-90	U-238
2	N/A	56%	50%	50%	50%	50%	55%	51%	50%	50%
Core	N/A	10%	9%	9%	9%	9%	10%	14%	9%	10%
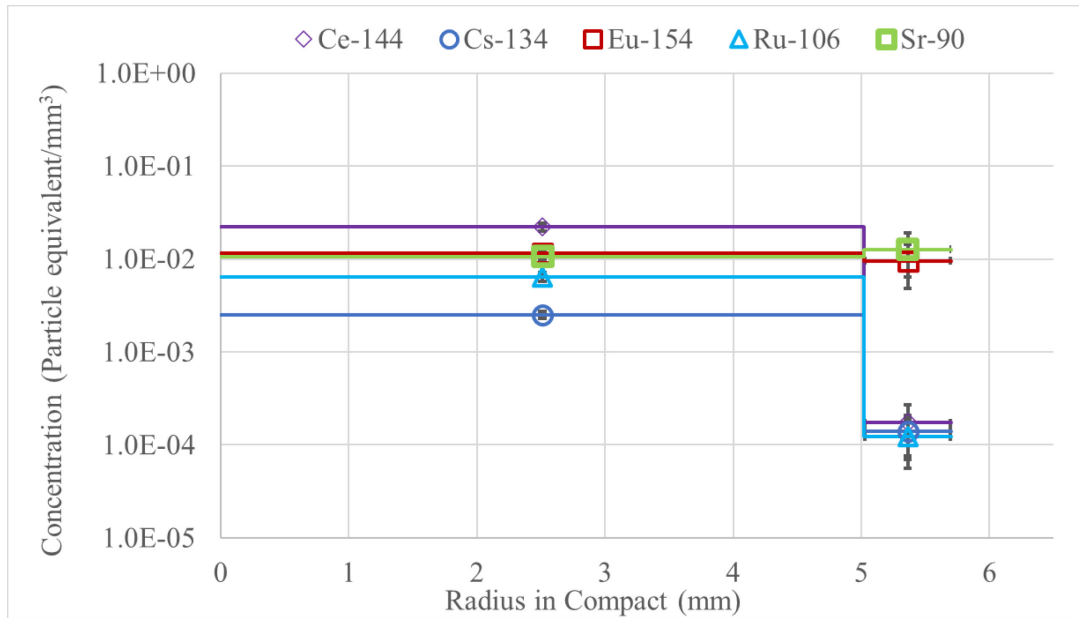
Figure 29. Radial concentrations of fission products in Compact 3-1 expressed in units of particle equivalents per mm^3. No concentrations are shown for Segment 1.
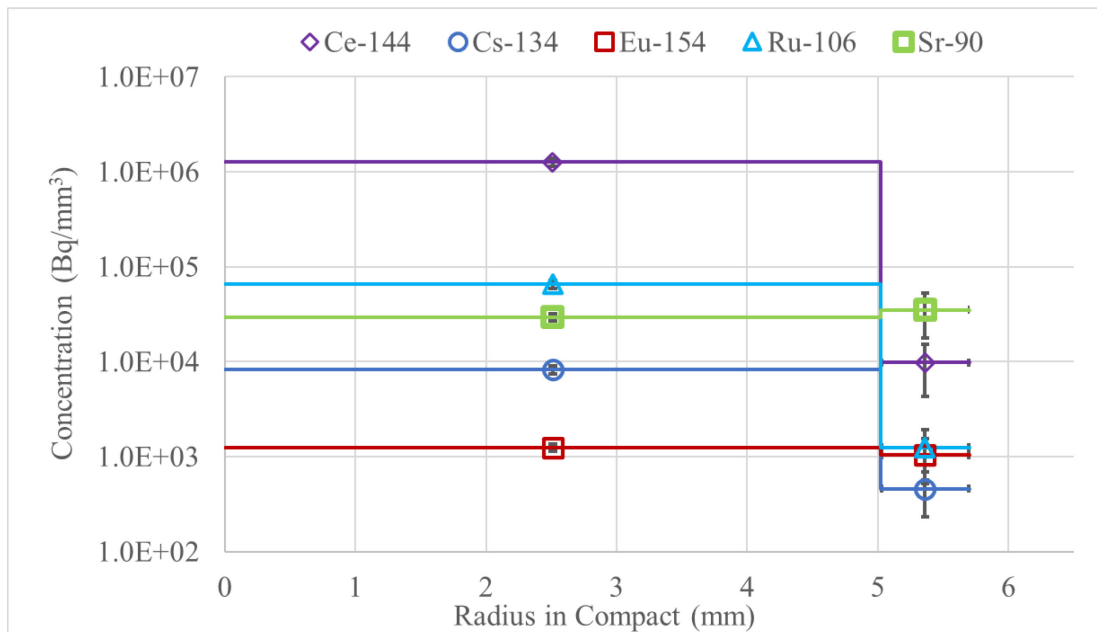
Figure 30. Radial concentrations of fission products in Compact 3-1 expressed in units of Bq per mm^3. No concentrations are shown for Segment 1.
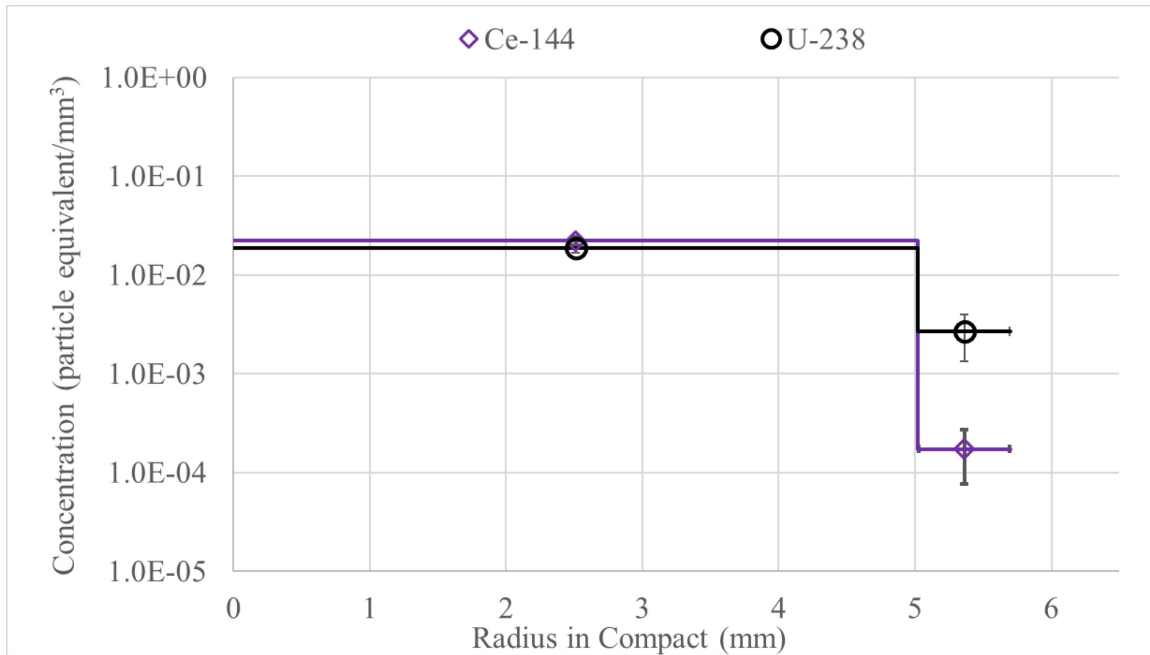
Figure 31. Comparison of U-238 and Ce-144 radial concentration profiles in Compact 3-1. No concentrations are shown for Segment 1.

5.5.   Compact 8-1 Radial Fission Product Profiles

Compact 8-1 (TAVA 1165°C) was reirradiated and then heated in the FACS furnace at 1200°C prior to RDLBL. Details on the ATR irradiation, NRAD reirradiation, and FACS tests were given in Sections 2.1 and 2.2. The EOI TAVA irradiation temperature and burnup for Compact 8-1 are like those for other Capsule 3 and Capsule 8 compacts that were subjected to as-irradiated and post-FACS RDLBL. The FACS test showed no signs of SiC or TRISO failure, and the RDLBL results (Section 4.5) corroborate this. Some uneven material removal was noted during RDLBL of this compact (Section 3.5).

The radial concentrations of fission product inventories are listed in Table 49, and Table 50 gives the error on the concentration by accounting for the measurement errors on the compact's dimensions and the fission product activity. Figure 32 and Figure 33 give the radial concentration profiles for selected fission products in Compact 8-1 in units of particle equivalents/mm^3 and Bq/mm^3, respectively. Figure 34 compares the concentration profiles of Ce-144 and U-238.

Despite a FACS temperature not much hotter than its TAVA irradiation temperature, the U-238 profile in this compact shows a noticeably more gradual and steady decrease with increasing radius, compared to most as-irradiated AGR-3/4 compacts. In 80% of the as-irradiated compacts, there were sharp reductions in U concentration spanning one or two orders of magnitude from the core to the adjacent radial segment, and then the profiles were relatively flat with increasing radius (see Figure 47 in Stempien and Cai [2024a]). Here, Compact 8-1's core concentration of U-238 is lower than most as-irradiated compacts, and outside of the core, its Segment 3 concentration is relatively high compared to as-irradiated compacts, while its concentrations in Segments 1 and 2 are about average relative to as-irradiated compacts (Stempien and Cai 2024a). In Compact 8-1's core and Segment 3, the Ce-144 concentrations are about average compared to as-irradiated compacts (see Figure 48 in Stempien and Cai [2024a]). In Compact 8-1's Segments 1 and 2, the Ce-144 concentrations are on the low end of the ranges measured in as-irradiated compacts.

Compact 8-1's Eu and Sr concentrations are relatively flat, with little difference between the concentrations in the core and Segments 2 and 1. The maximum Sr and Eu concentrations, however,

occur in Segment 3 (just outside of the core), where they are roughly twice as high as in the core and Segments 2 and 1. As-irradiated compacts with flat profiles or profiles that slightly increase with radius include Compacts 8-3, 7-4, and 7-3 (TAVA 1213, 1319, and 1376°C, respectively) (see Figures 49 and 50 in Stempien and Cai [2024a]). FACS-tested Compacts 3-2 (Figure 20) and 8-2 (Figure 23) have increases in Eu and Sr concentrations when moving outward from Segment 3 to their thin surface Segments 2 and 1. The shapes of the Eu and Sr profiles in Compact 8-1 are somewhat in between those of the high-irradiation-temperature as-irradiated compacts (i.e., 8-3, 7-4, and 7-3) and those with EOI burnups and average temperatures similar to Compact 8-1 that were safety-tested at 1400°C+ (i.e., 3-2 and 8-2). The maximum in Segment 3 could be a consequence of transport of a relatively small amount of these fission products out of the compact core during the 1200°C FACS test.

The Cs-134 profile in Compact 8-1 shows a steady decrease in concentration with increasing radius. The core concentration is on the low end of the range measured in as-irradiated compacts (see Figure 51 in Stempien and Cai [2024a]). It is higher than as-irradiated Compacts 12-3 and 8-3 and similar to as-irradiated Compacts 7-4 and 5-3. The concentrations and the shape of the Compact 8-1 Cs-134 profile most closely resembles that of Compact 8-2 (Figure 23), which had a similar EOI burnup and TAVA temperature and was FACS-tested at 1400°C.

Table 49. Radial fission product concentrations expressed in three different units for each segment of Compact 8-1.

Concentration	Segment	Ag-110m	Ce-144	Cs-134	Cs-137	Eu-154	Eu-155	Ru-106	Sb-125	Sr-90	U-238
Bq/mm^3	1	N/A	1.91E+4	1.26E+2	2.29E+2	4.14E+3	3.37E+3	6.67E+3	2.35E+2	8.02E+4	N/A
	2	N/A	2.75E+4	3.45E+2	9.58E+2	3.08E+3	2.28E+3	7.83E+3	9.81E+1	6.34E+4	
	3	N/A	1.56E+5	1.62E+3	5.27E+3	1.16E+4	8.65E+3	2.26E+4	2.94E+2	2.38E+5	
	core	N/A	1.30E+6	8.43E+3	1.13E+4	5.44E+3	4.44E+3	2.02E+5	1.27E+3	9.05E+4	
Fraction/mm^3	1	N/A	1.54E-7	1.37E-8	3.14E-8	1.43E-5	1.69E-5	2.58E-7	3.95E-7	1.28E-5	2.00E-7
	2	N/A	2.22E-7	3.75E-8	1.31E-7	1.06E-5	1.14E-5	3.03E-7	1.65E-7	1.01E-5	7.71E-7
	3	N/A	1.26E-6	1.76E-7	7.23E-7	4.00E-5	4.33E-5	8.74E-7	4.96E-7	3.79E-5	4.34E-6
	core	N/A	1.05E-5	9.15E-7	1.54E-6	1.87E-5	2.22E-5	7.80E-6	2.14E-6	1.44E-5	6.76E-6
Particle Equivalents /mm^3	1	N/A	2.95E-4	2.63E-5	6.02E-5	2.73E-2	3.23E-2	4.94E-4	7.59E-4	2.46E-2	3.83E-4
	2	N/A	4.25E-4	7.20E-5	2.52E-4	2.03E-2	2.19E-2	5.80E-4	3.17E-4	1.94E-2	1.48E-3
	3	N/A	2.42E-3	3.37E-4	1.39E-3	7.67E-2	8.31E-2	1.68E-3	9.52E-4	7.28E-2	8.33E-3
	core	N/A	2.01E-2	1.76E-3	2.96E-3	3.59E-2	4.26E-2	1.50E-2	4.10E-3	2.77E-2	1.30E-2

Table 50. Uncertainties in the Compact 8-1 concentrations given in Table 49.

Uncertainty of Concentrations	Ag-110m	Ce-144	Cs-134	Cs-137	Eu-154	Eu-155	Ru-106	Sb-125	Sr-90	U-238
1	N/A	35%	21%	20%	20%	20%	21%	21%	20%	20%
2	N/A	17%	13%	13%	13%	13%	17%	19%	13%	13%
3	N/A	45%	41%	41%	41%	41%	47%	46%	41%	41%
core	N/A	4%	2%	3%	3%	3%	3%	5%	2%	4%
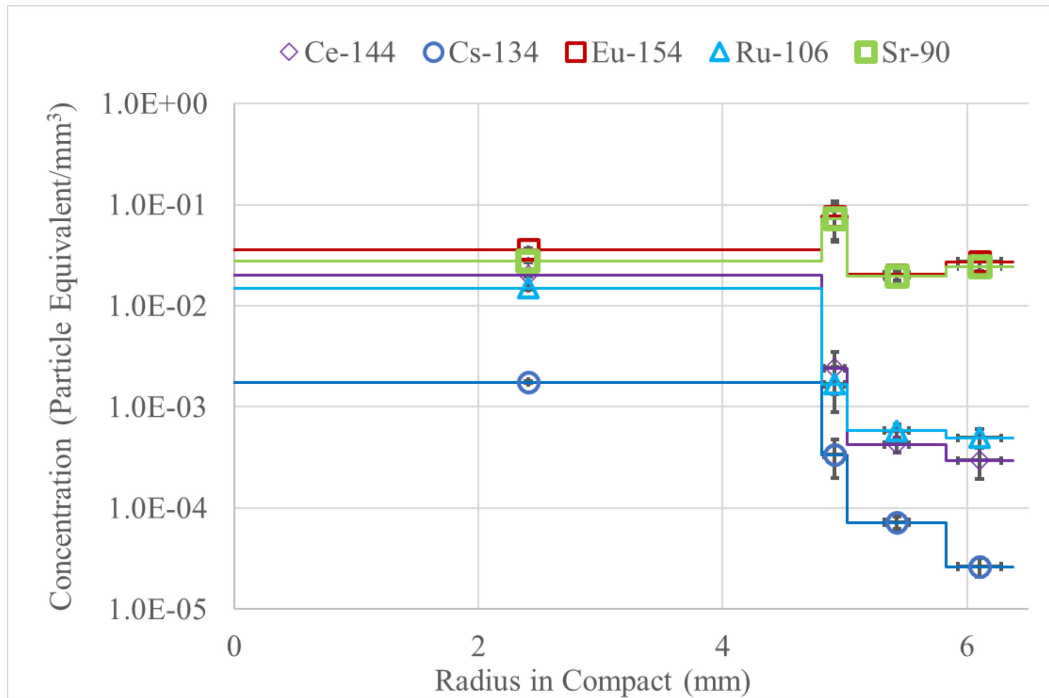
Figure 32. Compact 8-1 fission product radial concentration profiles in units of particle equivalents/mm^3.
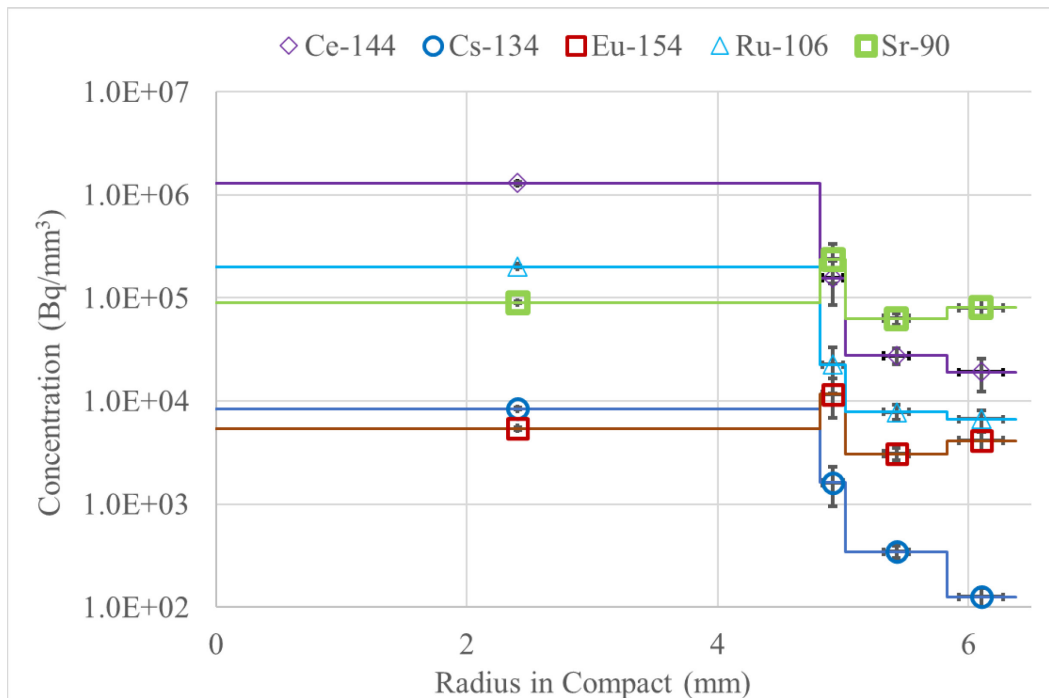
Figure 33. Compact 8-1 fission product radial concentration profiles in units of Bq/mm^3.
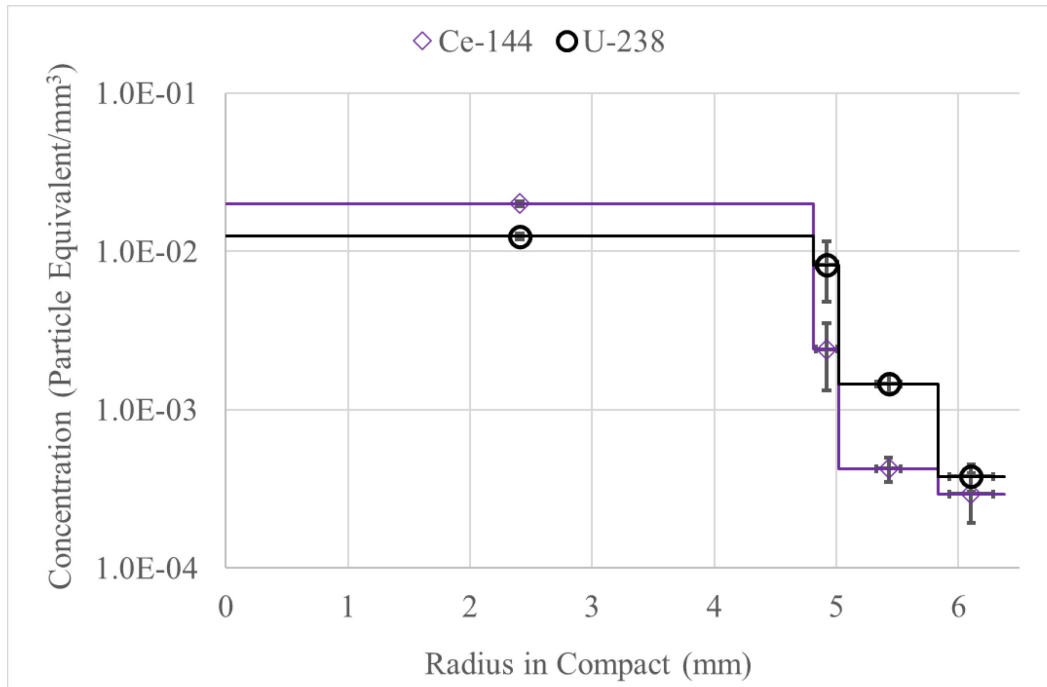
Figure 34. Comparison of Ce-144 and U-238 radial concentration profiles for Compact 8-1.

5.6. Comparisons of Fission Product Radial Concentration Profiles

In this section, the radial fission product concentration profiles among compacts from the same capsule are compared. Some of these compacts had been heated in the FACS furnace, and some were in the as-irradiated state when RDLBL was performed. The radial concentrations for selected fission products in Compacts 3-1 and 3-2 are shown in Figure 35, Figure 36 summarizes the same information for all four compacts from Capsule 8, and Figure 37 summarizes the concentration profiles for Capsule 1 compacts. The shaded regions around each line represent the error bands (when available).

For Compact 3-1, the results from Segment 1, which was very thin (about 0.6 mm thick), were not included in Figure 35 because multiple driver particles were accidentally broken and leached during the process, and reasonable corrections could not be made. The concentrations from as-irradiated Compact 3-3 also were not included because of the widespread accidental damage in that compact that occurred during RDLBL (Stempien and Cai 2024a). The core concentrations of Ce-144 in Compacts 3-1 and 3-2 were similar. There were similarly large reductions in the Ce-144 concentrations from the core to the outer segments for both Compacts 3-1 and 3-2. Segments 1 and 2 of Compact 3-2 (the two outermost segments) had large error bands that overlapped with the Segment 3 concentrations, making it difficult to conclude anything about the relative Ce-144 behavior in those regions. There was no detectable Ce-144 released during the FACS tests of Compacts 3-1 and 3-2. Compared to the available Ce-144 profiles in as-irradiated compacts from other capsules (Figure 48 in Stempien and Cai [2024a]), the core Ce-144 concentrations in Compacts 3-1 and 3-2 are toward the high end of the as-irradiated range and the concentrations in the radial segments of Compacts 3-1 are toward the bottom end of the range. Without trusted examples from as-irradiated Capsule 3 compacts for comparison, no conclusions on the impact of FACS testing on the Ce-144 can be made.

84

Compacts 3-1 and 3-2 had similar Cs-134 core concentrations, with very similar reductions from the core to the adjacent radial segment. This shape is similar to what was seen for Ce-144, but unlike Ce, there were signs of significant Cs transport in the total Cs inventories measured via RDLBL (which demonstrated that Cs from the DTF particles was released from the compacts), the significantly lower volumetric concentrations summarized in Figure 35, and the FACS tests (where about 0.9 particle equivalents of Cs-134 were driven out of the compacts during the tests).

Both Compacts 3-1 and 3-2 had relatively flat Eu concentration profiles, but the concentrations in Compact 3-1 were higher than in Compact 3-2, except near the surface, where they were similar. The lower core concentration in Compact 3-2 with a sudden increase in the adjacent radial segments could be from a combination of its higher irradiation temperature (closer to 1200°C[c]) and the 48 h it spent at 1700°C after the 300 h at 1600°C. There were 14.9 particle equivalents of Eu-154 releasing during Compact 3-2 FACS tests, while 4.5 were released during the Compact 3-1 FACS test. The Sr-90 profiles in these compacts were similar to the Eu-154 profiles.
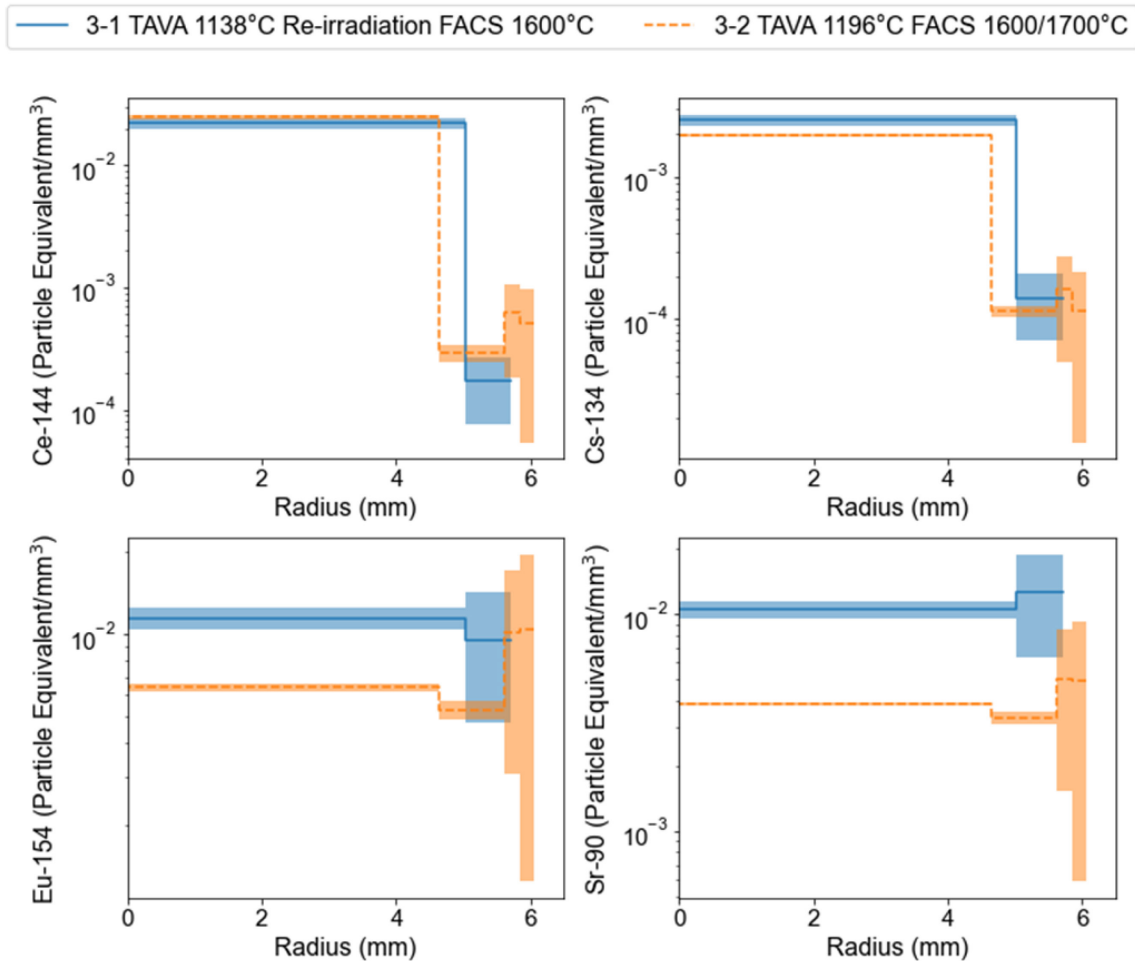
Figure 35. Comparison of Ce-144, Cs-134, Eu-154, and Sr-90 radial concentration profiles for Compacts 3-1 and 3-2. The shaded areas are the corresponding error bands.

---

[c] An acceleration in the Eu release rate at temperatures ≥1200°C has been noted previously (Stempien, Cai, and Demkowicz 2023).

The concentration profiles for selected fission products in all Capsule 8 compacts are summarized in Figure 36. This includes the present RDLBL results for FACS-tested Compacts 8-1 and 8-2 and the as-irradiated RDLBL results reported previously for Compacts 8-3 (Stempien and Cai 2024a) and 8-4 (Helmreich et al. 2021). Figure 36 (a) applies an estimated correction to the concentrations in Compact 8-2 Segment 3, and Figure 36(b) does not have a correction to Compact 8-2 Segment 3. Both representations are provided here because certain end uses of these data may be better suited by the corrected or uncorrected data sets.

As discussed in Sections 4.2 and 5.2, the evidence suggests that two in-pile SiC failures occurred in TRISO particles from Compact 8-2 Segment 3. A correction can be made by subtracting up to 2 particle-equivalent inventories from the measured inventory in the first post-burn leach of Compact 8-2 Segment 3. The corrected value represents an estimate of the concentration due only to the matrix and diver-particle OPyC inventories in Segment 3. The uncorrected case represents the real concentration profile, which includes the inventory recovered from the two failed-SiC TRISO driver particles, the compact matrix, and other driver particle OPyC inventories in Segment 3.

The correction potentially introduces biases. For example, it may overcorrect the matrix (and OPyC) inventory in Segment 3, making it artificially low. This is because the correction assumes that any radionuclide or actinide inventory in the first post-burn leach in Segment 3 that is ≤2.0 particle equivalents is due solely to those two particles. Some may be from those particles, but some may be from other sources, and some of the failed-SiC-particle inventory may be in other segments of the compact. Those other segments would be biased high from the inventory that originated in the failed-SiC particles that remains uncorrected in those segments.

As Figure 36 shows, the core concentrations of Ce-144 have the same order of magnitude for all four compacts, and these are comparable to the core concentrations measured in the FACS-tested Capsule 3 compacts (Figure 35). Like the Capsule 3 compacts, there were large drops in the Ce-144 concentrations between the cores and the adjacent radial segments in these Capsule 8 compacts. In Compacts 8-1, 8-3, and 8-4, the Ce-144 concentration decreased with increasing radius. In Compact 8-2, the Ce-144 profile decreases with increasing radius (as in the uncorrected case in Figure 36b). With the correction applied in Figure 36a, the estimated matrix concentration has a local minimum in Segment 3.

The Segment-1 concentrations of Cs-134 in FACS-tested Compacts 8-1 and 8-2 were lower than the Segment-1 concentrations in as-irradiated Compacts 8-3 and 8-4 because the FACS tests drove additional Cs-134 out of the compacts. Compact 8-2 had no measurable Cs-134 in Segment 1, and the shape of the Cs-134 concentration profiles in Compact 8-2 are similar in both the corrected and uncorrected representations.

In the Capsule 8 compacts, the Eu and Sr concentrations in the core were all similar. Note that the y-axis scales in the plots for Eu and Sr are different than for Ce and Cs. As-irradiated Compact 8-3 had slightly higher Eu and Sr concentrations in Segment 1 than in the core. The difference in the core and Segment 1 concentrations of Eu-154 in Compact 8-3 may not be statistically significant given the error bars overlap. As-irradiated Compact 8-4 had a slightly higher Eu-154 concentration in Segment 1 than in Segment 2, and its Sr-90 concentration decreased with increasing radius. The FACS-tested compacts (8-1 and 8-2) had pronounced local maxima in Eu-154 and Sr-90 concentrations in the radial segments outside of the core. Compact 8-1 had its local maxima in Eu and Sr in Segment 3, and Compact 8-2 had its local maxima in Eu and Sr in Segment 2. The presence of these local maxima may be a result of the FACS tests, and the relative locations of these local maxima may reflect the FACS temperatures, where the compact tested at 1200°C had Sr and Eu local maxima in Segment 3, and the compact tested at 1400°C had local maxima farther out from the core, in Segment 2.
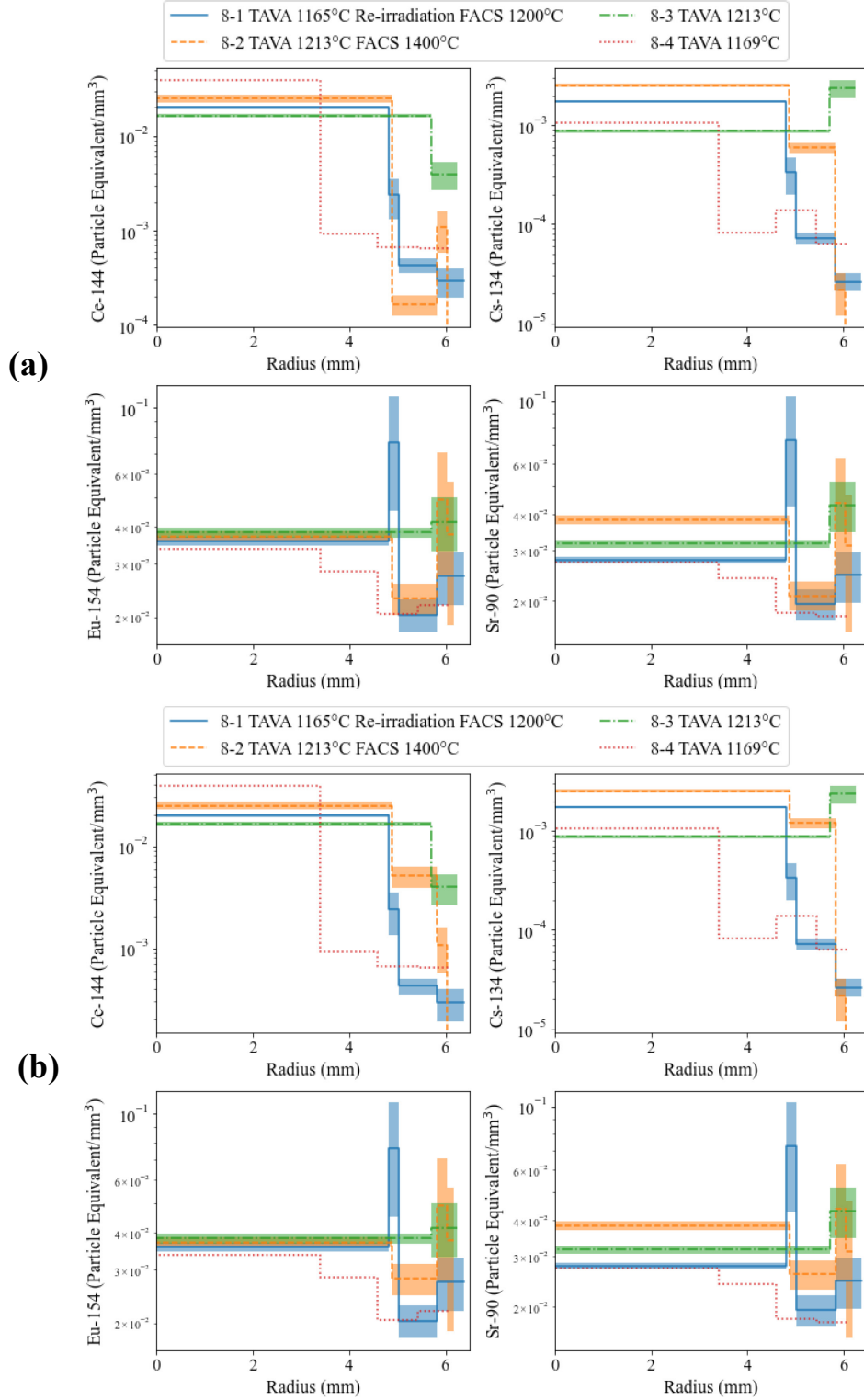
Figure 36. Radial concentration profiles for all four compacts in Capsule 8 (a) with an estimated correction for two failed-SiC particles in Compact 8-2 Segment 3, and (b) without a correction. The shaded area is the corresponding error band. The error bands for Compact 8-4 were not reported. No Ce-144 and no Cs-134 was detected in Segment 1 from Compact 8-2.

87

Figure 37 compares the radial fission product profiles for key nuclides from Capsule 1 compacts. Compacts 1-3 and 1-4 were both subjected to as-irradiated RDLBL at ORNL (Helmreich et al. 2022; Hunn et al. 2020). Compact 1-2 was reirradiated and FACS tested before undergoing RDLBL at INL. In Compact 1-2, the core concentrations of Ce-144 and Eu-154 are not believed to be erroneously high (possibly from an error in the radiochemistry), but the core concentrations of Cs-134 and Sr-90 are believed to be reasonable (see Sections 4.3.3 and 5.3 for discussion). The Compact 1-2 radial concentrations (outside the core) are believed to be reasonable for all nuclides. The Ce and Eu concentrations in the two radial segments from Compact 1-2 are comparable to those measured in the as-irradiated compacts. In typical fashion, the radial concentrations of Sr-90 are very similar to those of Eu-154 in Compact 1-2. The Cs-134 concentrations in Compact 1-2 are generally lower than those of the as-irradiated compacts, likely the result of the 1400°C FACS test that drove about 14 particle equivalents out of the compact. Compacts 1-2 and 1-4 both had local maxima in Cs-134 near the compact surface (Segment 1); therefore, these local maxima appear to be possible both in the as-irradiated state and after FACS testing.
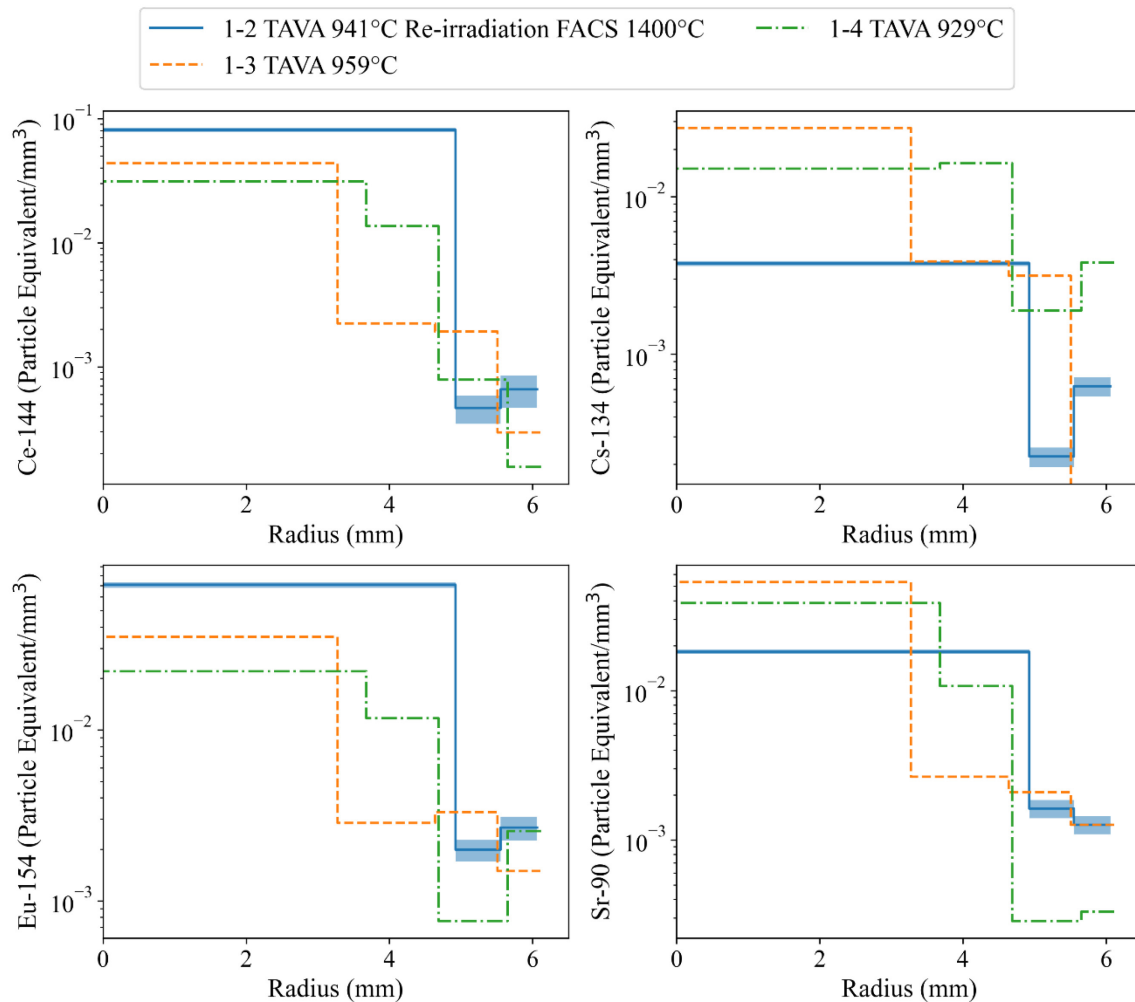
Figure 37. Comparison of the Ce-144, Cs-134, Eu-154, and Sr-90 radial concentration profiles for Capsule 1 compacts. The shaded areas for Compact 1-2 represent the error bands. Note that the core concentrations of Ce-144 and Eu-154 in Compact 1-2 are believed to be from erroneous measurements (see discussion in Sections 4.3.3 and 5.3).

6.   SUMMARY AND CONCLUSION

The AGR-3/4 experiment was specifically designed to investigate the migration of fission products in fuel-compact graphitic matrix and reactor graphite components. The irradiation experiment consisted of fuel compacts containing roughly 1898 TRISO-coated driver-fuel particles and 20 DTF particles aligned along the compact center to intentionally release fission products during irradiation to migrate through and out of the compact. The RDLBL method was employed to measure the concentrations of key fission product isotopes (Ag, Ce, Cs, Eu, Ru, Sr) and actinides (U and Pu) in the compacts outside of the SiC coatings of the TRISO-coated driver particles as a function of the radial position in the compacts. This kind of analysis was completed previously on as-irradiated AGR-3/4 fuel compacts and other subsets of AGR-3/4 compacts after post-irradiation heating in the FACS furnace (both with and without reirradiation in NRAD) (Hunn et al. 2020; Helmreich et al. 2021; Helmreich et al. 2022; Stempien and Cai 2024a). This report has focused on the results of INL's analyses of five FACS-tested compacts. Three of these were reirradiated in the NRAD reactor prior to FACS testing (Stempien et al. 2021b), and two of which were FACS tested without reirradiation (Stempien and Cai 2024b).

In generating the radial segments from each compact, a total of about 30-45% of the compact volume was removed from prior to the final deconsolidation of the remaining compact "core" that contained the DTF particles. The RDLBL technique proved challenging to implement and employ in a hot-cell environment, and several sources of uncertainty were identified.

- There were particles damaged during the RDLBL process (e.g., when compacts detached from the deconsolidation rod). There was also some evidence in a couple compacts that a few TRISO-coated driver-particles could have experienced in-pile SiC layer failure or SiC-layer failure during the 1600°C FACS tests. However, historically, in-pile SiC failure and SiC failure in a 1600°C safety test is very unlikely. In some cases, corrections for accidental TRISO particle damage incurred during RDLBL processes could be attempted. Any accidental TRISO particle damage incurred during PIE or possible in-pile or in-FACS degradation complicated the interpretation of the results, because it introduced another source of fission products besides the DTF particles at a discrete point in time. The evidence suggests that two TRISO-coated driver particles in Compact 8-2 experienced in-pile SiC failure, and the tradeoffs associated with making a correction for those failures were discussed. The corrections were intended to estimate the matrix (and OPyC) inventories of fission products by subtracting out the influence of damaged or failed fuel. This may over- or under-correct for the exposed driver fuel kernels.

- The deconsolidation process was intended to remove material from the compacts with axial and azimuthal uniformity. However, uneven material removal was observed in Compacts 1-2 and 8-1, resulting in a final core shape more like a conical frustum than a cylinder. In those cases, there was no axial uniformity because, for example, the diameter of the remaining compact at one end is noticeably smaller than the diameter at the other end. If there is an axial gradient in fission product content (e.g., the top has more of a given nuclide than the bottom) and more of the top was removed during RDLBL, this might artificially increase the apparent concentration in the affect compact segment(s).

- The RDLBL method was assumed to generate concentric annular segments, but in some cases (e.g. Compact 8-2), at least some portion of the RDLBL appeared to have uneven azimuthal material removal that presented as a compact that "wobbled" as it rotated. This may have some unknown impact on the true radius of the center of a given segment and it could artificially dilute or concentrate the inventory in a given segment. Some of these effects could conceivably average-out.

The total inventories and the radial concentration profiles of fission products and actinides measured from RDLBL were compared among as-irradiated compacts that underwent RDLBL at INL and as-irradiated and FACS-tested compacts that underwent RDLBL at ORNL. Measurements of condensable and gaseous fission products from the FACS tests were referenced to aid in the interpretation of the RDLBL results (Stempien et al. 2021b; Stempien and Cai 2024b). The AGR-3/4 irradiation-capsule mass balances (Stempien et al. 2018b) were also considered because they show the inventory of fission products released from the fuel compacts, while the RDLBL shows the inventory of fission products retained in the fuel compacts outside of the SiC layer of intact TRISO-coated particles. Key conclusions drawn from this work are as follows.

- Compacts with EOI burnup and TAVA irradiation temperature had similar Ce-144 core concentrations and sharp reductions in concentration from the core to the adjacent radial segment. This was the case regardless of whether the compact had been FACS-tested or not, and it indicates there was little transport within the compact of Ce-144 that was produced in the DTF particles.

- Like Ce-144, Ru-106 from the DTF particles was retained in the compact despite generally lower fractional quantities of Ru-106 than Ce-144 being measured in the post-FACS RDLBLs. It was concluded that the recovery of Ru-106 from the RDLBL operations was often noticeably low relative to the actinide and Ce-144 recoveries, which has been noted previously in AGR-2 and recently in the as-irradiated AGR-3/4 RDLBLs.

- The mass balances suggested that a significant amount of the Cs-134 produced in the DTF particles was released during the irradiation in ATR. As-irradiated RDLBL supported this and showed retention of about 35-75% of the DTF inventory of Cs-134 in compacts with TAVA irradiation temperatures from about 850 to 959°C. From about 1000°C to 1400°C, the Cs-134 retained in the as-irradiated compacts ranged from 5-20% of the DTF inventory. FACS-tested compacts generally had lower Cs-134 concentrations in the segment near the compact surface than did as-irradiated compacts. This is from Cs-134 transport outward during the post-irradiation FACS tests, from which Cs-134 releases from the compacts were also recorded.

- The RDLBLs of Compacts 8-1 and 8-2 detected a total of about 51-53 particle equivalents of Eu-154. This is evidence of Eu-154 release from intact TRISO-coated driver particles in addition to the DTF particles. The fact that only a couple tenths of a particle equivalent of Eu-154 were released during the FACS tests for Compacts 8-1 (1200°C FACS) and 8-2 (1400°C FACS) demonstrates that, at these temperatures, the compact matrix is capable of retaining roughly all Eu-154 that migrated out of the particles. As-irradiated compacts commonly had flat or radially decreasing Eu-154 profiles, but compacts that were FACS tested may have flat profiles or profiles with local Eu-154 maxima, suggesting intra-compact Eu-154 transport with little release from the compact. Sr-90 was found to behave similarly to Eu-154.

  The potential for Eu and Sr diffusion through intact TRISO coatings has been well documented (Demkowicz et al. 2015b; Stempien et al. 2021a; Stempien, Cai, and Demkowicz 2023); however, despite some diffusion through intact coatings, most of that Eu and Sr is still retained in the compact matrix and particle OPyC layers. A recent report on RDLBLs of as-irradiated AGR-3/4 fuel compacts (Stempien and Cai 2024a, Cai, and Demkowicz 2023) showed little or no release from the driver particles until compact TAVA temperatures exceeded 1050°C. From 1050 to 1169°C, the RDLBL inventories increased sharply and exceeded 20 particle equivalents, indicating significant release of Eu and Sr through intact driver particles, with retention within the compact matrix and OPyC. Between 1213 and 1376°C, the Eu and Sr inventories in the RDLBL solutions plateaued at 3.5 and 2.0 times higher than at 1050°C, respectively. From the capsule mass balances, however, the inventories of these nuclides outside the fuel compacts increased sharply between 1190 and 1345°C. This behavior shows that diffusive release of Eu and Sr

through intact TRISO coatings accelerates above 1050°C, but these nuclides are still largely retained in the compact until 1190°C. Above 1190°C, diffusive release through intact coatings continues to increase, but release from the compact altogether also accelerates.

- There was no Ag-110m measured via RDLBL of these FACS-tested compacts, which was consistent with all previous as-irradiated AGR-3/4 RDLBLs (Hunn et al. 2020; Helmreich et al. 2021; Helmreich et al. 2022; Stempien and Cai 2024a). Two factors have made it impossible to quantify Ag-110m in these RDLBLs. One factor is that generally very little of the Ag-110m released through intact TRISO coatings and from DTF particles is retained in the compact matrix, where it can be measured via DLBL (Demkowicz et al. 2015b; Stempien et al. 2021a). Instead, Ag-110m diffuses relatively rapidly through the matrix and is mostly released from the compact altogether. Comparing the Ag-110m mass balance to the Ag-110m inventories measured from FACS testing also supports this assertion. Second, the long delay between the end of the ATR irradiation and these RDLBL exams resulted in substantial radioactive decay of Ag-110m such that the total inventory was significantly reduced.

Ongoing work aims to derive usable transport parameters from the AGR-3/4 fission product profiles. The concentration profiles and fission product releases from the FACS tests are being compared to fission product transport models, and it may be possible to determine effective diffusivities for some of the fission products from these data.

7.   REFERENCES

Bess, J. D., J. B. Briggs, and R. M. Lell. 2014. "Neutron Radiography (NRAD) reactor 64-Element Core Upgrade." INL/EXT-13-29628, Idaho National Laboratory, Idaho Falls, ID. https://doi.org/10.2172/1120810.

Collin, B. P. 2015a. "AGR-3/4 Irradiation Test Final As-Run Report." INL/EXT-15-35550, Rev. 0, Idaho National Laboratory, Idaho Falls, ID. https://doi.org/10.2172/1196553.

Collin, B. P., 2015b, "AGR-3/4 Irradiation Experiment Test Plan." PLN-3867, Rev. 1, Idaho National Laboratory, Idaho Falls, ID.

Demkowicz, P. A., et al. 2012. "The Fuel Accident Condition Simulator (FACS) furnace system for high temperature performance testing of VHTR fuel." *Nuclear Engineering and Design* 251: 164–172. https://doi.org/10.1016/j.nucengdes.2011.10.048.

Demkowicz, P. A., et al. 2015a. "First high temperature safety tests of AGR-1 TRISO fuel with the Fuel Accident Condition Simulator (FACS) furnace." *Journal of Nuclear Materials* 464: 320–330. https://doi.org/10.1016/j.jnucmat.2015.05.006.

Demkowicz, P. A., et al. 2015b. "AGR-1 Post Irradiation Examination Final Report." INL/EXT-15-36407, Idaho National Laboratory, Idaho Falls, ID. https://doi.org/10.2172/1236801.

Gleicher, F. 2018. "ESA-29 NRAD In-core Irradiation of AGR Compacts." ECAR-4055, Idaho National Laboratory, Idaho Falls, ID.

Harp, J. M., J. D. Stempien, and P. A. Demkowicz. 2021. "Gamma Spectrometry Examination of the AGR-3/4 Irradiation." INL/EXT-20-58254, Idaho National Laboratory, Idaho Falls, ID. https://doi.org/10.2172/1844232.

Hawkes, G. 2016. "AGR-3/4 Daily As-Run Thermal Analyses." ECAR-2807, Rev. 1, Idaho National Laboratory, Idaho Falls, ID.

Helmreich, G., Hunn, J.D., Montgomery, F. C., and D. J. Skitt. 2022. "Radial Deconsolidation and Leach-Burn-Leach of AGR-3/4 Compacts 1-3, 4-3, 10-1, and 10-2." ORNL/TM-2022/2586, Oak Ridge National Laboratory, Oak Ridge, TN. https://doi.org/10.2172/1887677.

Helmreich, G. W., J. D. Hunn, F. C. Montgomery, and D. J. Skitt. 2021. "Radial Deconsolidation and Leach-Burn-Leach of AGR-3/4 Compacts 8-4 and 7-4." ORNL/TM-2021/2178, Oak Ridge National Laboratory, Oak Ridge, TN. https://doi.org/10.2172/1820768.

Helmreich, G., F. C. Montgomery, and J. D. Hunn. 2015. "Development of a Radial Deconsolidation Method." ORNL/TM-2015/699, Oak Ridge National Laboratory. Oak Ridge, TN. https://doi.org/10.2172/1235005.

Humrickhouse, P. W. et al. 2016. "Modeling and Analysis of Fission Product Transport in the AGR-3/4 Experiment." International Topical Meeting on High Temperature Reactor Technology (HTR2016), Paper 18693, Las Vegas, NV, November 7–11. https://www.osti.gov/servlets/purl/1358376.

Humrickhouse, P. W., et al. 2018. "Preliminary Estimation of Fission Product Diffusion Coefficients from AGR-3/4 Data." In proceedings of the High Temperature Reactor, HTR2018, Warsaw, Poland, Paper HTR 2018-3096, October 2018

Hunn, J. D., F. C. Montgomery, D. J. Skitt, and G. W. Helmreich. 2020. "Radial Deconsolidation and Leach-Burn-Leach of AGR-3/4 Compacts 1-4 and 10-4." ORNL/TM-2020/1707, Oak Ridge National Laboratory, Oak Ridge, TN. https://doi.org/10.2172/1709104.

Hunn, J. D., et al. 2016. "Detection and Analysis of Particles with Failed SiC in AGR-1 Fuel Compacts." *Nuclear Engineering and Design* 306: 36–46. https://doi.org/10.1016/j.nucengdes.2015.12.011.

Hunn, J. D., et al. 2015. "PIE on Safety-Tested AGR-1 Compact 4-2-2." ORNL/TM-2015/033, Rev. 0. Oak Ridge National Laboratory, Oak Ridge, TN.

Hunn, J.D., et al. 2014. "Fabrication and Characterization of Driver Fuel Particles, Designed-to-Fail Fuel Particles, and Fuel Compacts for the US AGR-3/4 Irradiation Test." *Nuclear Engineering and Design* 271: 123–130. https://doi.org/10.1016/j.nucengdes.2013.11.020.

Hunn, J. D., et al., 2013. "AGR-1 Irradiated Compact 4-4-2 PIE Report: Evaluation of As-Irradiated Fuel Performance with Leach Burn Leach, IMGA, Materialography, and X-ray Tomography." ORNL/TM-2013/236, Oak Ridge National Laboratory, Oak Ridge, TN. https://info.ornl.gov/sites/publications/files/pub141765.pdf.

Hunn, J. D, M. P. Trammell, and F. C. Montgomery. 2011. "Data Compilation for AGR-3/4 Designed-to-Fail (DTF) Fuel Compact Lot (LEU03-10TOP2/LEU03-07DTF-OP1)-Z." ORNL/TM-2011/124, Oak Ridge National Laboratory, Oak Ridge, TN.

Hunn, J. D. and Miller, J. H. 2009. "Data Compilation for AGR-3/4 Designed-to-Fail (DTF) Fuel Particle Batch LEU04-02DTF." ORNL/TM-2008/193, Oak Ridge National Laboratory, Oak Ridge, TN. https://doi.org/10.2172/940336.

Hunn, J.D. and Lowden, R. A. 2007. "Data Compilation for AGR-3/4 Driver Fuel Coated Particle Composite LEU03-09T." ORNL/TM-2007/019, Oak Ridge National Laboratory, Oak Ridge, TN. https://doi.org/10.2172/931362.

Idaho National Laboratory. 2022. "Technical Program Plan for INL Advanced Reactor Technologies Advanced Gas Reactor Fuel Development and Qualification Program." PLN-3636, Rev. 11, Idaho National Laboratory, Idaho Falls, ID.

Kercher, A. K., et al. 2011. "Data Compilation for AGR-3/4 Designed-to-Fail (DTF) Fuel Particle Batch LEU03-07DTF." ORNL/TM-2011/109, Oak Ridge National Laboratory, Oak Ridge, TN. https://doi.org/10.2172/1649083.

Kercher, A. K. and J. D. Hunn. 2006. "Results from ORNL Characterization of Nominal 350 μm LEUCO Kernels (LEU03) from the BWXT G73V-20-69303 Composite." ORNL/TM-2006/552, Oak Ridge National Laboratory, Oak Ridge, TN. https://doi.org/10.2172/974612.

Riet, Adriaan A. 2023. "Status of Modifications to the AGR-3/4 Fission Product Transport Model." INL/RPT-23-74853, Idaho National Laboratory. Idaho Falls, ID. https://inldigitallibrary.inl.gov/sites/sti/sti/Sort_68062.pdf.

Riet, A. A. 2022. "Reconstruction of Fission Product Distribution from Tomographic Scans in TRISO Fuel Graphitic Matrix and Nuclear Grade Graphites." INL/RPT-22-67635, Idaho National Laboratory, Idaho Falls, ID. https://inldigitallibrary.inl.gov/sites/sti/sti/Sort_61515.pdf.

Riet, A. A. and J. D. Stempien. 2022. "Comparison of AGR-3/4 Fission Product Transport Model to Measurements and Extraction of Diffusivities via Analytical Fits." INL/RPT-22-69040, Idaho National Laboratory, Idaho Falls, ID. https://inldigitallibrary.inl.gov/sites/sti/sti/Sort_63493.pdf.

Stempien, J. D., and L. Cai. 2024a. "Radial Deconsolidation and Leach-Burn-Leach of Eight As-Irradiated AGR-3/4 TRISO Fuel Compacts." INL/RPT-24-77357, Idaho National Laboratory, Idaho Falls, ID. https://www.osti.gov/biblio/2337443.

Stempien, J.D. and L. Cai. 2024b. "Post-irradiation Heating Tests of As-Irradiated AGR-3/4 TRISO Fuel Compacts." INL/RPT-24-80447, Idaho National Laboratory, Idaho Falls, ID.

Stempien, J. D., L. Cai, and P. A. Demkowicz. 2023. "AGR TRISO Fuel Fission Product Release Data Summary." INL/RPT-23-74651, Idaho National Laboratory, Idaho Falls, ID. https://www.osti.gov/biblio/2202411.

Stempien, J. D. 2021. "Measurement of Fission Product Concentration Profiles in AGR-3/4 TRISO Fuel Graphitic Matrix and Nuclear Graphites." INL/EXT-21-62863, Idaho National Laboratory, Idaho Falls, ID. https://www.osti.gov/biblio/1811841.

Stempien, J. D., et al. 2021a. "AGR-2 TRISO Fuel Post-Irradiation Examination Final Report." INL/EXT-21-64279, Idaho National Laboratory, Idaho Falls, ID. https://www.osti.gov/biblio/1822447.

Stempien, J.D., et al. 2021b. "Reirradiation and Heating Testing of AGR-3/4 TRISO Fuels." In proceedings of the International Conference on High-Temperature Reactor Technology (HTR 2021), Paper HTR 2021-3004, Virtual Conference, June 2–4.

Stempien, J. D. 2020. "AGR-2 Compact 6-4-1 Post-Irradiation Examination Results." INL/EXT-18-45418, Idaho National Laboratory, Idaho Falls, ID. https://www.osti.gov/biblio/1897106.

Stempien, J. D., et al. 2018a. "Preliminary results from the first round of post-irradiation heating tests of fuel compacts from the US AGR-3/4 irradiation." In proceedings of HTR 2018, International Conference on High Temperature Reactor Technology, Paper HTR 2018-323, Warsaw, Poland, October 8–11. https://www.osti.gov/biblio/1478513

Stempien, J. D., et al. 2018b. "AGR-3/4 Experiment Preliminary Mass Balance." INL/EXT-18-46049, Idaho National Laboratory, Idaho Falls, ID. https://doi.org/10.2172/1558760.

Stempien, J. D. 2017. "Radial Deconsolidation and Leach-burn-leach of AGR-3/4 Compacts 3-3, 12-1, and 12-3." INL/EXT-17-43182, Idaho National Laboratory, Idaho Falls, ID. https://doi.org/10.2172/1408764.

Sterbentz, J. W. 2015. "JMOCUP As-Run Daily Physics Depletion Calculation for the AGR-3/4 TRISO Particle Experiment in ATR Northeast Flux Trap." Rev. 1, ECAR-2753, Idaho National Laboratory, July 2015.

Appendix A

Additional RDLBL Data

The tables in this appendix present the RDLBL data for select fission products in terms of activity (Bq) and compact fraction of compacts in Section 4. This appendix also documents select actinides in terms of mas (μg) and compact fraction. These tables report the same results as in Section 4, but they use different units.

A-1. Compact 3-2

Table 51. Activities of fission products measured in the solutions from the radial deconsolidation of Compact 3-2. All values were decay-corrected to AGR-3/4 EOI + 1 day.

Activity (Bq)		Ag-110m	Ce-144	Cs-134	Cs-137	Eu-154	Eu-155	Ru-106	Sb-125	Sr-90
Segment #1	Decon	<4E+05	1.89E+06	2.75E+04	7.65E+04	3.32E+04	2.48E+04	4.66E+06	<1E+04	5.38E+05
	Pre-burn leach 1	<7E+05	<7E+05	6.96E+03	1.10E+04	1.16E+04	9.32E+03	1.33E+06	<1E+04	9.90E+04
	Pre-burn leach 2	<4E+05	<7E+05	5.74E+03	7.26E+03	2.08E+03	<4E+03	5.38E+05	<7E+03	2.26E+04
	Post-burn leach 1	<7E+05	<2E+06	<7E+03	3.49E+03	7.14E+04	6.13E+04	<4E+05	<1E+04	7.15E+05
	Post-burn leach 2	<4E+05	6.60E+05	<3E+03	3.77E+03	1.04E+03	<4E+03	2.57E+05	<7E+03	2.69E+04
	SUM (MDA = 0)	0	2.55E+06	4.02E+04	1.02E+05	1.19E+05	9.54E+04	6.78E+06	0	1.40E+06
Segment #2	Decon	<7E+05	2.37E+06	5.91E+04	1.41E+05	2.17E+04	1.63E+04	4.03E+06	<2E+04	3.05E+05
	Pre-burn leach 1	<4E+05	8.18E+05	<7E+03	1.96E+04	1.08E+04	9.22E+03	1.67E+06	<7E+03	1.06E+05
	Pre-burn leach 2	<4E+05	<1E+06	<7E+03	3.20E+03	<2E+03	<4E+03	<4E+05	<7E+03	1.85E+04
	Post-burn leach 1	<7E+05	<2E+06	<7E+03	2.99E+03	8.76E+04	7.21E+04	<7E+05	<1E+04	1.04E+06
	Post-burn leach 2	<4E+05	<1E+06	<7E+03	<7E+02	<2E+03	<4E+03	<4E+05	<7E+03	1.85E+03
	SUM (MDA = 0)	0	3.18E+06	5.91E+04	1.67E+05	1.20E+05	9.76E+04	5.70E+06	0	1.47E+06
Segment #3	Decon	<1E+06	2.00E+06	1.42E+05	3.22E+05	4.48E+04	3.18E+04	4.28E+06	<3E+04	6.54E+05
	Pre-burn leach 1	<7E+05	<1E+06	<7E+03	5.30E+03	1.68E+04	1.38E+04	2.63E+06	<1E+04	1.59E+05
	Pre-burn leach 2	<7E+05	<1E+06	<7E+03	1.52E+03	1.41E+03	9.23E+02	<7E+05	<1E+04	1.68E+04
	Post-burn leach 1	<3E+06	5.34E+07	2.37E+06	2.45E+06	2.81E+05	1.99E+05	<3E+06	<1E+05	5.72E+06
	Post-burn leach 1 Correction	<3E+06	3.62E+06	0	0	1.67E+05	1.22E+05	<3E+06	<1E+05	2.86E+06
	Post-burn leach 2	<4E+05	<1E+06	1.19E+04	1.78E+04	4.27E+03	4.10E+03	<7E+05	<1E+04	1.68E+03
	SUM (MDA = 0)	0	5.54E+07	2.53E+06	2.80E+06	3.48E+05	2.50E+05	6.91E+06	0	6.55E+06
	SUM (MDA = 0) Correction	0	5.62E+06	1.54E+05	3.46E+05	2.34E+05	1.73E+05	6.91E+06	0	3.70E+06
Core	Decon	<7E+05	1.09E+08	2.01E+06	4.50E+06	6.04E+04	4.42E+04	3.32E+07	<4E+04	1.09E+06
	Pre-burn leach 1	<2E+06	1.38E+08	2.08E+06	4.46E+06	9.82E+04	7.58E+04	6.80E+07	<1E+05	2.51E+06
	Pre-burn leach 2	<7E+05	8.98E+06	8.30E+04	1.61E+05	5.08E+03	<7E+03	2.56E+06	1.51E+04	4.62E+04
	Post-burn leach 1	<3E+06	7.81E+08	1.58E+06	1.82E+06	4.50E+05	3.27E+05	1.21E+07	2.69E+05	5.59E+06
	Post-burn leach 2	<7E+05	2.09E+06	6.95E+04	1.06E+05	<3E+03	<7E+03	6.01E+06	2.38E+04	1.10E+04
	SUM (MDA = 0)	0	1.04E+09	5.83E+06	1.10E+07	6.14E+05	4.47E+05	1.22E+08	3.08E+05	9.25E+06
Compact TOTAL (MDA = 0)		0	1.10E+09	8.45E+06	1.41E+07	1.20E+06	8.90E+05	1.41E+08	3.08E+05	1.87E+07
Compact TOTAL (MDA = 0)		0	1.05E+09	6.08E+06	1.17E+07	1.09E+06	8.13E+05	1.41E+08	3.08E+05	1.58E+07

Table 52. Fraction (M/C) of the compact inventory of fission products measured in the solutions from the radial deconsolidation of Compact 3-2. All values were decay-corrected to AGR-3/4 EOI + 1 day.

Compact Fraction		Ag-110m	Ce-144	Cs-134	Cs-137	Eu-154	Eu-155	Ru-106	Sb-125	Sr-90
Segment #1	Decon	<6E-03	1.98E-05	4.07E-06	1.22E-05	1.52E-04	1.68E-04	2.37E-04	<2E-05	9.81E-05
	Pre-burn leach 1	<1E-02	<8E-06	1.03E-06	1.76E-06	5.31E-05	6.29E-05	6.75E-05	<2E-05	1.81E-05
	Pre-burn leach 2	<6E-03	<8E-06	8.50E-07	1.16E-06	9.50E-06	<2E-05	2.74E-05	<2E-05	4.13E-06
	Post-burn leach 1	<1E-02	<2E-05	<1E-06	5.57E-07	3.26E-04	4.14E-04	<2E-05	<2E-05	1.30E-04
	Post-burn leach 2	<6E-03	6.92E-06	<4E-07	6.01E-07	4.74E-06	<2E-05	1.31E-05	<2E-05	4.91E-06
	SUM (MDA = 0)	0	2.68E-05	5.95E-06	1.63E-05	5.46E-04	6.45E-04	3.45E-04	0	2.56E-04
Segment #2	Decon	<1E-02	2.48E-05	8.75E-06	2.25E-05	9.90E-05	1.10E-04	2.05E-04	<4E-05	5.56E-05
	Pre-burn leach 1	<6E-03	8.57E-06	<1E-06	3.12E-06	4.94E-05	6.23E-05	8.50E-05	<2E-05	1.93E-05
	Pre-burn leach 2	<6E-03	<1E-05	<1E-06	5.10E-07	<8E-06	<2E-05	<2E-05	<2E-05	3.37E-06
	Post-burn leach 1	<1E-02	<2E-05	<1E-06	4.77E-07	4.00E-04	4.87E-04	<4E-05	<2E-05	1.90E-04
	Post-burn leach 2	<6E-03	<1E-05	<1E-06	<1E-07	<8E-06	<2E-05	<2E-05	<2E-05	3.38E-07
	SUM (MDA = 0)	0	3.34E-05	8.75E-06	2.66E-05	5.49E-04	6.59E-04	2.90E-04	0	2.69E-04
Segment #3	Decon	<2E-02	2.10E-05	2.10E-05	5.13E-05	2.05E-04	2.15E-04	2.18E-04	<6E-05	1.19E-04
	Pre-burn leach 1	<1E-02	<2E-05	<1E-06	8.46E-07	7.66E-05	9.33E-05	1.34E-04	<2E-05	2.91E-05
	Pre-burn leach 2	<1E-02	<2E-05	<1E-06	2.42E-07	6.45E-06	6.24E-06	<4E-05	<2E-05	3.07E-06
	Post-burn leach 1	<4E-02	5.59E-04	3.51E-04	3.92E-04	1.28E-03	1.35E-03	<2E-04	<3E-04	1.04E-03
	Post-burn leach 1 Correction	<4E-02	3.79E-05	0	0	7.63E-04	8.25E-04	<2E-04	<3E-04	5.22E-04
	Post-burn leach 2	<6E-03	<1E-05	1.76E-06	2.84E-06	1.95E-05	2.77E-05	<4E-05	<2E-05	3.06E-07
	SUM (MDA = 0)	0	5.80E-04	3.74E-04	4.47E-04	1.59E-03	1.69E-03	3.52E-04	0	1.20E-03
	SUM (MDA = 0) Correction	0	5.89E-05	2.28E-05	5.53E-05	1.07E-03	1.17E-03	3.52E-04	0	6.74E-04
Core	Decon	<1E-02	1.15E-03	2.98E-04	7.17E-04	2.76E-04	2.99E-04	1.69E-03	<8E-05	1.99E-04
	Pre-burn leach 1	<3E-02	1.45E-03	3.08E-04	7.12E-04	4.49E-04	5.12E-04	3.46E-03	<2E-04	4.57E-04
	Pre-burn leach 2	<1E-02	9.41E-05	1.23E-05	2.56E-05	2.32E-05	<5E-05	1.30E-04	3.14E-05	8.42E-06
	Post-burn leach 1	<4E-02	8.18E-03	2.35E-04	2.91E-04	2.06E-03	2.21E-03	6.15E-04	5.58E-04	1.02E-03
	Post-burn leach 2	<1E-02	2.19E-05	1.03E-05	1.69E-05	<1E-05	<5E-05	3.06E-04	4.93E-05	2.01E-06
	SUM (MDA = 0)	0	1.09E-02	8.64E-04	1.76E-03	2.81E-03	3.02E-03	6.21E-03	6.39E-04	1.69E-03
Compact TOTAL (MDA = 0)		0	1.15E-02	1.25E-03	2.25E-03	5.49E-03	6.01E-03	7.20E-03	6.39E-04	3.41E-03
Compact TOTAL (MDA = 0) Correction		0	1.10E-02	9.01E-04	1.86E-03	4.97E-03	5.49E-03	7.20E-03	6.39E-04	2.89E-03

Table 53. Masses for select actinides from ICP-MS of solutions of Compact 3-2.

Mass (µg)		Pu-239	Pu-240	U-234	U-235	U-236	U-238
Segment #1	Decon	0.24	0.07	0.10	7.72	2.17	77.77
	Pre-burn leach 1	0.04	<3E-02	<3E-02	0.06	<3E-02	0.59
	Pre-burn leach 2	<3E-02	<3E-02	<3E-02	<4E-02	<3E-02	0.22
	Post-burn leach 1	0.18	0.08	<2E-02	0.22	0.05	2.05
	Post-burn leach 2	0.05	<2E-02	<2E-02	0.18	0.07	2.32
	SUM (MDA = 0)	0.51	0.15	0.10	8.17	2.29	82.95
Segment #2	Decon	0.26	0.09	0.19	13.77	3.94	138.00
	Pre-burn leach 1	0.08	<2E-02	<2E-02	1.10	0.29	11.10
	Pre-burn leach 2	<3E-02	<3E-02	<3E-02	0.05	<3E-02	0.52
	Post-burn leach 1	0.23	0.12	<3E-02	0.28	0.09	3.05
	Post-burn leach 2	<3E-02	<3E-02	<3E-02	<4E-02	<3E-02	<1E-01
	SUM (MDA = 0)	0.57	0.20	0.19	15.20	4.32	152.66
Segment #3	Decon	0.23	0.08	0.23	16.57	4.79	168.33
	Pre-burn leach 1	<3E-02	<2E-02	<2E-02	0.19	0.05	1.77
	Pre-burn leach 2	<3E-02	<3E-02	<3E-02	<3E-02	<3E-02	<7E-02
	Post-burn leach 1	3.08	1.17	0.27	19.23	5.93	202.67
	Post-burn leach 2	0.03	<3E-02	<3E-02	0.07	<3E-02	0.64
	SUM (MDA = 0)	3.34	1.25	0.51	36.06	10.77	373.41
Core	Decon	7.66	2.73	2.34	167.00	49.60	1633.33
	Pre-burn leach 1	9.13	3.17	2.31	165.67	48.57	1640.00
	Pre-burn leach 2	0.46	0.16	<4E-02	0.28	0.06	2.62
	Post-burn leach 1	36.17	13.30	0.30	20.00	5.80	204.67
	Post-burn leach 2	0.20	0.07	<3E-02	0.08	<3E-02	0.71
	SUM (MDA = 0)	53.61	19.43	4.95	353.02	104.03	3481.33
Compact TOTAL (MDA = 0)		58.03	21.03	5.74	412.45	121.41	4090.35

Table 54. Compact fractions for select actinides from ICP-MS of solutions from Compact 3-2.

Compact Fraction		Pu-239	Pu-240	U-234	U-235	U-236	U-238
Segment #1	Decon	4.67E-05	4.17E-05	2.26E-04	2.42E-04	2.21E-04	2.27E-04
	Pre-burn leach 1	8.86E-06	<2E-05	<7E-05	1.84E-06	<3E-06	1.72E-06
	Pre-burn leach 2	<6E-06	<2E-05	<7E-05	<1E-06	<3E-06	6.45E-07
	Post-burn leach 1	3.61E-05	4.38E-05	<4E-05	6.75E-06	4.79E-06	5.97E-06
	Post-burn leach 2	9.02E-06	<1E-05	<4E-05	5.48E-06	7.08E-06	6.76E-06
	SUM (MDA = 0)	1.01E-04	8.54E-05	2.26E-04	2.56E-04	2.33E-04	2.42E-04
Segment #2	Decon	5.19E-05	5.13E-05	4.10E-04	4.31E-04	4.02E-04	4.02E-04
	Pre-burn leach 1	1.50E-05	<1E-05	<4E-05	3.45E-05	2.98E-05	3.24E-05
	Pre-burn leach 2	<6E-06	<2E-05	<7E-05	1.45E-06	<3E-06	1.51E-06
	Post-burn leach 1	4.61E-05	6.57E-05	<7E-05	8.91E-06	8.71E-06	8.88E-06
	Post-burn leach 2	<6E-06	<2E-05	<7E-05	<1E-06	<3E-06	<3E-07
	SUM (MDA = 0)	1.13E-04	1.17E-04	4.10E-04	4.76E-04	4.40E-04	4.45E-04
Segment #3	Decon	4.47E-05	4.51E-05	5.07E-04	5.19E-04	4.88E-04	4.91E-04
	Pre-burn leach 1	<6E-06	<1E-05	<4E-05	5.81E-06	4.79E-06	5.15E-06
	Pre-burn leach 2	<6E-06	<2E-05	<7E-05	<9E-07	<3E-06	<2E-07
	Post-burn leach 1	6.11E-04	6.68E-04	6.03E-04	6.02E-04	6.05E-04	5.91E-04
	Post-burn leach 2	6.05E-06	<2E-05	<7E-05	2.26E-06	<3E-06	1.87E-06
	SUM (MDA = 0)	6.62E-04	7.13E-04	1.11E-03	1.13E-03	1.10E-03	1.09E-03
Core	Decon	1.52E-03	1.56E-03	5.14E-03	5.23E-03	5.05E-03	4.76E-03
	Pre-burn leach 1	1.81E-03	1.81E-03	5.07E-03	5.19E-03	4.95E-03	4.78E-03
	Pre-burn leach 2	9.13E-05	9.17E-05	<9E-05	8.68E-06	6.42E-06	7.63E-06
	Post-burn leach 1	7.17E-03	7.59E-03	6.53E-04	6.26E-04	5.91E-04	5.97E-04
	Post-burn leach 2	3.97E-05	3.91E-05	<7E-05	2.36E-06	<3E-06	2.08E-06
	SUM (MDA = 0)	1.06E-02	1.11E-02	1.09E-02	1.11E-02	1.06E-02	1.01E-02
Compact TOTAL (MDA = 0)		1.15E-02	1.20E-02	1.26E-02	1.29E-02	1.24E-02	1.19E-02

A-2. Compact 8-2

Table 55. Activities of fission products measured in the solutions from the radial deconsolidation of Compact 8-2. All values were decay-corrected to AGR-3/4 EOI + 1 day.

Compact 8-2										
Activity (Bq)		Ag-110m	Ce-144	Cs-134	Cs-137	Eu-154	Eu-155	Ru-106	Sb-125	Sr-90
Segment #1	Decon	<7E+05	<1E+06	<1E+04	3.78E+03	8.29E+04	5.55E+04	<7E+05	<1E+04	1.99E+06
	Pre-burn leach 1	<1E+06	<4E+06	<2E+04	1.10E+04	4.81E+04	3.53E+04	<1E+06	<2E+04	6.12E+05
	Pre-burn leach 2	<4E+05	<1E+06	<3E+03	4.96E+03	2.65E+03	<4E+03	3.65E+05	<7E+03	5.34E+04
	Post-burn leach 1	<1E+06	<4E+06	<3E+04	8.84E+03	2.38E+05	1.61E+05	1.45E+06	<4E+04	3.90E+06
	Post-burn leach 2	<4E+05	<1E+06	<3E+03	2.48E+03	2.03E+03	2.23E+03	2.54E+05	<7E+03	1.29E+04
	SUM (MDA = 0)	0	0	0	3.11E+04	3.74E+05	2.54E+05	2.07E+06	0	6.57E+06
Segment #2	Decon	<7E+05	<2E+06	<1E+04	4.04E+03	1.15E+05	7.67E+04	<7E+05	<2E+04	2.53E+06
	Pre-burn leach 1	<1E+06	<2E+06	4.06E+03	7.29E+03	7.53E+04	5.55E+04	<1E+06	<2E+04	1.17E+06
	Pre-burn leach 2	<3E+05	<4E+05	1.15E+03	1.91E+03	3.36E+03	2.47E+03	5.32E+04	<3E+03	7.60E+04
	Post-burn leach 1	<1E+06	6.13E+06	4.99E+03	7.80E+03	5.60E+05	4.18E+05	<1E+06	1.73E+04	1.05E+07
	Post-burn leach 2	<1E+06	<2E+06	5.62E+02	1.49E+03	4.47E+02	3.55E+02	<7E+05	1.62E+03	1.01E+04
	SUM (MDA = 0)	0	6.13E+06	1.08E+04	2.25E+04	7.55E+05	5.53E+05	5.32E+04	1.90E+04	1.43E+07
Segment #3	Decon	<2E+06	<4E+06	2.03E+04	4.84E+04	2.52E+05	1.73E+05	<1E+06	1.30E+04	5.76E+06
	Pre-burn leach 1	<2E+06	<4E+06	8.39E+03	1.20E+04	1.50E+05	1.16E+05	<3E+06	<4E+04	2.27E+06
	Pre-burn leach 2	<7E+05	<1E+06	<7E+03	1.78E+03	7.86E+03	5.66E+03	<7E+05	<1E+04	1.29E+05
	Post-burn leach 1	<4E+06	1.10E+08	1.20E+06	1.45E+06	1.29E+06	9.75E+05	1.46E+07	2.23E+05	2.49E+07
	Post-burn leach 1 Correction	<4E+06	0	0	0	9.81E+05	7.72E+05	0	0	1.83E+07
	Post-burn leach 2	<1E+06	3.72E+06	1.13E+06	1.16E+06	9.35E+03	7.80E+03	1.44E+06	<4E+04	4.63E+05
	SUM (MDA = 0)	0	1.14E+08	2.36E+06	2.67E+06	1.71E+06	1.28E+06	1.60E+07	2.36E+05	3.35E+07
	SUM (MDA = 0) Correction	0	3.72E+06	1.16E+06	1.22E+06	1.40E+06	1.07E+06	9.61E+05	1.30E+04	2.69E+07
Core	Decon	<2E+06	2.16E+08	2.62E+06	5.54E+06	6.74E+05	4.96E+05	6.85E+07	1.48E+05	1.82E+07
	Pre-burn leach 1	<7E+06	3.40E+08	3.95E+06	8.26E+06	6.80E+05	5.48E+05	1.07E+08	<3E+05	2.01E+07
	Pre-burn leach 2	<7E+06	1.05E+07	1.16E+06	1.10E+06	4.17E+04	3.41E+04	<7E+06	<1E+05	1.58E+06
	Post-burn leach 1	<1E+07	7.41E+08	3.03E+06	3.08E+06	3.91E+06	2.76E+06	1.34E+07	7.57E+05	7.63E+07
	Post-burn leach 2	<4E+06	1.97E+07	9.09E+05	9.81E+05	3.22E+04	2.46E+04	3.86E+06	<1E+05	1.23E+06
	SUM (MDA = 0)	0	1.33E+09	1.17E+07	1.90E+07	5.34E+06	3.87E+06	1.93E+08	9.05E+05	1.17E+08
Compact TOTAL (MDA = 0)		0	1.45E+09	1.40E+07	2.17E+07	8.18E+06	5.95E+06	2.11E+08	1.16E+06	1.72E+08
Compact TOTAL (MDA = 0) Correction		0	1.34E+09	1.28E+07	2.02E+07	7.87E+06	5.75E+06	1.84E+08	9.37E+05	1.65E+08

Table 56. Fraction (M/C) of the compact inventory of fission products measured in the solutions from the radial deconsolidation of Compact 8-2. All values were decay-corrected to AGR-3/4 EOI + 1 day.

Compact Fraction		Ag-110m	Ce-144	Cs-134	Cs-137	Eu-154	Eu-155	Ru-106	Sb-125	Sr-90
Segment #1	Decon	<7E-03	<1E-05	<1E-06	5.17E-07	2.81E-04	2.86E-04	<3E-05	<2E-05	3.17E-04
	Pre-burn leach 1	<1E-02	<3E-05	<2E-06	1.50E-06	1.63E-04	1.82E-04	<6E-05	<4E-05	9.74E-05
	Pre-burn leach 2	<3E-03	<1E-05	<3E-07	6.77E-07	8.98E-06	<2E-05	1.43E-05	<1E-05	8.50E-06
	Post-burn leach 1	<1E-02	<3E-05	<4E-06	1.21E-06	8.09E-04	8.28E-04	5.70E-05	<6E-05	6.21E-04
	Post-burn leach 2	<3E-03	<1E-05	<3E-07	3.38E-07	6.89E-06	1.15E-05	9.99E-06	<1E-05	2.05E-06
	SUM (MDA = 0)	0	0	0	4.24E-06	1.27E-03	1.31E-03	8.13E-05	0	1.05E-03
Segment #2	Decon	<7E-03	<2E-05	<1E-06	5.51E-07	3.91E-04	3.94E-04	<3E-05	<3E-05	4.02E-04
	Pre-burn leach 1	<1E-02	<2E-05	4.29E-07	9.94E-07	2.55E-04	2.85E-04	<4E-05	<3E-05	1.86E-04
	Pre-burn leach 2	<2E-03	<3E-06	1.22E-07	2.61E-07	1.14E-05	1.27E-05	2.09E-06	<4E-06	1.21E-05
	Post-burn leach 1	<1E-02	5.62E-05	5.28E-07	1.07E-06	1.90E-03	2.15E-03	<4E-05	2.99E-05	1.68E-03
	Post-burn leach 2	<1E-02	<2E-05	5.94E-08	2.04E-07	1.52E-06	1.83E-06	<3E-05	2.79E-06	1.60E-06
	SUM (MDA = 0)	0	5.62E-05	1.14E-06	3.08E-06	2.56E-03	2.85E-03	2.09E-06	3.27E-05	2.28E-03
Segment #3	Decon	<2E-02	<3E-05	2.15E-06	6.61E-06	8.56E-04	8.89E-04	<6E-05	2.23E-05	9.16E-04
	Pre-burn leach 1	<2E-02	<3E-05	8.87E-07	1.64E-06	5.07E-04	5.96E-04	<1E-04	<6E-05	3.61E-04
	Pre-burn leach 2	<7E-03	<1E-05	<8E-07	2.43E-07	2.67E-05	2.91E-05	<3E-05	<2E-05	2.06E-05
	Post-burn leach 1	<3E-02	1.01E-03	1.27E-04	1.98E-04	4.37E-03	5.01E-03	5.73E-04	3.84E-04	3.96E-03
	Post-burn leach 1 Correction	<3E-02	0	0	0	3.33E-03	3.97E-03	0	0	2.92E-03
	Post-burn leach 2	<1E-02	3.41E-05	1.19E-04	1.58E-04	3.17E-05	4.01E-05	5.67E-05	<6E-05	7.37E-05
	SUM (MDA = 0)	0	1.05E-03	2.49E-04	3.64E-04	5.79E-03	6.57E-03	6.30E-04	4.06E-04	5.33E-03
	SUM (MDA = 0) Correction	0	3.41E-05	1.22E-04	1.66E-04	4.75E-03	5.52E-03	3.78E-05	2.23E-05	4.29E-03
Core	Decon	<2E-02	1.98E-03	2.76E-04	7.56E-04	2.29E-03	2.55E-03	2.69E-03	2.55E-04	2.89E-03
	Pre-burn leach 1	<7E-02	3.12E-03	4.18E-04	1.13E-03	2.31E-03	2.82E-03	4.20E-03	<4E-04	3.20E-03
	Pre-burn leach 2	<7E-02	9.66E-05	1.23E-04	1.50E-04	1.42E-04	1.75E-04	<3E-04	<2E-04	2.51E-04
	Post-burn leach 1	<1E-01	6.79E-03	3.20E-04	4.20E-04	1.33E-02	1.42E-02	5.28E-04	1.30E-03	1.21E-02
	Post-burn leach 2	<3E-02	1.80E-04	9.61E-05	1.34E-04	1.09E-04	1.26E-04	1.52E-04	<2E-04	1.96E-04
	SUM (MDA = 0)	0	1.22E-02	1.23E-03	2.59E-03	1.81E-02	1.99E-02	7.58E-03	1.56E-03	1.87E-02
Compact TOTAL (MDA = 0)		0	1.33E-02	1.48E-03	2.96E-03	2.77E-02	3.06E-02	8.29E-03	2.00E-03	2.73E-02
Compact TOTAL (MDA = 0) Correction		0	1.23E-02	1.36E-03	2.76E-03	2.67E-02	2.96E-02	7.25E-03	1.61E-03	2.63E-02

Table 57. Masses for select actinides from ICP-MS of solutions of Compact 8-2.

	Compact 8-2					
Mass (µg)	Pu-239	Pu-240	U-234	U-235	U-236	U-238
Segment #1 Decon	0.02	<9E-03	<9E-03	0.11	0.02	1.03
Pre-burn leach 1	<7E-02	<2E-02	<4E-02	0.10	<3E-02	0.87
Pre-burn leach 2	<3E-02	<1E-02	<3E-02	<7E-02	<2E-02	0.10
Post-burn leach 1	0.11	0.08	<4E-02	0.09	0.04	1.09
Post-burn leach 2	<7E-02	<2E-02	<4E-02	<8E-02	<3E-02	<2E-01
SUM (MDA = 0)	0.13	0.08	0.00	0.30	0.06	3.08
Segment #2 Decon	<2E-02	<9E-03	<1E-02	<4E-02	<2E-02	0.36
Pre-burn leach 1	<8E-02	<2E-02	<4E-02	<9E-02	<3E-02	<3E-01
Pre-burn leach 2	<9E-02	<3E-02	<5E-02	<1E-01	<3E-02	<3E-01
Post-burn leach 1	0.43	0.30	<4E-02	0.66	0.15	11.27
Post-burn leach 2	<8E-02	<2E-02	<4E-02	<1E-01	<3E-02	<3E-01
SUM (MDA = 0)	0.43	0.30	0.00	0.66	0.15	11.62
Segment #3 Decon	<2E-02	<9E-03	<9E-03	0.23	0.08	2.88
Pre-burn leach 1	<7E-02	<2E-02	<4E-02	<8E-02	<3E-02	0.31
Pre-burn leach 2	<9E-02	<3E-02	<5E-02	<1E-01	<3E-02	<3E-01
Post-burn leach 1	4.93	2.22	0.42	24.03	10.40	321.33
Post-burn leach 1 Correction	0	0.44	0	0	0	0
Post-burn leach 2	0.46	0.19	<6E-02	2.14	0.90	28.67
SUM (MDA = 0)	5.39	2.41	0.42	26.40	11.38	353.19
SUM (MDA = 0) Correction	0.46	0.64	0	2.37	0.98	31.86
Core Decon	15.43	5.31	2.07	124.33	52.23	1533.33
Pre-burn leach 1	24.60	9.31	2.70	160.67	68.70	2086.67
Pre-burn leach 2	0.34	0.18	<4E-02	0.25	0.11	3.36
Post-burn leach 1	13.10	7.25	0.44	24.73	10.70	328.33
Post-burn leach 2	0.99	0.43	0.08	4.32	1.87	58.30
SUM (MDA = 0)	54.46	22.48	5.29	314.30	133.61	4010.00
Compact TOTAL (MDA = 0)	60.41	25.27	5.71	341.67	145.20	4377.89
Compact TOTAL (MDA = 0) Correction	55.47	23.50	5.29	317.63	134.80	4056.56

Table 58. Compact fractions for select actinides from ICP-MS of solutions from Compact 8-2.

Compact 8-2		Pu-239	Pu-240	U-234	U-235	U-236	U-238
Compact Fraction		Pu-239	Pu-240	U-234	U-235	U-236	U-238
Segment #1	Decon	3.69E-06	<5E-06	<2E-05	4.58E-06	2.11E-06	3.03E-06
	Pre-burn leach 1	<1E-05	<1E-05	<9E-05	4.05E-06	<3E-06	2.55E-06
	Pre-burn leach 2	<6E-06	<5E-06	<7E-05	<3E-06	<2E-06	2.80E-07
	Post-burn leach 1	2.23E-05	3.96E-05	<9E-05	3.75E-06	3.31E-06	3.22E-06
	Post-burn leach 2	<1E-05	<1E-05	<9E-05	<3E-06	<3E-06	<6E-07
	SUM (MDA = 0)	2.60E-05	3.96E-05	0.00E+00	1.24E-05	5.42E-06	9.09E-06
Segment #2	Decon	<4E-06	<5E-06	<2E-05	<2E-06	<2E-06	1.05E-06
	Pre-burn leach 1	<2E-05	<1E-05	<9E-05	<4E-06	<3E-06	<9E-07
	Pre-burn leach 2	<2E-05	<2E-05	<1E-04	<4E-06	<3E-06	<9E-07
	Post-burn leach 1	8.49E-05	1.52E-04	<9E-05	2.70E-05	1.41E-05	3.32E-05
	Post-burn leach 2	<2E-05	<1E-05	<9E-05	<4E-06	<3E-06	<9E-07
	SUM (MDA = 0)	8.49E-05	1.52E-04	0.00E+00	2.70E-05	1.41E-05	3.42E-05
Segment #3	Decon	<4E-06	<5E-06	<2E-05	9.55E-06	7.66E-06	8.47E-06
	Pre-burn leach 1	<1E-05	<1E-05	<9E-05	<3E-06	<3E-06	9.22E-07
	Pre-burn leach 2	<2E-05	<2E-05	<1E-04	<4E-06	<3E-06	<9E-07
	Post-burn leach 1	9.85E-04	1.13E-03	9.98E-04	9.85E-04	9.61E-04	9.47E-04
	Post-burn leach 1 Correction	0	8.85E-05	0	0	0	0
	Post-burn leach 2	9.11E-05	9.82E-05	<1E-04	8.76E-05	8.30E-05	8.44E-05
	SUM (MDA = 0)	1.08E-03	1.23E-03	9.98E-04	1.08E-03	1.05E-03	1.04E-03
	SUM (MDA = 0) Correction	9.11E-05	1.87E-04	0	9.71E-05	9.07E-05	9.38E-05
Core	Decon	3.08E-03	2.71E-03	4.91E-03	5.10E-03	4.83E-03	4.52E-03
	Pre-burn leach 1	4.91E-03	4.74E-03	6.39E-03	6.59E-03	6.35E-03	6.15E-03
	Pre-burn leach 2	6.74E-05	9.21E-05	<9E-05	1.01E-05	9.82E-06	9.91E-06
	Post-burn leach 1	2.62E-03	3.70E-03	1.03E-03	1.01E-03	9.88E-04	9.67E-04
	Post-burn leach 2	1.98E-04	2.19E-04	1.83E-04	1.77E-04	1.72E-04	1.72E-04
	SUM (MDA = 0)	1.09E-02	1.15E-02	1.25E-02	1.29E-02	1.23E-02	1.18E-02
Compact TOTAL (MDA = 0)		1.21E-02	1.29E-02	1.35E-02	1.40E-02	1.34E-02	1.29E-02
Compact TOTAL (MDA = 0) Correction		1.11E-02	1.18E-02	1.25E-02	1.30E-02	1.25E-02	1.20E-02

A-3. Compact 1-2

Table 59. Activities of fission products measured in the solutions from the radial deconsolidation of Compact 1-2. All values were decay-corrected to AGR-3/4 EOI + 1 day.

Compact 1-2										
Activity (Bq)		Ag-110m	Ce-144	Cs-134	Cs-137	Eu-154	Eu-155	Ru-106	Sb-125	Sr-90
Segment #1	Decon	<3E+05	5.31E+06	3.19E+03	6.89E+03	1.26E+03	1.15E+03	7.43E+05	<2E+03	5.39E+04
	Pre-burn leach 1	<1E+05	<3E+05	1.42E+04	1.60E+04	4.86E+02	<3E+02	1.97E+05	<1E+03	1.75E+04
	Pre-burn leach 2	<3E+05	<3E+05	7.33E+03	7.30E+03	1.26E+02	<4E+02	<1E+05	<1E+03	5.31E+03
	Post-burn leach 1	<2E+05	1.18E+06	7.04E+03	8.11E+03	2.98E+03	2.20E+03	<7E+04	<7E+02	8.74E+04
	Post-burn leach 2	<1E+05	<2E+05	5.60E+03	5.66E+03	<2E+02	1.18E+02	<7E+04	<7E+02	4.09E+03
	SUM (MDA = 0)	0	6.50E+06	3.73E+04	4.39E+04	4.85E+03	3.46E+03	9.40E+05	0	1.68E+05
Segment #2	Decon	<4E+05	9.58E+06	6.63E+03	1.80E+04	1.10E+03	6.53E+02	1.83E+06	<4E+03	4.76E+04
	Pre-burn leach 1	<7E+04	<1E+05	6.10E+03	7.17E+03	3.33E+02	2.80E+02	1.03E+05	1.07E+03	1.01E+04
	Pre-burn leach 2	<2E+05	1.41E+06	6.67E+03	7.74E+03	2.13E+03	2.16E+03	<7E+04	<1E+03	5.87E+04
	Post-burn leach 1	<3E+05	<4E+05	1.17E+04	1.58E+04	5.32E+03	3.61E+03	<2E+05	<2E+03	1.25E+05
	Post-burn leach 2	<2E+05	<4E+05	2.78E+04	2.62E+04	<2E+02	<4E+02	<7E+04	<2E+03	4.88E+03
	SUM (MDA = 0)	0	1.10E+07	5.89E+04	7.49E+04	8.89E+03	6.71E+03	1.93E+06	1.07E+03	2.47E+05
Segment #3	Decon	<3E+05	1.39E+07	1.04E+04	3.01E+04	1.71E+03	1.21E+03	1.54E+06	4.24E+03	1.42E+05
	Pre-burn leach 1	<1E+05	<3E+05	9.81E+03	1.50E+04	9.45E+02	5.76E+02	4.78E+05	<1E+03	4.23E+04
	Pre-burn leach 2	<2E+05	<3E+05	5.69E+03	7.47E+03	2.91E+02	2.16E+02	<1E+05	<1E+03	6.83E+03
	Post-burn leach 1	<2E+05	<7E+05	9.45E+03	1.59E+04	8.31E+03	5.87E+03	<7E+04	2.22E+03	4.02E+05
	Post-burn leach 2	<1E+05	<3E+05	3.55E+03	4.85E+03	2.17E+02	<2E+02	1.01E+05	<7E+02	4.23E+03
	SUM (MDA = 0)	0	1.39E+07	3.89E+04	7.32E+04	1.15E+04	7.88E+03	2.11E+06	6.46E+03	5.97E+05
Core	Decon	<7E+05	5.67E+08	6.03E+04	1.70E+05	4.28E+04	5.10E+04	6.14E+06	2.01E+04	4.71E+06
	Pre-burn leach 1	<1E+07	3.77E+09	1.30E+06	3.42E+06	1.59E+05	2.07E+05	4.68E+08	2.18E+05	8.11E+06
	Pre-burn leach 2	<7E+06	2.10E+08	3.77E+05	6.46E+05	1.76E+04	2.04E+04	1.36E+08	1.24E+05	5.11E+06
	Post-burn leach 1	<1E+07	4.26E+09	5.65E+05	1.39E+06	1.27E+06	1.86E+06	3.86E+07	2.36E+05	1.11E+06
	Post-burn leach 2	<7E+06	1.27E+08	1.08E+05	1.13E+05	9.40E+03	1.16E+04	5.73E+07	4.82E+04	5.68E+06
	SUM (MDA = 0)	0	8.94E+09	2.41E+06	5.74E+06	1.50E+06	2.15E+06	7.07E+08	6.46E+05	2.47E+07
Compact TOTAL (MDA = 0)		0	8.97E+09	2.55E+06	5.94E+06	1.53E+06	2.17E+06	7.12E+08	6.54E+05	2.58E+07

Table 60. Fraction (M/C) of the compact inventory of fission products measured in the solutions from the radial deconsolidation of Compact 1-2. All values were decay-corrected to AGR-3/4 EOI + 1 day.

Compact Fraction		Ag-110m	Ce-144	Cs-134	Cs-137	Eu-154	Eu-155	Ru-106	Sb-125	Sr-90
					Compact 1-2					
Segment #1	Decon	<1E-02	2.38E-05	2.46E-06	2.33E-06	2.93E-05	2.23E-05	7.31E-05	<1E-06	1.95E-05
	Pre-burn leach 1	<4E-03	<1E-06	1.09E-05	5.41E-06	1.13E-05	<4E-06	1.93E-05	<1E-06	6.34E-06
	Pre-burn leach 2	<7E-03	<2E-06	5.66E-06	2.47E-06	2.93E-06	<8E-06	<1E-05	<1E-06	1.92E-06
	Post-burn leach 1	<7E-03	5.30E-06	5.44E-06	2.75E-06	6.90E-05	4.26E-05	<1E-05	<7E-07	3.17E-05
	Post-burn leach 2	<4E-03	<8E-07	4.32E-06	1.91E-06	<3E-06	2.28E-06	<1E-05	<7E-07	1.48E-06
	SUM (MDA = 0)	0.00E+00	2.91E-05	2.88E-05	1.49E-05	1.12E-04	6.71E-05	9.25E-05	0.00E+00	6.10E-05
Segment #2	Decon	<2E-02	4.29E-05	5.12E-06	6.09E-06	2.56E-05	1.27E-05	1.80E-04	<4E-06	1.73E-05
	Pre-burn leach 1	<2E-03	<7E-07	4.71E-06	2.43E-06	7.72E-06	5.43E-06	1.01E-05	8.44E-07	3.65E-06
	Pre-burn leach 2	<6E-03	6.30E-06	5.15E-06	2.62E-06	4.94E-05	4.19E-05	<1E-05	<9E-07	2.13E-05
	Post-burn leach 1	<7E-03	<2E-06	9.03E-06	5.35E-06	1.23E-04	7.00E-05	<2E-05	<2E-06	4.55E-05
	Post-burn leach 2	<6E-03	<2E-06	2.15E-05	8.87E-06	<5E-06	<8E-06	<1E-05	<2E-06	1.77E-06
	SUM (MDA = 0)	0.00E+00	4.92E-05	4.55E-05	2.53E-05	2.06E-04	1.30E-04	1.90E-04	8.44E-07	8.95E-05
Segment #3	Decon	<9E-03	6.22E-05	8.03E-06	1.02E-05	3.96E-05	2.35E-05	1.51E-04	3.35E-06	5.13E-05
	Pre-burn leach 1	<4E-03	<2E-06	7.57E-06	5.06E-06	2.19E-05	1.12E-05	4.71E-05	<1E-06	1.53E-05
	Pre-burn leach 2	<6E-03	<1E-06	4.39E-06	2.53E-06	6.74E-06	4.19E-06	<2E-05	<9E-07	2.48E-06
	Post-burn leach 1	<6E-03	<2E-06	7.30E-06	5.38E-06	1.93E-04	1.14E-04	<1E-05	1.75E-06	1.46E-04
	Post-burn leach 2	<4E-03	<1E-06	2.74E-06	1.64E-06	5.02E-06	<4E-06	9.93E-06	<4E-07	1.53E-06
	SUM (MDA = 0)	0.00E+00	6.22E-05	3.00E-05	2.48E-05	2.66E-04	1.53E-04	2.08E-04	5.10E-06	2.17E-04
Core	Decon	<2E-02	2.54E-03	4.65E-05	5.77E-05	9.92E-04	9.89E-04	6.04E-04	1.59E-05	1.71E-03
	Pre-burn leach 1	<4E-01	1.69E-02	1.00E-03	1.16E-03	3.69E-03	4.01E-03	4.61E-02	1.72E-04	2.94E-03
	Pre-burn leach 2	<4E-01	9.40E-04	2.91E-04	2.19E-04	4.09E-04	3.95E-04	1.34E-02	9.82E-05	1.85E-03
	Post-burn leach 1	<4E-01	1.91E-02	4.36E-04	4.71E-04	2.95E-02	3.61E-02	3.80E-03	1.86E-04	4.04E-04
	Post-burn leach 2	<1E-01	5.71E-04	8.36E-05	3.83E-05	2.18E-04	2.25E-04	5.64E-03	3.81E-05	2.06E-03
	SUM (MDA = 0)	0.00E+00	4.00E-02	1.86E-03	1.94E-03	3.48E-02	4.18E-02	6.95E-02	5.10E-04	8.97E-03
Compact TOTAL (MDA = 0)		0.00E+00	4.02E-02	1.97E-03	2.01E-03	3.54E-02	4.21E-02	7.01E-02	5.16E-04	9.35E-03

Table 61. Masses for select actinides from ICP-MS of solutions of Compact 1-2.

Mass (µg)		Pu-239	Pu-240	U-234	U-235	U-236	U-238
				Compact 1-2			
Segment #1	Decon	0.15	0.03	0.10	10.07	1.02	61.67
	Pre-burn leach 1	0.02	0.01	<4E-03	0.25	0.05	8.38
	Pre-burn leach 2	<7E-03	<4E-03	<2E-03	0.02	0.00	0.06
	Post-burn leach 1	0.02	<4E-03	<2E-03	0.07	0.01	1.34
	Post-burn leach 2	<8E-03	<4E-03	<2E-03	<7E-03	<5E-04	<4E-02
	SUM (MDA = 0)	0.19	0.03	0.10	10.41	1.08	71.45
Segment #2	Decon	0.31	0.06	0.18	18.37	1.83	109.33
	Pre-burn leach 1	0.01	<3E-03	<2E-03	0.07	0.01	0.41
	Pre-burn leach 2	0.02	<4E-03	<2E-03	0.05	0.01	0.96
	Post-burn leach 1	<1E-02	<5E-03	<3E-03	0.04	0.01	0.30
	Post-burn leach 2	<8E-03	<4E-03	<2E-03	0.01	<2E-03	0.14
	SUM (MDA = 0)	0.33	0.06	0.18	18.54	1.85	111.13
Segment #3	Decon	0.37	0.07	0.19	19.97	1.94	116.00
	Pre-burn leach 1	0.01	0.00	<5E-04	0.03	0.00	0.20
	Pre-burn leach 2	<2E-03	<8E-04	<5E-04	<2E-03	<2E-04	<9E-03
	Post-burn leach 1	0.00	<5E-04	<3E-04	0.01	0.00	0.05
	Post-burn leach 2	<2E-03	<8E-04	<5E-04	<2E-03	<2E-04	<9E-03
	SUM (MDA = 0)	0.38	0.07	0.19	20.00	1.94	116.25
Core	Decon	12.60	2.26	3.23	337.33	32.80	2016.67
	Pre-burn leach 1	18.00	3.20	2.18	225.00	21.93	1340.00
	Pre-burn leach 2	0.14	0.03	0.01	0.54	0.05	3.55
	Post-burn leach 1	4.73	0.85	0.06	6.46	0.63	39.37
	Post-burn leach 2	0.03	0.01	0.00	0.11	0.01	0.72
	SUM (MDA = 0)	35.50	6.35	5.48	569.44	55.43	3400.30
Compact TOTAL (MDA = 0)		36.41	6.51	5.94	618.38	60.30	3699.13

Table 62. Compact fractions for select actinides from ICP-MS of solutions from Compact 1-2.

Compact Fraction		Pu-239	Pu-240	U-234	U-235	U-236	U-238
Segment #1	Decon	4.15E-05	4.33E-05	1.73E-04	1.70E-04	1.83E-04	1.75E-04
	Pre-burn leach 1	6.33E-06	7.81E-06	<7E-06	4.18E-06	9.03E-06	2.37E-05
	Pre-burn leach 2	<2E-06	<6E-06	<4E-06	2.93E-07	1.48E-07	1.76E-07
	Post-burn leach 1	4.71E-06	<6E-06	<4E-06	1.12E-06	1.99E-06	3.81E-06
	Post-burn leach 2	<2E-06	<6E-06	<4E-06	<1E-07	<9E-08	<1E-07
	SUM (MDA = 0)	5.25E-05	5.11E-05	1.73E-04	1.75E-04	1.94E-04	2.02E-04
Segment #2	Decon	8.37E-05	8.47E-05	3.20E-04	3.10E-04	3.27E-04	3.10E-04
	Pre-burn leach 1	2.47E-06	<4E-06	<4E-06	1.12E-06	1.11E-06	1.16E-06
	Pre-burn leach 2	4.56E-06	<6E-06	<4E-06	8.61E-07	1.77E-06	2.71E-06
	Post-burn leach 1	<3E-06	<7E-06	<5E-06	7.03E-07	1.21E-06	8.38E-07
	Post-burn leach 2	<2E-06	<6E-06	<4E-06	2.41E-07	<4E-07	3.86E-07
	SUM (MDA = 0)	9.07E-05	8.47E-05	3.20E-04	3.13E-04	3.32E-04	3.15E-04
Segment #3	Decon	9.95E-05	9.89E-05	3.36E-04	3.37E-04	3.48E-04	3.29E-04
	Pre-burn leach 1	3.40E-06	1.93E-06	<9E-07	4.52E-07	4.54E-07	5.79E-07
	Pre-burn leach 2	<5E-07	<1E-06	<9E-07	<3E-08	<4E-08	<3E-08
	Post-burn leach 1	5.88E-07	<7E-07	<5E-07	1.26E-07	1.90E-07	1.30E-07
	Post-burn leach 2	<5E-07	<1E-06	<9E-07	<3E-08	<4E-08	<3E-08
	SUM (MDA = 0)	1.04E-04	1.01E-04	3.36E-04	3.37E-04	3.48E-04	3.29E-04
Core	Decon	3.42E-03	3.39E-03	5.82E-03	5.69E-03	5.88E-03	5.71E-03
	Pre-burn leach 1	4.89E-03	4.79E-03	3.93E-03	3.79E-03	3.93E-03	3.80E-03
	Pre-burn leach 2	3.89E-05	3.81E-05	9.31E-06	9.08E-06	8.67E-06	1.01E-05
	Post-burn leach 1	1.28E-03	1.28E-03	1.10E-04	1.09E-04	1.14E-04	1.12E-04
	Post-burn leach 2	7.57E-06	8.66E-06	2.83E-06	1.79E-06	1.68E-06	2.03E-06
	SUM (MDA = 0)	9.64E-03	9.50E-03	9.87E-03	9.60E-03	9.94E-03	9.63E-03
Compact TOTAL (MDA = 0)		9.89E-03	9.74E-03	1.07E-02	1.04E-02	1.08E-02	1.05E-02

A-4. Compact 3-1

Table 63. Activities of fission products measured in the solutions from the radial deconsolidation of Compact 3-1. All values were decay-corrected to AGR-3/4 EOI + 1 day.

Compact 3-1									
Activity (Bq)		Ag-110m	Ce-144	Cs-134	Cs-137	Eu-154	Eu-155	Ru-106	Sb-125	Sr-90
Segment #1	Decon	<1E+06	6.13E+07	2.21E+05	5.11E+05	8.44E+04	6.92E+04	8.69E+06	1.12E+05	2.81E+06
	Pre-burn leach 1	<2E+06	<4E+06	1.17E+06	1.45E+06	2.45E+04	1.99E+04	9.41E+05	2.33E+04	6.47E+05
	Pre-burn leach 2	<2E+06	<4E+06	4.40E+05	5.32E+05	5.50E+03	4.18E+03	<1E+06	<2E+04	2.65E+05
	Post-burn leach 1	<4E+06	3.45E+08	6.92E+06	8.04E+06	5.63E+05	4.60E+05	4.95E+07	6.46E+05	1.59E+07
	Post-burn leach 2	<2E+06	<7E+06	2.44E+06	2.87E+06	2.33E+04	2.19E+04	2.18E+06	7.50E+04	1.18E+06
	SUM (MDA = 0)	0.00E+00	4.06E+08	1.12E+07	1.34E+07	7.01E+05	5.75E+05	6.13E+07	8.56E+05	2.08E+07
Segment #2	Decon	<3E+05	2.79E+06	7.49E+04	2.41E+05	2.41E+04	1.95E+04	1.11E+05	<3E+03	1.32E+06
	Pre-burn leach 1	<7E+05	<1E+06	2.39E+04	3.38E+04	2.90E+04	2.60E+04	2.44E+05	5.81E+03	1.07E+06
	Pre-burn leach 2	<7E+05	<1E+06	1.16E+04	1.13E+04	2.38E+03	1.97E+03	<4E+05	2.62E+03	1.71E+05
	Post-burn leach 1	<2E+06	<3E+06	1.19E+04	1.08E+04	2.37E+05	1.90E+05	<1E+06	1.03E+04	7.45E+06
	Post-burn leach 2	<7E+05	<1E+06	8.28E+03	7.81E+03	2.76E+03	2.35E+03	<3E+05	1.96E+03	2.15E+04
	SUM (MDA = 0)	0.00E+00	2.79E+06	1.31E+05	3.05E+05	2.96E+05	2.40E+05	3.55E+05	2.07E+04	1.00E+07
Core	Decon	<1E+06	1.11E+08	5.34E+05	1.63E+06	9.49E+04	8.16E+04	6.23E+06	<1E+04	3.23E+06
	Pre-burn leach 1	<4E+06	3.05E+08	3.11E+06	3.53E+06	3.02E+05	2.50E+05	4.52E+07	1.16E+05	8.28E+06
	Pre-burn leach 2	<3E+06	6.29E+06	1.04E+06	1.13E+06	9.00E+03	1.07E+04	2.24E+06	3.72E+04	4.36E+05
	Post-burn leach 1	<1E+07	8.20E+08	3.32E+06	3.70E+06	8.19E+05	6.54E+05	7.65E+06	2.72E+05	1.71E+07
	Post-burn leach 2	<7E+05	<3E+06	8.70E+04	9.67E+04	9.47E+03	7.92E+03	2.99E+06	3.12E+04	3.42E+04
	SUM (MDA = 0)	0.00E+00	1.24E+09	8.10E+06	1.01E+07	1.23E+06	1.00E+06	6.43E+07	4.57E+05	2.90E+07
Compact TOTAL (MDA = 0)		0	1.71E+09	1.96E+07	2.43E+07	2.32E+06	1.89E+06	1.35E+08	1.45E+06	6.27E+07

Table 64. Fraction (M/C) of the compact inventory of fission products measured in the solutions from the radial deconsolidation of Compact 3-1. All values were decay-corrected to AGR-3/4 EOI + 1 day.

Compact 3-1										
Compact Fraction		Ag-110m	Ce-144	Cs-134	Cs-137	Eu-154	Eu-155	Ru-106	Sb-125	Sr-90
Segment #1	Decon	<2E-02	5.61E-04	3.50E-05	8.37E-05	4.03E-04	4.68E-04	4.46E-04	2.33E-04	5.24E-04
	Pre-burn leach 1	<3E-02	<3E-05	1.85E-04	2.38E-04	1.17E-04	1.35E-04	4.83E-05	4.85E-05	1.21E-04
	Pre-burn leach 2	<3E-02	<3E-05	6.96E-05	8.71E-05	2.62E-05	2.82E-05	<8E-05	<4E-05	4.95E-05
	Post-burn leach 1	<5E-02	3.16E-03	1.10E-03	1.32E-03	2.69E-03	3.11E-03	2.54E-03	1.34E-03	2.97E-03
	Post-burn leach 2	<3E-02	<7E-05	3.86E-04	4.70E-04	1.11E-04	1.48E-04	1.12E-04	1.56E-04	2.20E-04
	SUM (MDA = 0)	0.00E+00	3.72E-03	1.77E-03	2.19E-03	3.34E-03	3.89E-03	3.15E-03	1.78E-03	3.89E-03
Segment #2	Decon	<4E-03	2.56E-05	1.19E-05	3.95E-05	1.15E-04	1.32E-04	5.70E-06	<7E-06	2.46E-04
	Pre-burn leach 1	<1E-02	<1E-05	3.79E-06	5.53E-06	1.38E-04	1.76E-04	1.25E-05	1.21E-05	1.99E-04
	Pre-burn leach 2	<1E-02	<1E-05	1.83E-06	1.85E-06	1.14E-05	1.33E-05	<2E-05	5.44E-06	3.20E-05
	Post-burn leach 1	<3E-02	<3E-05	1.88E-06	1.77E-06	1.13E-03	1.28E-03	<6E-05	2.15E-05	1.39E-03
	Post-burn leach 2	<1E-02	<1E-05	1.31E-06	1.28E-06	1.32E-05	1.59E-05	<1E-05	4.07E-06	4.01E-06
	SUM (MDA = 0)	0.00E+00	2.56E-05	2.07E-05	5.00E-05	1.41E-03	1.62E-03	1.82E-05	4.31E-05	1.87E-03
Core	Decon	<2E-02	1.01E-03	8.46E-05	2.67E-04	4.53E-04	5.52E-04	3.20E-04	<3E-05	6.03E-04
	Pre-burn leach 1	<5E-02	2.80E-03	4.93E-04	5.78E-04	1.44E-03	1.69E-03	2.32E-03	2.42E-04	1.55E-03
	Pre-burn leach 2	<4E-02	5.76E-05	1.65E-04	1.85E-04	4.30E-05	7.25E-05	1.15E-04	7.73E-05	8.15E-05
	Post-burn leach 1	<2E-01	7.51E-03	5.25E-04	6.05E-04	3.91E-03	4.42E-03	3.93E-04	5.67E-04	3.18E-03
	Post-burn leach 2	<1E-02	<2E-05	1.38E-05	1.58E-05	4.52E-05	5.35E-05	1.53E-04	6.49E-05	6.39E-06
	SUM (MDA = 0)	0.00E+00	1.14E-02	1.28E-03	1.65E-03	5.90E-03	6.78E-03	3.30E-03	9.51E-04	5.42E-03
Compact TOTAL (MDA = 0)		0	1.57E-02	3.11E-03	3.98E-03	1.11E-02	1.28E-02	6.91E-03	3.01E-03	1.17E-02

Table 65. Masses for select actinides from ICP-MS of solutions of Compact 3-1.

	Compact 3-1						
Mass (µg)		Pu-239	Pu-240	U-234	U-235	U-236	U-238
Segment #1	Decon	3.73	1.28	0.70	49.67	14.70	492.00
	Pre-burn leach 1	0.13	0.04	0.01	1.01	0.30	10.63
	Pre-burn leach 2	0.02	0.00	<2E-03	0.04	0.01	0.41
	Post-burn leach 1	17.00	5.90	1.44	101.00	29.87	1010.00
	Post-burn leach 2	0.32	0.11	0.04	2.54	0.75	26.67
	SUM (MDA = 0)	21.20	7.34	2.18	154.26	45.63	1539.71
Segment #2	Decon	0.01	0.00	0.00	0.31	0.09	136.00
	Pre-burn leach 1	<4E-03	<7E-04	<7E-04	0.00	0.00	0.02
	Pre-burn leach 2	<6E-03	<9E-04	<1E-03	<2E-03	<5E-06	<6E-03
	Post-burn leach 1	<5E-03	<8E-04	<9E-04	<2E-03	0.00	0.01
	Post-burn leach 2	<4E-03	<7E-04	<7E-04	<2E-03	0.00	<4E-03
	SUM (MDA = 0)	0.01	0.00	0.00	0.31	0.09	136.03
Core	Decon	13.37	4.41	3.42	242.67	69.73	2470.00
	Pre-burn leach 1	13.83	4.84	1.08	73.40	22.23	768.00
	Pre-burn leach 2	0.28	0.10	<4E-03	0.23	0.06	2.30
	Post-burn leach 1	27.23	9.97	0.07	3.52	1.03	36.57
	Post-burn leach 2	0.05	0.02	<6E-04	0.02	0.00	0.24
	SUM (MDA = 0)	54.76	19.34	4.58	319.83	93.06	3277.10
Compact TOTAL (MDA = 0)		75.97	26.68	6.77	474.41	138.78	4952.85

Table 66. Compact fractions for select actinides from ICP-MS of solutions from Compact 3-1.

Compact 3-1							
Compact Fraction		Pu-239	Pu-240	U-234	U-235	U-236	U-238
Segment #1	Decon	7.09E-04	7.33E-04	1.52E-03	1.49E-03	1.53E-03	1.43E-03
	Pre-burn leach 1	2.38E-05	2.34E-05	3.05E-05	3.04E-05	3.09E-05	3.10E-05
	Pre-burn leach 2	2.97E-06	2.84E-06	<4E-06	1.27E-06	1.21E-06	1.21E-06
	Post-burn leach 1	3.23E-03	3.37E-03	3.12E-03	3.03E-03	3.11E-03	2.94E-03
	Post-burn leach 2	6.15E-05	6.28E-05	7.67E-05	7.62E-05	7.82E-05	7.77E-05
	SUM (MDA = 0)	4.03E-03	4.19E-03	4.75E-03	4.63E-03	4.74E-03	4.49E-03
Segment #2	Decon	1.94E-06	1.91E-06	9.57E-06	9.37E-06	9.39E-06	3.96E-04
	Pre-burn leach 1	<8E-07	<4E-07	<2E-06	5.47E-08	4.90E-08	5.22E-08
	Pre-burn leach 2	<1E-06	<5E-07	<2E-06	<6E-08	<5E-10	<2E-08
	Post-burn leach 1	<9E-07	<5E-07	<2E-06	<6E-08	3.86E-08	3.79E-08
	Post-burn leach 2	<8E-07	<4E-07	<2E-06	<6E-08	1.94E-09	<1E-08
	SUM (MDA = 0)	1.94E-06	1.91E-06	9.57E-06	9.42E-06	9.48E-06	3.97E-04
Core	Decon	2.54E-03	2.52E-03	7.44E-03	7.29E-03	7.25E-03	7.20E-03
	Pre-burn leach 1	2.63E-03	2.76E-03	2.36E-03	2.20E-03	2.31E-03	2.24E-03
	Pre-burn leach 2	5.23E-05	5.57E-05	<9E-06	6.76E-06	6.63E-06	6.70E-06
	Post-burn leach 1	5.17E-03	5.69E-03	1.53E-04	1.06E-04	1.07E-04	1.07E-04
	Post-burn leach 2	1.01E-05	1.13E-05	<1E-06	7.04E-07	4.53E-07	6.86E-07
	SUM (MDA = 0)	1.04E-02	1.10E-02	9.95E-03	9.60E-03	9.67E-03	9.55E-03
Compact TOTAL (MDA = 0)		1.44E-02	1.52E-02	1.47E-02	1.42E-02	1.44E-02	1.44E-02

A-5. Compact 8-1

Table 67. Activities of fission products measured in the solutions from the radial deconsolidation of Compact 8-1. All values were decay-corrected to AGR-3/4 EOI + 1 day.

	Compact 8-1									
Activity (Bq)		Ag-110m	Ce-144	Cs-134	Cs-137	Eu-154	Eu-155	Ru-106	Sb-125	Sr-90
Segment #1	Decon	<1E+06	<4E+06	1.30E+04	3.72E+04	1.86E+05	1.38E+05	<7E+05	1.57E+04	4.23E+06
	Pre-burn leach 1	<7E+05	1.39E+06	1.05E+04	1.21E+04	3.48E+04	3.04E+04	1.47E+05	1.16E+04	7.54E+05
	Pre-burn leach 2	<1E+06	<2E+06	1.65E+03	2.20E+03	1.03E+04	9.33E+03	<1E+06	5.12E+03	1.20E+05
	Post-burn leach 1	Discard	3.59E+06	6.43E+03	6.82E+03	8.50E+05	7.01E+05	1.60E+06	2.46E+04	1.58E+07
	Post-burn leach 2	<4E+05	<1E+06	1.38E+03	1.45E+03	9.62E+02	6.19E+02	<4E+05	4.24E+03	2.25E+04
	SUM (MDA = 0)	7.35E+06	4.98E+06	3.29E+04	5.98E+04	1.08E+06	8.79E+05	1.74E+06	6.12E+04	2.09E+07
Segment #2	Decon	<1E+06	<3E+06	1.08E+05	3.09E+05	1.28E+05	8.91E+04	1.20E+06	<1E+04	3.47E+06
	Pre-burn leach 1	<1E+06	<2E+06	3.77E+03	1.24E+04	7.36E+04	5.46E+04	<1E+06	3.99E+03	1.75E+06
	Pre-burn leach 2	<7E+05	<1E+06	2.52E+03	1.60E+03	5.79E+03	3.93E+03	<4E+05	1.40E+03	9.51E+04
	Post-burn leach 1	<3E+06	9.47E+06	4.21E+03	5.38E+03	8.52E+05	6.36E+05	1.50E+06	2.43E+04	1.65E+07
	Post-burn leach 2	<7E+05	<1E+06	8.52E+02	1.08E+03	2.33E+03	1.86E+03	<4E+05	4.07E+03	3.87E+04
	SUM (MDA = 0)	0	9.47E+06	1.19E+05	3.30E+05	1.06E+06	7.85E+05	2.70E+06	3.38E+04	2.18E+07
Segment #3	Decon	<7E+05	5.37E+06	1.21E+05	4.06E+05	7.17E+04	5.53E+04	1.83E+06	<1E+04	3.05E+06
	Pre-burn leach 1	<7E+05	<1E+06	3.49E+03	7.23E+03	4.52E+04	3.00E+04	<7E+05	<7E+03	9.04E+05
	Pre-burn leach 2	<7E+05	<1E+06	3.17E+03	3.81E+03	6.51E+03	5.17E+03	<3E+05	<3E+03	1.15E+05
	Post-burn leach 1	<3E+06	7.26E+06	<1E+04	6.07E+03	8.14E+05	6.07E+05	<2E+06	2.13E+04	1.51E+07
	Post-burn leach 2	<1E+06	<1E+06	2.69E+03	3.19E+03	1.43E+03	1.05E+03	<4E+05	2.45E+03	2.06E+04
	SUM (MDA = 0)	0	1.26E+07	1.31E+05	4.26E+05	9.39E+05	6.99E+05	1.83E+06	2.38E+04	1.92E+07
Core	Decon	<2E+06	1.79E+08	1.16E+06	3.54E+06	2.37E+05	2.05E+05	3.69E+07	1.38E+05	7.70E+06
	Pre-burn leach 1	<7E+06	1.61E+08	2.22E+06	2.78E+06	3.04E+05	2.21E+05	1.19E+08	1.47E+05	6.50E+06
	Pre-burn leach 2	<4E+06	1.18E+07	3.26E+05	2.80E+05	4.41E+04	3.14E+04	4.61E+06	4.37E+04	9.58E+05
	Post-burn leach 1	<7E+06	8.30E+08	3.51E+06	3.24E+06	4.35E+06	3.57E+06	1.65E+07	7.68E+05	6.69E+07
	Post-burn leach 2	<3E+06	<7E+06	4.56E+05	4.05E+05	1.27E+04	9.30E+03	6.76E+06	5.69E+04	1.86E+05
	SUM (MDA = 0)	0	1.18E+09	7.67E+06	1.02E+07	4.95E+06	4.04E+06	1.84E+08	1.15E+06	8.23E+07
Compact TOTAL (MDA = 0)		0	1.21E+09	7.95E+06	1.11E+07	8.03E+06	6.40E+06	1.90E+08	1.27E+06	1.44E+08

Table 68. Fraction (M/C) of the compact inventory of fission products measured in the solutions from the radial deconsolidation of Compact 8-1. All values were decay-corrected to AGR-3/4 EOI + 1 day.

Compact 8-1										
Compact Fraction		Ag-110m	Ce-144	Cs-134	Cs-137	Eu-154	Eu-155	Ru-106	Sb-125	Sr-90
Segment #1	Decon	<9E-03	<3E-05	1.41E-06	5.10E-06	6.40E-04	6.90E-04	<3E-05	2.64E-05	6.76E-04
	Pre-burn leach 1	<6E-03	1.12E-05	1.14E-06	1.66E-06	1.20E-04	1.52E-04	5.67E-06	1.96E-05	1.20E-04
	Pre-burn leach 2	<9E-03	<1E-05	1.79E-07	3.02E-07	3.56E-05	4.67E-05	<4E-05	8.63E-06	1.92E-05
	Post-burn leach 1	Discard	2.89E-05	6.98E-07	9.36E-07	2.92E-03	3.51E-03	6.16E-05	4.14E-05	2.52E-03
	Post-burn leach 2	<3E-03	<1E-05	1.50E-07	1.99E-07	3.31E-06	3.10E-06	<1E-05	7.16E-06	3.58E-06
	SUM (MDA = 0)	5.84E-02	4.01E-05	3.58E-06	8.20E-06	3.72E-03	4.40E-03	6.73E-05	1.03E-04	3.34E-03
Segment #2	Decon	<9E-03	<2E-05	1.17E-05	4.24E-05	4.41E-04	4.46E-04	4.62E-05	<2E-05	5.54E-04
	Pre-burn leach 1	<1E-02	<2E-05	4.10E-07	1.70E-06	2.53E-04	2.73E-04	<4E-05	6.73E-06	2.79E-04
	Pre-burn leach 2	<6E-03	<9E-06	2.74E-07	2.20E-07	1.99E-05	1.96E-05	<1E-05	2.36E-06	1.52E-05
	Post-burn leach 1	<2E-02	7.63E-05	4.58E-07	7.38E-07	2.93E-03	3.18E-03	5.79E-05	4.10E-05	2.63E-03
	Post-burn leach 2	<6E-03	<9E-06	9.26E-08	1.48E-07	8.02E-06	9.32E-06	<1E-05	6.86E-06	6.19E-06
	SUM (MDA = 0)	0	7.63E-05	1.29E-05	4.52E-05	3.65E-03	3.93E-03	1.04E-04	5.69E-05	3.49E-03
Segment #3	Decon	<6E-03	4.32E-05	1.32E-05	5.56E-05	2.47E-04	2.77E-04	7.06E-05	<2E-05	4.86E-04
	Pre-burn leach 1	<6E-03	<1E-05	3.79E-07	9.91E-07	1.55E-04	1.50E-04	<3E-05	<1E-05	1.44E-04
	Pre-burn leach 2	<6E-03	<9E-06	3.44E-07	5.22E-07	2.24E-05	2.59E-05	<1E-05	<6E-06	1.84E-05
	Post-burn leach 1	<2E-02	5.85E-05	<2E-06	8.32E-07	2.80E-03	3.04E-03	<7E-05	3.60E-05	2.41E-03
	Post-burn leach 2	<9E-03	<1E-05	2.92E-07	4.37E-07	4.91E-06	5.23E-06	<1E-05	4.12E-06	3.29E-06
	SUM (MDA = 0)	0	1.02E-04	1.42E-05	5.84E-05	3.23E-03	3.50E-03	7.06E-05	4.01E-05	3.06E-03
Core	Decon	<2E-02	1.44E-03	1.26E-04	4.86E-04	8.15E-04	1.03E-03	1.43E-03	2.32E-04	1.23E-03
	Pre-burn leach 1	<6E-02	1.30E-03	2.41E-04	3.81E-04	1.04E-03	1.10E-03	4.59E-03	2.48E-04	1.04E-03
	Pre-burn leach 2	<3E-02	9.47E-05	3.54E-05	3.85E-05	1.52E-04	1.57E-04	1.78E-04	7.38E-05	1.53E-04
	Post-burn leach 1	<6E-02	6.68E-03	3.81E-04	4.44E-04	1.50E-02	1.79E-02	6.38E-04	1.30E-03	1.07E-02
	Post-burn leach 2	<2E-02	<6E-05	4.95E-05	5.56E-05	4.38E-05	4.66E-05	2.61E-04	9.60E-05	2.97E-05
	SUM (MDA = 0)	0	9.51E-03	8.33E-04	1.40E-03	1.70E-02	2.02E-02	7.10E-03	1.94E-03	1.31E-02
Compact TOTAL (MDA = 0)		0	9.73E-03	8.63E-04	1.52E-03	2.76E-02	3.21E-02	7.34E-03	2.14E-03	2.30E-02

Table 69. Masses for select actinides from ICP-MS of RDLBL solutions of Compact 8-1.

Compact 8-1							
Mass (µg)		Pu-239	Pu-240	U-234	U-235	U-236	U-238
Segment #1	Decon	0.03	0.01	0.01	0.64	0.25	8.10
	Pre-burn leach 1	0.01	0.01	0.01	0.58	0.03	2.33
	Pre-burn leach 2	0.01	<4E-03	<2E-03	0.01	0.00	0.10
	Post-burn leach 1	0.60	0.42	0.01	0.54	0.24	7.07
	Post-burn leach 2	0.03	0.02	<1E-03	0.01	0.00	0.08
	SUM (MDA = 0)	0.69	0.46	0.03	1.77	0.51	17.67
Segment #2	Decon	0.31	0.09	0.11	6.26	2.68	83.07
	Pre-burn leach 1	<4E-02	<3E-02	<3E-02	0.14	0.06	1.58
	Pre-burn leach 2	<2E-02	<2E-02	<2E-02	<2E-02	<2E-02	0.11
	Post-burn leach 1	0.45	0.30	<2E-02	0.40	0.17	5.18
	Post-burn leach 2	0.02	<2E-02	<2E-02	<2E-02	<2E-02	<6E-02
	SUM (MDA = 0)	0.78	0.39	0.11	6.80	2.91	89.93
Segment #3	Decon	0.45	0.13	0.15	8.64	3.65	112.00
	Pre-burn leach 1	<2E-02	<2E-02	<2E-02	0.21	0.05	1.87
	Pre-burn leach 2	<2E-02	<2E-02	<2E-02	<2E-02	<2E-02	0.04
	Post-burn leach 1	0.42	0.28	<2E-02	0.40	0.17	4.98
	Post-burn leach 2	<3E-02	<3E-02	<3E-02	<3E-02	<3E-02	<5E-02
	SUM (MDA = 0)	0.86	0.41	0.15	9.25	3.86	118.89
Core	Decon	15.13	5.15	2.04	116.00	48.53	1453.33
	Pre-burn leach 1	6.96	2.84	0.61	33.90	14.30	410.33
	Pre-burn leach 2	0.19	0.12	<4E-03	0.12	0.05	1.51
	Post-burn leach 1	13.33	7.54	0.34	17.23	7.48	218.67
	Post-burn leach 2	0.06	0.03	0.00	0.12	0.05	1.46
	SUM (MDA = 0)	35.68	15.68	3.00	167.37	70.40	2085.30
Compact TOTAL (MDA = 0)		38.01	16.94	3.28	185.19	77.69	2311.80

Table 70. Compact fraction for select actinides from ICP-MS of RDLBL solutions of Compact 8-1.

Compact 8-1		Pu-239	Pu-240	U-234	U-235	U-236	U-238
Compact Fraction							
Segment #1	Decon	6.07E-06	4.11E-06	2.56E-05	2.59E-05	2.31E-05	2.39E-05
	Pre-burn leach 1	2.70E-06	3.01E-06	1.26E-05	2.32E-05	2.46E-06	6.87E-06
	Pre-burn leach 2	1.55E-06	<2E-06	<5E-06	4.12E-07	1.84E-07	2.86E-07
	Post-burn leach 1	1.15E-04	2.06E-04	2.63E-05	2.18E-05	2.18E-05	2.08E-05
	Post-burn leach 2	6.15E-06	1.08E-05	<2E-06	2.42E-07	1.49E-07	2.29E-07
	SUM (MDA = 0)	1.32E-04	2.24E-04	6.44E-05	7.15E-05	4.77E-05	5.21E-05
Segment #2	Decon	5.90E-05	4.28E-05	2.52E-04	2.52E-04	2.48E-04	2.45E-04
	Pre-burn leach 1	<8E-06	<1E-05	<7E-05	5.48E-06	5.20E-06	4.65E-06
	Pre-burn leach 2	<4E-06	<1E-05	<5E-05	<8E-07	<2E-06	3.19E-07
	Post-burn leach 1	8.56E-05	1.48E-04	<5E-05	1.63E-05	1.61E-05	1.53E-05
	Post-burn leach 2	4.23E-06	<1E-05	<5E-05	<8E-07	<2E-06	<2E-07
	SUM (MDA = 0)	1.49E-04	1.91E-04	2.52E-04	2.74E-04	2.70E-04	2.65E-04
Segment #3	Decon	8.53E-05	6.25E-05	3.52E-04	3.48E-04	3.38E-04	3.30E-04
	Pre-burn leach 1	<4E-06	<1E-05	<5E-05	8.39E-06	4.60E-06	5.52E-06
	Pre-burn leach 2	<4E-06	<1E-05	<5E-05	<8E-07	<2E-06	1.07E-07
	Post-burn leach 1	7.97E-05	1.37E-04	<5E-05	1.61E-05	1.53E-05	1.47E-05
	Post-burn leach 2	<6E-06	<1E-05	<7E-05	<1E-06	<3E-06	<1E-07
	SUM (MDA = 0)	1.65E-04	2.00E-04	3.52E-04	3.73E-04	3.58E-04	3.51E-04
Core	Decon	2.90E-03	2.50E-03	4.82E-03	4.68E-03	4.50E-03	4.29E-03
	Pre-burn leach 1	1.33E-03	1.38E-03	1.44E-03	1.37E-03	1.33E-03	1.21E-03
	Pre-burn leach 2	3.69E-05	5.74E-05	<9E-06	4.81E-06	4.18E-06	4.45E-06
	Post-burn leach 1	2.56E-03	3.66E-03	8.08E-04	6.95E-04	6.93E-04	6.45E-04
	Post-burn leach 2	1.17E-05	1.46E-05	5.85E-06	4.73E-06	4.20E-06	4.30E-06
	SUM (MDA = 0)	6.84E-03	7.61E-03	7.07E-03	6.75E-03	6.53E-03	6.15E-03
Compact TOTAL (MDA = 0)		7.28E-03	8.23E-03	7.74E-03	7.47E-03	7.20E-03	6.82E-03